Regulation of spindle assembly checkpoint signalling and silencing during mitosis

Timoteo Enrique Felipe Kuijt

ISBN: 978-94-6375-745-4

Cover: Timoteo E.F. Kuijt
Printed by: Ridderprint | www.ridderprint.nl

Regulation of spindle assembly checkpoint signalling and silencing during mitosis

Regulatie van spoel-controlepunt signalering en demping tijdens mitose

(met een samenvatting in het Nederlands)

Proefschrift

ter verkrijging van de graad van doctor aan de
Universiteit Utrecht
op gezag van de
rector magnificus, prof.dr. H.R.B.M. Kummeling,
ingevolge het besluit van het college voor promoties
in het openbaar te verdedigen op

donderdag 20 februari 2020 des middags te 2.30 uur

door

Timoteo Enrique Felipe Kuijt

geboren op 12 juli 1987
te Bogota, Colombia

Promotor: Prof. dr. G.J.P.L. Kops

Stilte Ruimte Alleen een Merel die Zingt

Table of content

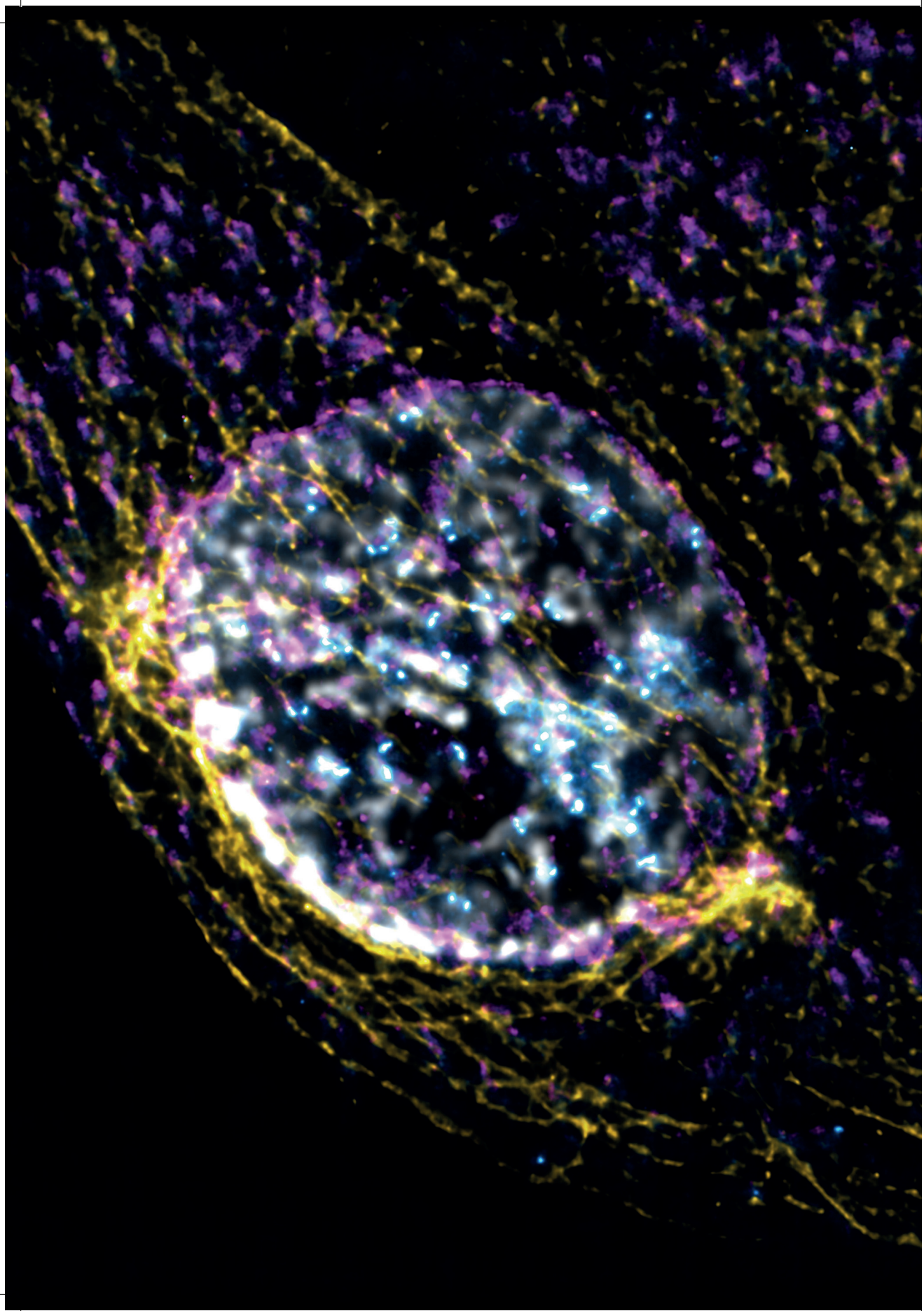

Chapter 1

General introduction

Symphony of Cell Division

The biological drive of most living organisms is to transmit their genetic information to their progeny. Organisms transmit their genetic information by a stunning performance known as mitosis or cell division. During development and adulthood of multicellular organisms, innumerable cell divisions take place to create new life, facilitate growth and preserve healthy tissue homeostasis. The cell's genetic information is encoded on DNA strands that are looped around histones, forming structures known as chromosomes. In humans, each parent contributes a haploid set of 23 chromosomes to their progeny and the diploid human genome is thus composed of 46 chromosomes. When cells divide, the genetic information encoded on those 46 chromosomes is distributed equally across the two daughter cells ensuring no genetic information is lost.

Leading up to every cell division event, cells progress through successive phases to prepare for the division. These phases are collectively known as the cell cycle, and it begins in G1-phase (Gap 1), where the parental cell increases in size and prepares the instruments needed for the synthesis (S) phase (**Figure 1A**). During S-phase, the chromosomes are carefully duplicated, as are the centrosomes, required for cell division at a later phase. The duplicated chromosomes are kept together by ring-shaped cohesin complexes, forming 46 duets that each are known as a pair of sister chromatids. Following S-phase, cells enter G2-phase (Gap 2), where errors made during DNA copying are resolved and the stage is set for the final phase of the cell cycle. This final phase is known as mitosis (M-phase), where the mother cell physically splits and sister chromatids are equally segregated to the daughter cells. The newly formed daughter cells each progress to G1-phase and a consecutive cell cycle starts.

Cacophony of Cell Division

Errors in chromosome segregation can result in daughter cells that deviate in chromosome content (karyotype) from their parental cell, a cellular state known as aneuploidy. The consequences of aneuploidy are deregulation of signalling pathways[1], cellular stress[2], cell cycle arrest[3, 4] and cell death. Especially during early development, aneuploidy is lethal[5], with a few exceptions such as trisomy 21 (causing Down syndrome)[6, 7]. In adulthood, aneuploidy is mostly found associated with the diseases collectively known as cancer[8, 9]. Chromosomes can be lost or gained and even break, creating complex rearrangements[10-12]. Instability of the genome can alter expression of tumour suppressor genes and oncogenes, resulting in cell cycle deregulation and uncontrolled cell division[1, 2, 13-15]. Furthermore, cancer cells exhibit higher frequencies of chromosome missegregation[16, 17], a phenotype known as chromosomal instability (CIN). As such, in a population of cancer cells, CIN drives karyotype heterogeneity and this, combined with ongoing selection, promotes cancer cell adaptation and survival[18, 19]. To

prevent aneuploidy and CIN, progression through mitosis is carefully regulated by cell cycle checkpoints. Mutations in these checkpoint pathways can induce CIN and thus contribute to oncogenic transformation[20-22].

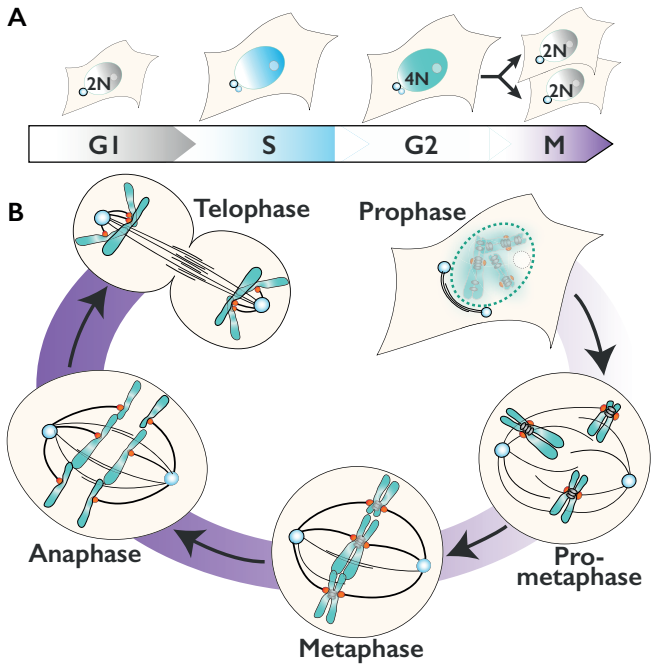

Figure 1. The symphony of cell division & the orchestration of mitosis. (**A**) The phases of the cell cycle presented in a linear course. Above each phase, a cartoon illustration of a cell in that phase is depicted. In G1 phase, the nucleus contains a diploid (2N) DNA content and the cell contains one centrosome (blue circle). In S-phase, DNA is replicated and a second centrosome is formed. During G2, the cell contains a replicated set of DNA (4N) and two centrosomes. (**B**) Five phases of mitosis. In **prophase,** microtubules (black lines) split centrosomes apart, and the nuclear envelope (dotted line around nucleus) starts to break down. Sister chromatids are held together by cohesin (grey) on arms and centromeres and chromosome condensation is initiated. In **prometaphase,** a kinetochore (red) is assembled on the centromere of each sister chromatids (green) and sister chromatids arms split as cohesin is removed. In **metaphase,** all chromosomes are bioriented at the cell equator and K-fibres generate pulling forces on kinetochores. In **anaphase,** cohesion is removed and sister chromatids are split. In **telophase**, sister chromatids are moved close to the opposing centrosomes.

Maestro of Mitosis

The cell cycle is conducted by several master regulator complexes. During each phase of the cell cycle, distinct cyclins are present to orchestrate tasks imperative to this specific phase[23, 24]. Cyclins are accompanied by an active enzymatic component, known as Cyclin-Dependent Kinases (CDKs) and cyclin/CDK complexes orchestrate cell cycle events by phosphorylating downstream substrates. The activity of cyclin/CDK complexes is tightly regulated by both inhibitory and activating pathways that together establish

a unidirectional order of the cell cycle. The expression of cyclin B1, the conductor of mitosis, is promoted by the S/G2-specific cyclin A2[25]. In G2-phase, newly synthesised cyclin B1 associates with CDK1, however the activity cyclin B1/CDK1 heterodimer complexes is actively suppressed by an inhibitory pathway[25, 26]. This suppression occurs by inhibitory phosphorylation on both cyclin B1/CDK1[27] and on CDK1-activating kinases (CAKs). Cells are ready to commence mitosis when high cyclin B1 protein levels are reached and clustering of cyclin B1/CDK1 create a local high concentration capable of overpowering the inhibitory signalling[28]. A switch-like transition between G2 and mitosis occurs as cyclin B1/CDK1 deposits activating phosphorylation on CAKs[29], further promoting its own activity. In addition, cyclin B1/CDK1 represses the inhibitory pathway by phosphorylation[30]. This enables rapid activation of cyclin B1/CDK1 and the G2/S-phase specific cyclin A2 protein is degraded, instigating the irreversible transition of G2 to mitosis[27, 31-33]. During mitosis, continuous cyclin B1/CDK1 activity is needed to orchestrates many downstream pathways that are essential for equal segregation of chromosomes to two daughter cells[34]. At the end of mitosis, cyclin B1 is targeted for degradation and by virtue of losing cyclin B1/CDK1 activity cell splitting is initiated[35].

Orchestrating Mitosis

Orchestrated by cyclin B1/CDK1 activity, cells undergo striking morphological changes at the onset of mitosis. Cells progress though mitosis in six strictly ordered phases[36] (**Figure 1B**), commencing with **prophase**. In this phase, chromosomes condense and cohesin complexes are removed from the sister chromatid arms while being preserved at centromeres, giving them their characteristic X-shape[37, 38]. In the cytoplasm, the microtubule meshwork is extensively reorganised by splitting up the duplicated centrosomes from which microtubule fibres are produced. Physically, the appearance of the cell changes to a globular form to accommodate the mitotic spindle aiding in efficient chromosome segregation[39]. The next phase is **prometaphase**, the phase in which cytoplasm and nucleus are united as nuclear envelope breakdown (NEB) occurs. In prometaphase the mitotic spindle assembles into a bipolar configuration with centrosomes emanating microtubules towards the centre of the cell. As the mitotic spindle takes shape, microtubules capture and congress chromosomes towards the equatorial plane of the cell. The forces required to move chromosomes around are generated by dynamic microtubules that can grow or shrink[40-42] and through microtubule-associated motor proteins[43, 44]. Each sister chromatid of a pair must attach to microtubules that emanate from opposite centrosomes, a configuration known as biorientation. It is only bioriented chromosomes that can support equal chromosome segregation, and thus all chromosomes must become bioriented before sister splitting is initiated. Bioriented chromosomes form a metaphase plate at the centre of the cell and only once all chromosomes have bioriented here, has the cell reached metaphase. During **metaphase**, the remaining cohesin-rings between sister chromatids are removed and cyclin B1 levels

rapidly drop. Within several minutes of losing cyclin B1/CDK1 activity, the irreversible transition from metaphase to anaphase is initiated[45]. In **anaphase**, the sister chromatids are separated and move towards opposing centrosomes by virtue of microtubule-shrinkage induced forces. This is followed by the movement of centrosomes towards the plasma membrane, further separating the sister chromatids apart. During **telophase,** the DNA decondenses as the nuclear envelope is reassembled around the chromosomes, and the mitotic spindle is disassembled. Apart from this, the morphology of the cell changes to accommodate physical separation into two cells. Physical separation in two daughter cells is finalised during **cytokinesis**, the sixth and final phase of mitosis.

Tuning Concert Pitch: Defining Kinetochore-Microtubule Attachments

After NEB, condensed sister chromatids lay scattered in the cell while assembly of the mitotic spindle is in motion. Interaction of sister chromatids with microtubules is mediated by kinetochores, intricate protein assemblies compiled on the centromeres of each sister chromatid[46]. At this stage, kinetochores start to form attachments to the spindle microtubules, initially often in the form of lateral interactions to the sides of the microtubule fibre. By means of microtubule-motor proteins, laterally attached kinetochores are first moved towards the minus ends of microtubules, embedded in the centrosomes and subsequently to the cell equator. Phases of microtubule-growth/shrinkage generate forces that preclude lateral kinetochore-attachments from stabilising. As a laterally attached kinetochore reaches the end of a microtubule fibre, the microtubule can either be released or convert into an end-on kinetochore attachment. End-on attachments can mature to resist microtubule forces, forming load-bearing kinetochore-microtubule interactions when the right conditions are met (discussed in section '*Sostenuto*' below). Equal chromosome segregation requires every chromosome to form load-bearing, mature kinetochore-microtubule attachments with a bioriented configuration. The human kinetochore has a binding capacity of 15-25 microtubules[47] which on mature bioriented kinetochores form thick snares known as kinetochore-fibres (K-fibres). Before unveiling the molecular aspects of how kinetochores bind microtubules, it is important to conceptualise the architecture of kinetochores. While often placing focus on a single core unit, it should be noted that in a more realistic representation of kinetochore architecture, many copies of this unit working in harmony compose the kinetochore.

Strings Attached: The Kinetochore Microtubule-Binding Interface

Sister chromatids are kept together at the centromeric constriction site during mitosis, which allows chromosomes to biorient and be segregated to opposite side of the cell in anaphase. Centromeres contain highly repetitive DNA (containing α-satellite repeats) on which specific histones are incorporated amongst canonical histones. Initially,

three centromere proteins (CENP-A, B and C) were identified to specifically localise to centromeres in human cells[48]. CENP-A is a component of the centromeric histone complex and epigenetically defines the location of centromeres on chromosomes. In addition to the α-satellite repeats, short 17-base pair repetitive motifs of centromeric DNA are bound by CENP-B[49]. CENP-C binds directly to CENP-A at centromeres[50, 51]. An additional 15 proteins were found at centromeres, that together with CENP-C are collectively known as Constitutive Centromere-Associated Network (CCAN) proteins. Several CCAN proteins are essential to preserve CENP-A at centromeres as CENP-A is replenished after each division to prevent catastrophic loss of the epigenetic centromere mark. The CCAN is an essential structural component of kinetochores as it additionally scaffolds the outer layer of the kinetochore which is composed of the KNL, MIS12 and NDC80 complexes (known as the KMN network) (**Figure 2A**).

The function of the KMN network is to interact directly with microtubules[52] and integrate signalling pathways that ensure proper chromosome segregation during mitosis. The MIS12 complex consists of four subunits (MIS12, DSN1, NNF1 and NSL1) and is the KMN backbone, stabilising KNL and NDC80 complexes at kinetochores. The KNL1 and NDC80 complexes are the two microtubule binding modules of the KMN network. The KNL-complex is composed of KNL1 and the stabilising subunit ZWINT1. KNL1 forms a podium for many signalling proteins that regulate the kinetochore biorientation process and duration of prometaphase (these roles of KNL1 are discussed in the section '*Fermata*' below). Additionally, KNL1 can directly bind microtubules[53], but the microtubule-binding affinity appears to be too weak to support chromosome segregation[53, 54] and the functional relevance of this feature is currently not clear.

The second microtubule-binding module of the KMN network is the NDC80 complex (NDC80-c)[55-58]. The NDC80-c is elongated in shape with a length of ±60nm[59, 60], and extends further outwards than the other KMN network components. (**Figure 2A**). The elongated shape of NDC80-c permits clustering of many NDC80-c on a confined surface. An estimate of 240 NDC80-c copies[61, 62] extends outward to create a Velcro-like surface to which multiple microtubules can bind[63]. Clustering of NDC80-c at kinetochores facilitates cooperative binding and permits formation of load-bearing attachments that are able to sustain forces generated by dynamically growing/shrinking microtubules[64-67]. NDC80-c is composed of two heterodimeric subcomplexes, the SPC24/SPC25 dimer that structurally links NDC80-c to the CCAN and MIS12 complexes[68], and the HEC1/NUF2 dimer that directly binds to microtubules via their calponin-homology (CH) domains[64, 69-71]. Apart from the CH-domain, an 80-residue long N-terminal tail exclusive to HEC1 increases the binding affinity NDC80-c to microtubules[70, 72, 73]. Perturbing this N-terminal tail's function, or any other microtubule-binding surface of NDC80-c, impairs the capacity of kinetochores to form load-bearing microtubule attachments and thus obstructs equally chromosome segregation[56-58].

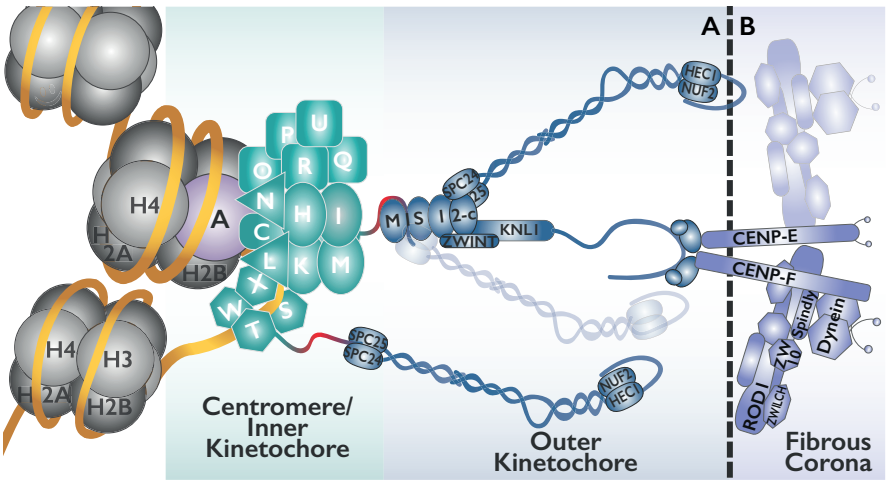

Figure 2. Centromere, kinetochore and auxiliary proteins take the stage. (**A**) Schematic model of a single repeat unit that composes the centromere and kinetochore. DNA (orange) is wrapped around canonical (Histone 3) and centromere-specific (lilac colour, CENP-A) nucleosomes. The CCAN (green, 16-subunits) composes the inner kinetochore and contacts DNA at the nucleosome-like CENP-STWX module. The two CCAN subunits CENP-C and CENP-T form the predominant connection (red tails) to the outer kinetochore (blue). The outer kinetochore (KMN-network) contains many additional signalling and MCC components that are not shown. The MIS12 complex potentially binds additional NDC80-c modules (semi-transparent NDC80-c). (**B**) Auxiliary components compose the fibrous corona which facilitates lateral attachments and chromosome-movement (CENP-E and dynein) during early mitosis. The fibrous corona extends beyond the outer kinetochore and might oligomerise (semi-transparent module), encapsulating the outer kinetochore.

Lateral attachments are mediated by auxiliary proteins of the kinetochore[74]. In the absence of microtubule attachments, kinetochores recruit and dynamically expand these auxiliary proteins to form a ring-like/crescent structure surrounding the sister kinetochores[75], called the fibrous corona[76] (**Figure 2B**). Fibrous corona proteins interact transiently with the kinetochore and facilitate chromosome movement and integration of signalling pathways imperative to biorientation[77]. The fibrous corona extents further outward from kinetochores than NDC80-c and can form a large surface to which initial microtubule attachments are established. In fact, an expanded fibrous corona promotes formation of lateral attachments, and obstructs microtubules from forming end-on attachments to NDC80-c until the corona is removed[76]. Assembly of the fibrous corona requires the RZZ-complex (ROD/ZW10/ZWILCH) which can oligomerise[76, 78, 79] and recruit the motor protein dynein[80-82] and dynein regulators CENP-F[83], Ndel1[84], NdeI[85], Lis1[86, 87], and CLIP170[88]. It is unknown why all these factors are recruited to the corona, but the dynein motor is required to remove corona components when microtubules bind to enable efficient end-on attachment to the Ndc80-c. Indeed, impairing dynein in this function blocks mitotic progression at metaphase[76, 89, 90]. The fibrous corona contains additional motor proteins such as CENP-E[43, 91, 92] and KIF2B[93], and regulators

of microtubule dynamics such as CLASPs[94] and EB1[95]. Chromosome movement towards centrosomes is directed by dynein[82], while CENP-E facilitates centrosome-to-metaphase plate congression[44]. Chromosome congression is further aided by kinetochore localisation of the microtubule-plus end tracking protein MCAK[44], and the SKAP-Astrin[96] and SKA-complexes[97-100]. The plus end-tracking properties of the SKA-complex support NDC80-c in maintaining end-on, load-bearing kinetochore-microtubule attachments[101-105].

Hitting the Right Snare: Stable Kinetochore-Microtubule Attachments

Kinetochores are not able to directly detect from which centrosome an attached microtubule originates, posing a restraint on the efficiency of chromosome biorientation. The process of biorientation is thus inherently error-prone and many intermediate configurations can precede biorientation of chromosomes (**Figure 3**)[106, 107]. When each kinetochore of a sister chromatid is bound to microtubules emanating from opposing centrosomes, a configuration known as **amphitelic** (bioriented) is reached. Early in prometaphase, centrosomes emanate many microtubules and some sister chromatids might be in close vicinity to one of the two centrosomes. The high density of spindle microtubules close to centrosomes increases the chance of forming undesired intermediate attachment configurations. By chance, only one kinetochore of a sister chromatid could form an end-on attachment to microtubules emanating from one centrosome, a configuration known as **monotelic**. Alternatively, both kinetochores could from end-on attachments to microtubules emanating from the same centrosome. This type of configuration is known as a **syntelic** attachment state. If monotelic or syntelic attachment states were to persist until anaphase, equal chromosome segregation would not occur and aneuploid daughter cells would be generated. Both monotelic and syntelic configurations cannot sustain pulling forces exerted by dynamic microtubules, making these types of attachments unstable and relatively short-lived. A more complicated configuration can occur when one kinetochore is attached to microtubules emanating from opposing centrosomes, termed merotelic attachments. **Merotelic** attachments can sustain forces generated by dynamic microtubules, and thus stable kinetochore-microtubule attachments are formed. A merotelic configuration can prevent equal chromosome segregation during anaphase if not detected.

Mitotic Metronomes: Mechanisms Ensuring Biorientation

To guard against errors in chromosome segregation, two surveillance mechanisms are active during mitosis. One such mechanism, the spindle assembly checkpoint (SAC), enables kinetochores to announce their attachment status to the whole cell and delay anaphase onset in the event that kinetochores are not attached to microtubules. The SAC composes a timer to prevent anaphase onset and ties kinetochore-attachment status to progression into anaphase. The second mechanism prevents end-on attachments from

maturing by continuously modulating the microtubule-binding affinity of the outer kinetochore. Each of these mechanisms involves careful coordination of many signalling proteins which occurs at kinetochores. Kinetochores thus not only form attachment sites for spindle microtubules, but serve as essential sensory and signalling hubs to ensure equal chromosome segregation.

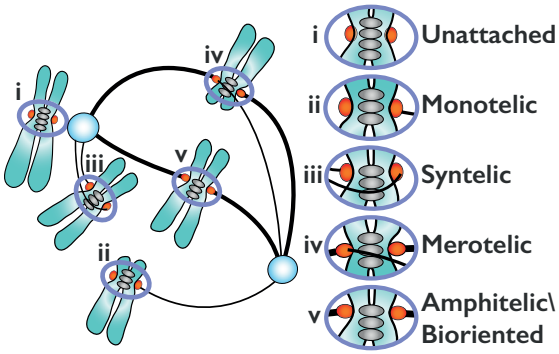

Figure 3. Hitting the right snare: chromosome biorientation. Schematic model of kinetochore-attachment configurations during mitosis, same components shown as in Figure 1. **i**) Unattached kinetochores are devoid of microtubule attachments. **ii**) In monotelic configuration, one kinetochore forms end-on microtubule-attachments. **iii**) In syntelic configuration, both kinetochores are attached to microtubules emanating from one centrosome. **iv**) In merotelic configuration, one kinetochore is attached to microtubules from both poles. **v**) In amphitelic attachments (bioriented), K-fibres generate kinetochore-tension and only this configuration supports equal segregation of sister chromatids during anaphase. The error correction pathway continuously destabilises configurations **ii-iv**, generating unattached kinetochores that can subsequently biorient when provided sufficient time. The spindle assembly checkpoint signal is generated at unattached kinetochores during prometaphase, delaying anaphase onset and permits biorientation of all chromosomes.

Sostenuto: Kinetochore Stretch & Error Correction

To sustain forces generated by microtubule-dynamics, end-on attached kinetochores undergo mechanical maturation[108, 109]. By virtue of these forces, tension is generated and, for example, the centromere (CENP-A) to outer kinetochore (HEC1) distance increases by ±30nm[110-113]. It is unclear if the mechanically exerted forces reshape the kinetochore or if the architecture of components within the kinetochore change their conformation[114]. Furthermore, the distance between sister centromeres (inter-kinetochore stretch) also increases as a result of tension in bioriented sister chromatids[113, 115]. Although currently controversial, inter- and intra-kinetochore-stretch may be essential to stabilise kinetochore-microtubule interactions and support equal chromosome segregation[114, 116-121].

In the absence of tension, the error correction pathway is active and promotes the release of microtubules by modulating the microtubule-binding affinity of outer kinetochore[119]. Upon formation of bioriented attachments, tension functions to counteract the activity of the error correction pathway, permitting maturation of bioriented attachments[122]. Merotelic attachments display inter-kinetochore stretch[119], yet

the error correction pathway detects and corrects this incorrect attachment, suggesting error correction activity is not solely regulated by inter-kinetochore stretch[120, 123-126].

The central performers in the error correction pathway form a quartet; featuring the active component Aurora B kinase[127, 128], the scaffold INCENP[129] and the regulatory members Survivin[130] and Borealin[131]. At the onset of mitosis this quartet of proteins localise to the chromosomes[132] and by prometaphase the complex is clustered at centromeres (reviewed in[133]) potentially through phase separation[134]. This complex displays additional dynamic localisation during later stages of mitosis and its name reflects the dynamic localisation: Chromosomal Passenger Complex (CPC) (reviewed by[135]). Activation of Aurora B occurs at onset of mitosis and is sustained during mitosis by CPC clustering at centromeres[136, 137]. Active Aurora B can diffuse away from centromeres, creating a gradient of activity that reaches distant substrates of Aurora B at kinetochores and beyond[54, 138, 139].

During onset of mitosis, Aurora B kinase phosphorylates several proteins to modulate the microtubule-binding affinity of the outer kinetochore. The primary substrate for Aurora B is the N-terminal tail of HEC1, where nine residues can be phosphorylated by Aurora B[72, 140, 141]. In the dephosphorylated state, the HEC1 tail is positively charged and together with additional positively charged residues in the HEC1/NUF2 CH-domains creates a high affinity module for the negatively charged isoelectric surface of microtubules[70, 73]. Phosphorylation of the HEC1-tail by Aurora B neutralises the positively charged tail and thereby reduces its affinity for microtubules[142]. Preventing HEC1 tail phosphorylation by mutating the phospho-residues to alanine results in hyper-stable microtubule-binding and failure of many chromosomes to biorient[72, 73]. Conversely, mutating these same residues to mimic phosphorylation impairs formation of stable kinetochore-microtubule attachments[72, 73]. This shows that modulating HEC1-tail phosphorylation by Aurora B is an important regulatory mechanism for forming stable end-on attachments.

HEC1 phosphorylation is dynamic: shortly after NEB the tail is highly phosphorylated and formation of end-on attachments strongly reduces phosphorylation[142]. Furthermore, inducing loss of kinetochore–microtubule attachments in prometaphase does not fully restore HEC1 phosphorylation to levels observed before NEB[142]. These observations suggest that Aurora B activity is counteracted during prometaphase. Indeed, kinetochores were found to recruit protein phosphatases 1 (PP1) and PP2A-B56 (B56) to kinetochores in prometaphase and both were implicated in regulating Aurora B activity[142-149]. Perturbing localisation or activity of either PP1 or B56 prevents formation of stable kinetochore microtubule attachments[143, 146, 150, 151]. Similarly, tethering Aurora B to the outer kinetochore to locally increase its activity prevented formation of stable attachments[139]. This demonstrates that Aurora B activity must be muffled to allow stable end-on attachments to be formed.

Two current models propose how Aurora B distinguishes between correct

(amphitelic) and incorrect (syntelic or merotelic kinetochore-microtubule attachment. One model posits that upon biorientation, as a result of either inter- or intra-kinetochore-stretch, Aurora B substrates are physically distanced from centromeric Aurora B activity[139, 152, 153]. Initial evidence comes from investigating the spatiotemporal activity of Aurora B using a Förster Resonance Energy Transfer (FRET-) biosensor specific for Aurora B[154]. This sensor reports on the local activity of Aurora B and when placed at outer kinetochores it was observed that microtubule-attachments reduced but did not fully switch off Aurora B activity[54, 138, 139]. Only bioriented kinetochores that were under tension lost all detectable Aurora B activity while Aurora B activity at the centromere in this condition was unaffected[54, 138, 139]. Furthermore, outer kinetochore substrates of Aurora B appear to be less phosphorylated than substrates closer to centromeres[54]. This spatial separation model proposes that a gradient of Aurora B originates from centromeres, reaching kinetochores only in the absence of the tension, and tension on amphitelic attachments preclude Aurora B activity. The second proposed model suggests that Aurora B activity is reduced on bioriented kinetochores as a result of reduced kinase recruitment, shifting towards phosphatase-directed dephosphorylation[155]. This model is supported by the observations that Aurora B itself localises to kinetochores but to a lesser extend when bioriented[142, 155-158]. Furthermore, centromere localisation of Aurora B was found not to be essential for its role in error correction arguing spatial separation cannot solely account for regulation of Aurora B activity by attachment states[158-160]. Both models are not mutually exclusive and possibly several proposed mechanisms regulate Aurora B in concert.

Aurora B regulates attachment stability not only via HEC1 phosphorylation, but also by regulating MCAK[161], CENP-E[162], KIF18A[163-165] SKA-complex[166] and KNL1[54, 147]. Regulation of MCAK localisation and activity by Aurora B affects microtubule stability in the vicinity of kinetochores and is important for biorientation[44, 161, 167-170]. Furthermore, Aurora B regulates the conversion of lateral to end-on attachments by CENP-E phosphorylation[77, 167] and the formation of stable end-on attachments by regulating kinetochore localisation of the SKA-complex[105, 166]. The phosphorylation of KNL1 by Aurora B regulates localisation of protein phosphatase 1 (PP1) to kinetochores by reducing PP1 binding to SSILK- and RVSF-motifs[171, 172] on KNL1[147, 173, 174]. The function of PP1 at kinetochores is unclear as both kinetochore-microtubule stabilisation and regulation of the SAC (see next paragraph) appear to be regulated by this phosphatase[162, 175]. Additional binding sites for PP1 recruitment to kinetochores are found in SKA[151], Astrin-SKAP[176], CENP-E[162] and KIF18A[164, 165, 177]. Recent work has identified numerous PP1 scaffolds to be phosphorylated by Aurora B and established Aurora B-dependent phosphorylation of PP1-binding motifs to be a recurring regulatory mechanism[178]. Aurora B may thus regulate kinetochore localisation of one of its own antagonising phosphatases.

Fermata: The SAC delays anaphase onset

The amount of time required for all sister chromatids to biorient varies per cell division due to the stochastic nature of this process. Once completed, cells rapidly progress from metaphase to anaphase by degrading key mitotic regulators, such as cyclin B1. To this end, the anaphase promoting complex/cyclosome (APC/C)[179], an E3-ubiquitin ligase complex, becomes active at metaphase. APC/C operates in conjunction with its coactivator CDC20[180-182] to recognise and ubiquitinate substrates after which these substrates are degraded by the proteasome[183-185]. The activity of the APC/C is carefully regulated to allow sufficient time for completion of biorientation and prevent anaphase onset in the presence of non-bioriented chromosomes. For this reason, the SAC halts mitotic progression in the event that kinetochores devoid of attachments are present. Unattached kinetochores operate as autonomous signalling platforms, proficient in producing the SAC signal and halting mitotic progression. These kinetochores are highly efficient in generate the SAC signal as a single kinetochore generates sufficient inhibition to prevent APC/C activation[186, 187]. Reminiscent to the workings of a rheostat, the SAC signal produced by one kinetochore is less strong than that of multiple kinetochores combined[186-189].

The physical manifestation of the SAC signal comes in the form of a soluble inhibitor known as the mitotic checkpoint complex (MCC)[190-194]. The MCC is a tetrameric complex composed of BUBR1, BUB3 and MAD2 that cooperate to bind CDC20 during mitosis[195-197]. During mitosis, APC/C is bound to CDC20 and the MCC presents itself as a pseudo-substrate, hereby blocking other substrates from being recognised[179, 190-194, 198]. APC/C can be liberated from MCC: the APC/C-subunit APC15 promotes ubiquitylation of CDC20 in MCC[198-200] and CDC20 is subsequently degraded by the proteasome[193, 198, 200-203]. As a result, CDC20 requires continuous synthesis and incorporation in newly produced MCC (**Figure 4A**).

Unattached kinetochores form receptors to cluster MCC components and catalyse the assembly of the MCC (**Figure 4B**)[187, 204, 205]. Crucial to orchestrating MCC production is the kinase MPS1 (discussed below). Kinetochore localisation of BUBR1:BUB3 is essential for MCC assembly and depends on the scaffold KNL1 and its binding partner BUB1[206-208]. The KNL1:BUB1 complex facilitates not only BUBR1 kinetochore localisation but additionally promotes localisation of CDC20 as well as MAD2[209, 210]. The latter occurs by direct binding of BUB1 to MAD1:MAD2 heterodimers that serves as a platform to activate MAD2. The activation of MAD2 occurs by inducing a conformational change from an inactive open- (O-MAD2) to an active closed-MAD2 (C-MAD2) form[211-214]. Kinetochore-MAD1 is bound to an active C-MAD2 conformer (MAD1:C-MAD2) and O-MAD2 is recruited after which the MAD1:C-MAD2 dimer functions as a template for O-MAD2 conversion to C-MAD2[215-217]. During the conversion of O-MAD2 to C-MAD2, CDC20 is bound by MAD2 and BUBR1 through several contact sites[192, 204, 216, 218]. Forming the C-MAD2-CDC20 subcomplex is the rate-limiting step in the production of MCC[216,

[219, 220]. Furthermore, perturbing MCC assembly overrides the SAC signal, resulting in APC/C activation and exit from mitosis irrespective of non-bioriented chromosomes that many exist[197, 204, 219].

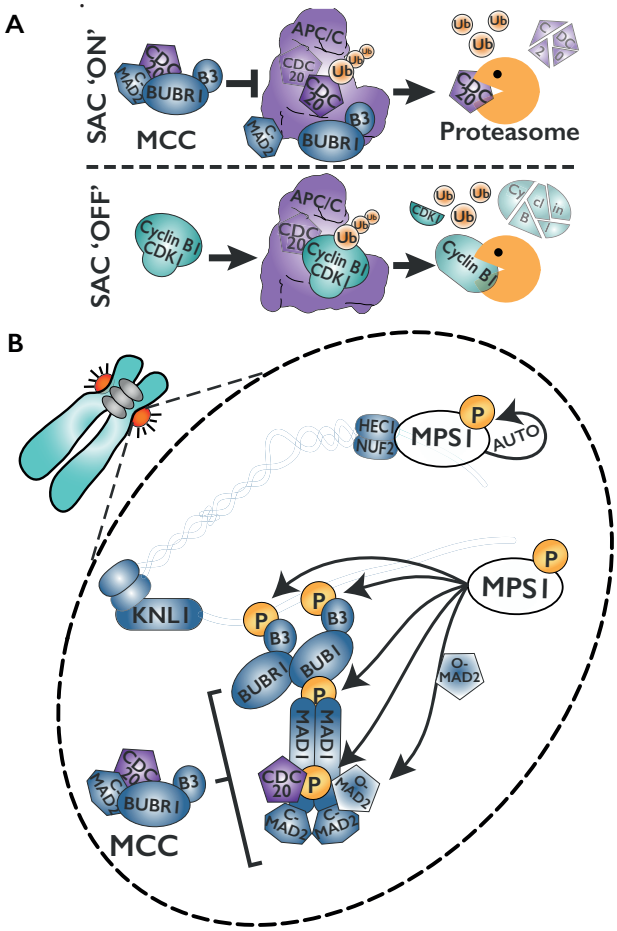

Figure 4. Function of MCC and the assembly of MCC at kinetochores. (**A**) Schematic representation of APC/C and MCC functions. In SAC 'ON', the MCC complex presents CDC20 as a substrate to APC/C and CDC20 is ubiquitinated while the other MCC components disassemble. Continuous CDC20 synthesis and MCC production are required to sustain APC/C inhibition and prevent recognition of other substrates. In SAC 'OFF', the APC/C is active and ubiquitinates cyclin B1/CDK1 (orange circle, 'Ub'). The proteasome subsequently degrades cyclin B1 and this will result in a reduction of cyclin B1/CDK1 activity and mitotic exit. (**B**) Schematic overview of MCC catalysis at an unattached kinetochore. The outer kinetochore components HEC1/NUF2 scaffold MPS1, the orchestrator of the SAC signal. MPS1 trans-autoactivates (T-loop phosphorylation, yellow circle, 'P') and rapid dissociates creating a gradient (diffuse blue colour) of MPS1 activity (see **Chapter 4**). A cascade of MPS1-directed phosphorylations follow, starting with KNL1 MELT-motifs to sequester BUB3:BUBR1 and BUB3:BUB1 complexes. This cascade continues with the phosphorylation of BUB1 to recruit the MAD1:C-MAD2 hetero-dimer and the subsequent phosphorylation of MAD1 to then promote CDC20 binding. MAD1:C-MAD2 binds an inactive O-MAD2 (promoted by MPS1) and the close proximity of CDC20 allows C-MAD2:CDC20 dimer formation. Assembled MCC complexes dissociate from the kinetochore to inhibit cytosolic APC/C complexes.

While during mitosis kinetochores facilitate the catalysis of MCC, mounting evidence suggests that a pool of interphase MCC is generated to support cyclin B1 accumulation in G2-phase[221-224]. During interphase, the MAD1:MAD2 complexes are bound to the nuclear pore protein TPR[225-227] and removal of MAD1:MAD2 from nuclear pores reduced G2-phase cyclin B1 levels, perturbing mitotic chromosome segregation[221].

Cadenza: Repertoire of MPS1 kinase functions

The virtuoso for generating the SAC signal from kinetochores is the kinase Monopolar Spindle 1 (MPS1). MCC assembly is facilitated by MPS1 kinase, which orchestrates recruitment of MCC components to kinetochores and promotes MAD2 conformational activation (**Figure 4B**). Recent work proposed that at onset of mitosis, MAD1 phosphorylation by MPS1 releases the MAD1:MAD2 complex from the nuclear pore, a prerequisite for bringing MAD1:MAD2 to kinetochores[228]. At the same time, MPS1 phosphorylation of KNL1 on TxxΩ-, MELT-, and SHT-motifs drives the recruitment of BUB3:BUB1 and BUB3:BUBR1 complexes[208, 229-233]. MPS1 subsequently phosphorylates BUB1 on multiple sites to initiate MAD1:MAD2[234-237] and CDC20[235, 238] recruitment. Additionally, MPS1-dependent recruitment of RZZ[76, 79, 239, 240] forms a second receptor for MAD1:MAD2[79, 241-243] enhancing SAC signalling at kinetochores[79, 242, 243]. Lastly, recent work identified MAD1 as a receptor for cyclin B1/CDK1 at kinetochores and this interaction enhances SAC signalling[244-247]. MPS1 thus also indirectly recruits cyclin B1/CDK1 to kinetochores to strengthening the SAC signal, but the mechanisms by which cyclin B1/CDK1 impacts the SAC are not fully understood yet. In conclusion, MPS1 activity is indispensable for establishing and maintaining the SAC signal and inhibiting MPS1 kinase rapidly exterminates it, resulting in chromosome segregation errors[248-253].

MPS1 protein kinase contains an N-terminal extension (NTE)[254] adjoined by a tetratricopeptide (TPR) domain[255], followed by a conserved middle-region (MR) and lastly a Serine/Threonine-specific protein kinase domain[256]. At the onset of mitosis, MPS1 translocates from the cytoplasm to the nucleus[257]. The nuclear translocation of MPS1 might depend on nuclear localisation signals found in the N-terminus[258] and TPR-domain[257]. Activation of MPS1 likely occurs through dimerisation *in vivo,* which allows intermolecular autoactivation of the kinase[251, 259, 260]. Both the NTE and TPR are implicated as putative dimerisation surfaces in MPS1[255, 261]. In addition, the NTE was proposed to inhibit MPS1 kinase activity, which is relieved through autophosphorylation of this segment[262]. Several additional autophosphorylation sites have been identified[251, 259, 263] of which phosphorylation at Thr676, the kinase T-loop, is essential for full activation[*251, 259, 260*].

In the absence of kinetochore-microtubule interactions, MPS1 binds the outer kinetochore proteins HEC1/NUF2[69, 248, 264]. The molecular binding site of MPS1 on HEC1/NUF2 was recently resolved and shown to be located on the CH-domains of both

HEC1 and NUF2[265, 266]. Phosphorylation of the NTE by MPS1 is required for binding to HEC1/NUF2, and the TPR-domain in MPS1 contributes separately to promote its kinetochore localisation[265]. In addition, the CDK1-mediated phosphorylation of MPS1 on Ser281 in the MR region was found to enhance MPS1 binding to NUF2[266-268]. Recent work has demonstrated that MPS1 localisation to kinetochores also requires binding to ARHGEF17[269]. It is unclear how MPS1 and ARHGEF17 molecularly interact and how this contributes to MPS1 kinetochore localisation. Regardless, kinetochore localisation of MPS1 is essential for SAC signalling: removal of either HEC1 or ARHGEF17 prevents MPS1 activation and impairs SAC signalling[269, 270], and this can be rescued by ectopic localisation of MPS1 to kinetochores[270] or centromeres[269]. Based on the observation that induced clustering of KNL1 and MPS1 in the cytoplasm can elicit a SAC signal[271], a current model for the requirement of the kinetochore is that it functions mainly as a scaffold for clustering the key SAC components.

While MPS1 principally acts to establish and maintain the SAC, additional functions during interphase and mitosis have been found (**Figure 5**). In interphase, MPS1 localises to the cytoplasm, and associates with centrosomes[250, 272]. In budding yeast, MPS1 was originally identified as a regulator of spindle pole body duplication[273]. The regulation of centrosome duplication by MPS1 might be conserved in humans[250, 274], although remains controversial[248, 253, 274]. In human cells, overexpression of MPS1 can induce centrosome reduplication although the efficient proteasomal degradation of MPS1 at the centrosome makes detection of this function in some cell types difficult[272] (reviewed in[275]). In addition to a potential role in the centrosome cycle, MPS1 was also found to localise to nuclear pore complexes in interphase cells[276]. As MAD1:MAD2 resides at nuclear pores, it was proposed that MPS1 might regulate interphase MCC production[221, 277]. Another possible role for MPS1 at nuclear pores is to stimulate disassociation of MAD1:MAD2 from nuclear pores, a prerequisite for kinetochore localisation of this complex[245].

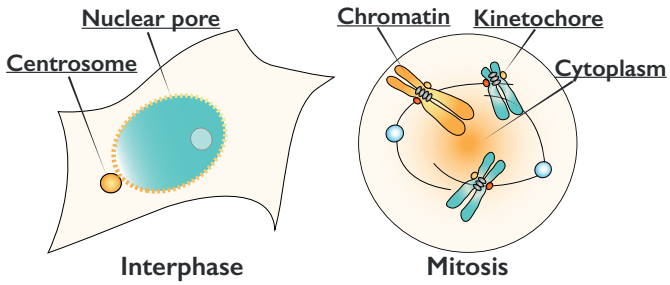

Figure 5. Repertoire of MPS1 functions during the cell cycle. Localisation of either MPS1 kinase or its substrates during the cell cycle, indicated by gold colouring. In interphase, MPS1 localises to centrosomes where it regulates centrosome duplication. Furthermore, MPS1 localises to the nuclear pores during this phase. In mitosis, MPS1 phosphorylates a condensin subunit at chromatin and MPS1 has several substrates at kinetochores (see **Figure 4**) to generate the SAC signal and orchestrate chromosome biorientation. During prometaphase, active MPS1 is released from kinetochores and reaches the cytoplasm.

During mitosis, MPS1 regulates biorientation through several pathways. Early work demonstrated that MPS1 phosphorylates Borealin and thereby promotes efficient Aurora B activation[278]. Recent work showed that MPS1 regulates expansion of the fibrous corona[76, 79] and thus indirectly supports dynein and CENP-E in biorientation. Furthermore, CENP-E as a substrate for MPS1 *in vivo*[239] and MPS1 might regulate CENP-E motor activity[279]. This study also showed that MPS1 phosphorylates SKA3 and acts to destabilise end-on microtubule attachments[239]. Retaining high levels of MPS1 activity at kinetochores in metaphase disrupted stabilisation of end on attachment[239]. This was however not observed in instances where other methods of retaining MPS1 at kinetochores were used[254, 280].

Doppio concerto: Integrating error correction and SAC signalling

The error correction pathway and the SAC are profoundly tied as destabilisation of microtubule-attachments elicits a SAC signal from unattached kinetochores. The key players of these two signalling pathways have extensive crosstalk at centromeres/kinetochores and are regulated by a set of protein phosphatases, recently reviewed in depth[148]. This section will summarise the cross-talk between MPS1 and Aurora B kinase and the opposing phosphatases involved.

At the onset of mitosis MPS1 and Aurora B ensure their mutual rapid activation. Aurora B activity promotes the interaction of MPS1 with HEC1/NUF2[270] in part through phosphorylation of HEC1's tail[266]. Once active, MPS1 promotes the recruitment of BUB1[229] kinase to KNL1 by phosphorylation of MELT-motifs[208, 232, 233]. Kinetochore clustering of BUB1 promotes its autoactivation and BUB1 then phosphorylates histone 2A on Thr120 (H2A-pT120) at pericentromeric chromatin[281]. This mark facilitates binding of Shugoshin 1[282, 283] (Sgo1) and possibly Sgo2[284] that in turn promotes centromeric clustering of the CPC. Through MPS1, Aurora B thus promotes its own localised activity. In a parallel pathway, MPS1 phosphorylates Borealin, further enhancing CPC centromere clustering[278]. Aurora B fortifies the recruitment of BUB1 by phosphorylating KNL1 to exclude PP1 from localising to kinetochores and dephosphorylating MELT-motifs[147, 150, 229, 285]. Furthermore, Aurora B activity promotes localisation of Sgo1 and Sgo2 to centromeres[168, 286], enhancing its own centromere clustering. MPS1 and Aurora B thus mutually promote their activation through several positive feedback pathways. It is thought this elaborate network creates a fast activation switch for both essential kinases and thus ensures fast initiation of error correction and the SAC.

After NEB, the activity of MPS1 and Aurora B are counteracted by phosphatases localised to the kinetochore and centromere. Counteracting these kinases after NEB might serve to prevent hyper-phosphorylation of substrates, precluding formation of end-on attachments and persistent SAC signalling. At centromeres, both Sgo1 and Sgo2 bind pools of PP2A-B56 and this counteracts Aurora B activity during mitosis[144, 287]. It

is unclear if and how the B56 pools associated with Sgo1 and Sgo2 are regulated during mitosis. The localisation of Sgo1 is not confined to the inner centromere, as a Sgo1-kinetochore pool has been described[288] and BUBR1 might promote kinetochore Sgo1 localisation[287, 289]. At kinetochores, MPS1-directed KNL1-phosphorylation enables the localisation of BUBR1 after NEB. BUBR1 in turn, binds a pool of PP2A-B56[145, 146] which counteract both Aurora B[143, 145, 146] and MPS1[290, 291] activity. The BUBR1-B56 interaction is promoted by both CDK1 and PLK1 phosphorylation on BUBR1[146, 149, 289]. Our current understanding of how different B56 pools regulate different kinases and substrates is limited by the complex cross-talk that various pathways display. As described above, Aurora B prevents PP1 phosphatase binding to KNL1 and regulates additional PP1 pools on SKA[166, 177], Astrin-SKAP[176] and CENP-E[162]. KNL1-PP1 dephosphorylates the MELT-motifs in KNL1, displacing BUBR1-B56 from kinetochores[150]. This ensures that after initial activation of Aurora B, the activity of either MPS1 or Aurora B at outer kinetochores is dampened. The activity of MPS1 is antagonised by PP1 phosphatase and this phosphatase is essential for SAC silencing in many species[53, 150, 173, 175, 229, 292, 293]. However, recent data in human cells suggests that the BUBR1-B56 pool might antagonise MPS1 at kinetochores[294].

Many additional putative Aurora B substrates have been identified to contain RVSF-motifs, revealing Aurora B as a regulator of PP1 localisation during mitosis[178]. In *Drosophila melanogaster* the activating T-loop phosphorylation on MPS1 is a direct substrate of PP1[295], recently it was proposed that the BUBR1-B56 pool in humans regulates T-loop phosphorylation of MPS1[294]. This would suggest PLK1 and Cyclin B1 regulate MPS1 activity at kinetochores as they phosphorylate BUBR1 and sequester B56.

Al fine: Silencing the SAC signal

In response to microtubule attachments, the SAC signal output at kinetochores is reduced by multiple pathways acting collectively. The exact state of kinetochore-microtubule interactions that satisfy the SAC has been under intense debate. Satisfaction of the SAC has been ascribed to tension across sister kinetochores generated by force-producing microtubule attachments[296], or to tension within a kinetochore as a result of microtubule dynamics[110, 117]. In agreement with this, the SAC can be activated when tension is reduced by addition of a microtubule-stabilising drug at metaphase[35]. A caveat in interpreting the impact that lack-of-tension has on the SAC is that it destabilizes kinetochore-microtubule interactions, causing unattached kinetochores. A potential mechanism for the impact of tension on the SAC was proposed by observations that changes of budding yeast kinetochore architecture sets up a barrier for MPS1 to reach its substrate KNL1[297]. Alternatively, experiments in which cells entered mitosis without having produced sister chromatids showed that formation of end-on kinetochore-microtubule attachments sufficed to silence the SAC[298]. It remains unclear if tension,

changes in kinetochore-architecture, or mere end-on microtubule interactions with the kinetochore is the primary event that shuts of the SAC.

As sister chromatids biorient, the proteins that generate the SAC signal and modifications on proteins must be removed in order to silence the SAC signal and permit progression into anaphase. An important step in SAC silencing occurs with initial end-on attachment. When the HEC1/NUF2-complex binds microtubules end-on, the binding of MPS1 is obstructed[265, 266]. This directly reduces the signal input for the production of MCC complexes at kinetochores with end-on attachments. Removal of MPS1 from kinetochores is prerequisite for SAC silencing as ectopic localisation of MPS1 on kinetochores blocks cells at metaphase[280]. Downstream of MPS1, MCC components that localise to kinetochores are removed upon formation of end-on attachments. The fibrous corona is stripped by the motor complex dynein. This is mediated by the kinetochore-specific dynein adaptor Spindly[80, 81, 89, 299, 300]. Furthermore, displacing the fibrous corona from the outer kinetochore reduces MAD1:MAD2[301] and cyclin B1/CDK1[246] complexes at kinetochores. Preventing the removal of MAD1 from kinetochores elicits a SAC response on bioriented kinetochores[302], demonstrating that MAD1 removal is a prerequisite step in SAC silencing, downstream of MPS1 removal.

SAC signalling is enabled through many phosphorylation sites that are deposited by MPS1, Aurora B and cyclin B1/CDK1. Various pools of PP1 and B56 contribute to counteracting the output of these kinases and dephosphorylate their substrates[303, 304]. An important contribution to SAC substrate dephosphorylation is made by the KNL1-bound PP1 pool[173, 292] which facilitates the dephosphorylation of MELT-motifs[150]. Through this, the clustering of BUBR1 and the BUB1-MAD1 complex is alleviated. Additional pools of PP1 are recruited to end-on attached kinetochores such as the SKA-complex[177] , Astrin-SKAP[176], KIF18A[164, 165] and CENP-E[162]. It remains unclear if these pools of PP1 contribute to SAC silencing or are important for maintaining stable end-on attachments.

In addition to halting the production of MCC complexes at kinetochores, MCC complexes are rapidly disassemble to free CDC20 and initiate APC/C activation at metaphase. The APC/C-subunit APC15 destabilises C-MAD2 in the MCC, causing the release of MAD2 from MCC[198-200, 222]. This occurs in concert with p31^{comet} (p31), that structurally mimics C-MAD2, promoting C-MAD2 extraction from the MCC[223, 305-308]. Furthermore, p31 sequesters C-MAD2 to the hexameric AAA+ ATPase TRIP13[223, 305, 306, 308, 309], a machine that can alter protein conformation states. TRIP13-p31 facilitate deactivation of MAD2 to the inactive O-MAD2 conformation[222, 310-313], effectively recycling MAD2 These mechanisms are active during mitosis, and are essential for efficient APC/C activation to occur at metaphase. Perturbing the function of either APC15[198, 200] or p31[223, 307, 308] delays progression from metaphase to anaphase, demonstrating the importance of disassembling MCC complexes in alleviating APC/C inhibition.

Scope of this thesis

The research presented in this thesis aims to augment our knowledge on how the SAC operates in mitosis. Accurate regulation of the SAC is essential for ensuring that mitosis occurs without errors in chromosome segregation. We focus on two outstanding questions related to the mechanisms that contribute to SAC silencing. We explore the reversible nature of SAC silencing by controlling kinetochore-localisation of a downstream component, revealing that kinetochore-MCC production is halted primarily by removing this downstream component. Furthermore, we explore which state of chromosome-microtubule interactions suffice for satisfaction of SAC in human cells by uncoupling biorientation and error correction from maintaining stable end-on kinetochore-microtubule attachment. Lastly, we investigate the activation and dynamic regulation of the kinase MPS1 by developing a live-cell activity reporter, laying the groundwork to further understand MPS1 regulation in cells.

In **Chapter 2** we address which event at kinetochores terminally silences the SAC signal by exploring the requirement for SAC reactivation after initial silencing at metaphase has occurred. At metaphase, the SAC is fully switched off, measurable by the degradation of cyclin B1. We temporally control MAD1 kinetochore localisation by chemically induced dimerisation of FKBP-FRB to assay if tethering MAD1 to kinetochores after the SAC has been silenced is sufficient to reactivate the SAC signal. Our data shows that in cells that have instigated mitotic exit, evidenced by cyclin B1 degradation, reinstating MAD1 kinetochore-localisation reactivates the SAC within several minutes. Furthermore, we find that this SAC reactivation still depends on MPS1 kinase activity, suggesting MPS1 is not fully silenced during the metaphase-to-anaphase transition.

Chapter 3 describes our work that focusses on understanding what state of chromosome-spindle interactions satisfies the SAC in cells. In the absence of tension, kinetochore-microtubule attachments are continuously destabilised by Aurora B, and this could activate the SAC. To explore if stable end-on microtubule-attachments are sufficient to satisfy the SAC, we devised an assay to uncouple loss-of-tension from attachment stability. We prevent formation of kinetochore-tension by inducing monopolar spindles in cells. At the same time, we express a HEC1-mutant that is relieved from Aurora B-dependent attachment destabilisation. We show that stable end-on attachments in the absence of tension between kinetochores or within a kinetochore is sufficient to silence the SAC. Silencing of the SAC thus does not require significant kinetochore tension and we establish an assay to further interrogate how attachments can silence the SAC and which mechanisms contribute to SAC silencing at kinetochores.

In **Chapter 4,** we sought to answer when and where MPS1 activation occurs and how its activity is modulated during mitosis. The SAC is activated by the kinase MPS1 at onset of mitosis but our understanding of where and how MPS1 activation is regulated and subsequently modulated is limited. We designed a live cell fluorescent sensor, tuned specifically for reporting on MPS1 kinase activity. We find that MPS1 activation occurs well before nuclear envelope breakdown (NEB), concentrating in the nucleus. Activation occurs with rapid, switch-like kinetics, and in a HEC1- and Aurora B-dependent manner. We further uncover a novel role for PP2A-B56 in regulating the timing of MPS1 activation in G2-phase. Lastly, we demonstrate our MPS1 activity sensor can detect subtle deregulation of MPS1 kinase signalling in cancer cells and 3D stem cell cultures.

In **Chapter 5** we summarise our findings in a general context and discuss the implications of our results. In consideration of recent developments in the field we define open questions and specify future research directions to further complement our understanding of how SAC regulation and silencing mechanisms operate during mitosis.

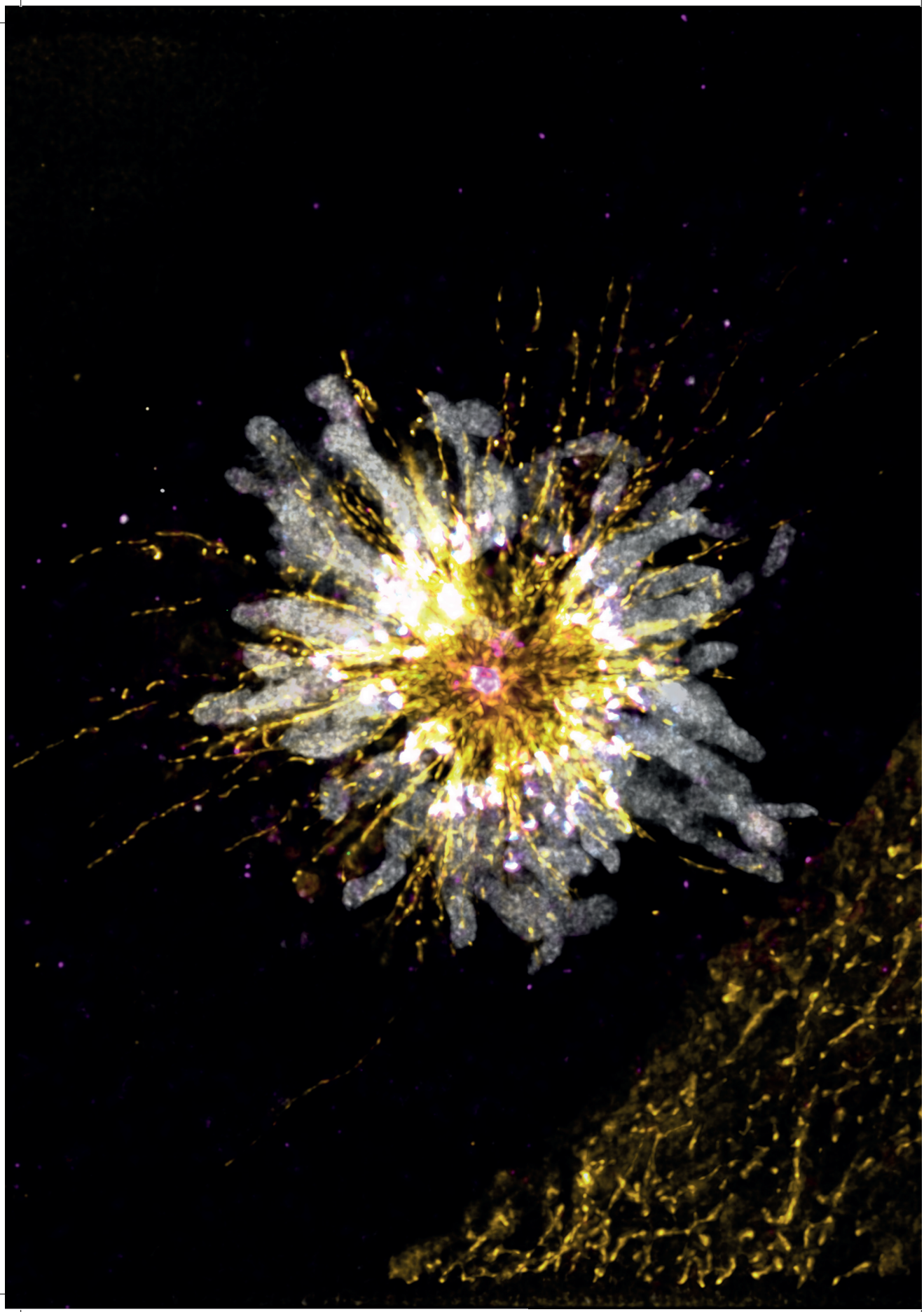

Chapter 2

Conditional targeting of MAD1 to kinetochores is sufficient to reactivate the spindle assembly checkpoint in metaphase

Timo E.F. Kuijt[1, 2], Manja Omerzu[1, 2], Adrian T. Saurin[1, 2 #], Geert J.P.L. Kops[1,2, 3]

[1]Molecular Cancer Research, [2]Center for Molecular Medicine, and [3]Cancer Genomics Netherlands, University Medical Center Utrecht, 3584 CG, Utrecht, The Netherlands.

[#] Present address: Medical Research Institute, Jacqui Wood Cancer Centre, University of Dundee, DD1 9SY Dundee, UK.

Chromosoma (2014) **123**: 471.

Abstract

Fidelity of chromosome segregation is monitored by the spindle assembly checkpoint (SAC). Key components of the SAC include MAD1, MAD2, BUB1, BUB3, BUBR1 and MPS1. These proteins accumulate on kinetochores in early prometaphase but are displaced when chromosomes attach to microtubules and/or biorient on the mitotic spindle. As a result, stable attachment of the final chromosome satisfies the SAC, permitting activation of the anaphase promoting complex/cyclosome (APC/C) and subsequent anaphase onset. SAC satisfaction is reversible however, as addition of taxol during metaphase stops cyclin B1 degradation by the APC/C. We now show that targeting MAD1 to kinetochores during metaphase is sufficient to re-establish SAC activity after initial silencing. Using rapamycin-induced heterodimerisation of FKBP-MAD1 to FRB-MIS12 and live monitoring of cyclin B1 degradation, we show that timed relocalisation of MAD1 during metaphase can stop cyclin B1 degradation without affecting chromosome-spindle attachments. APC/C inhibition represented true SAC reactivation, as FKBP-MAD1 required an intact MAD2-interaction motif and MPS1 activity to accomplish this. Our data show that MAD1 kinetochore localisation dictates SAC activity and imply that SAC regulatory mechanisms downstream of MAD1 remain functional in metaphase.

Introduction

Whole chromosome alterations to the karyotype is hazardous to eukaryotic cells[314]. As such, a surveillance mechanism named the spindle assembly checkpoint (SAC) has evolved to protect cells from chromosome segregation errors during cell divisions. Our recent comparative genomic analysis showed that this checkpoint was likely present in the last eukaryotic common ancestor, since most protein components of the SAC can be identified in species throughout the eukaryotic tree of life[315]. The SAC monitors the state of attachment of chromosomes to microtubules of the mitotic spindle, and halts the cell cycle until all chromosomes have achieved stable biorientation. Unattached kinetochores and/or kinetochores of non-bioriented chromosomes recruit a subset of SAC components that contribute to the generation of a wait-anaphase signal[316, 317]. Central to this is the MAD1-MAD2 complex that is stably associated with unattached kinetochores[318]. MAD1-MAD2 catalyses production of an inhibitor of the anaphase-promoting complex/cyclosome (APC/C), resulting in maintenance of sister chromatid cohesion and of the mitotic state[215, 319, 320]. A current model of SAC signalling is as follows: various activities at kinetochores, including BUB1, MPS1 and Rod-ZW10-Zwilch, contribute to recruitment of the MAD1-MAD2 complex[69, 236, 240, 241, 252, 264, 277, 321-328]. This complex in turn binds soluble MAD2 molecules and converts these into a form that allows association with CDC20, an essential mitotic cofactor of the APC/C[318]. The MAD2-CDC20 complex then binds BUBR1/BUB3 and this four-subunit protein

complex, now referred to as the MCC (mitotic checkpoint complex) is directed to the APC/C[191, 192, 218, 219, 319, 329-334]. MCC-bound APC/C is incapable of poly-ubiquitinating its metaphase substrates securin and cyclin B1, at least in large part due to the actions of BUBR1, which occupies a substrate-recognition site on CDC20 and likely has additional inhibitory interactions with the APC/C[192, 203, 218, 329, 335-338].

Stable attachment of kinetochores to microtubules causes removal of SAC proteins, thereby negating their ability to generate MCC[317]. It was recently shown by Maldonado and Kapoor that removal of MAD1 is a key step in shutting down SAC signalling at kinetochores. Preventing its release after microtubule binding by tethering it to the constitutive kinetochore protein MIS12 delayed anaphase onset[302]. In agreement with this, we showed previously that similar tethering of MPS1 prevented anaphase in human cells and this coincided with persistent MAD1 localisation to attached, bioriented kinetochores[280]. While attachment of kinetochores leads to progressive weakening of SAC signalling[188], full SAC silencing awaits stable biorientation of all chromosomes. In addition to removal of MAD1 from kinetochores, such silencing requires disassembly of MCC and release of APC/C activity, followed by degradation of cyclin B1 and securin[198-200, 223, 307, 339, 340]. SAC silencing is, however, reversible. Addition of taxol to cells that had initiated cyclin B1 degradation at metaphase was able to rapidly halt further cyclin B1 degradation[35, 186]. Since taxol reduces inter-sister tension and allows a subset of kinetochore-microtubule interactions to be released[341], SAC reactivation by taxol in metaphase most likely involved full reactivation of the SAC signalling cascade in response to loss of attachment.

We set out to examine if MAD1 kinetochore binding is the determining factor in switching the SAC between the ON and OFF state. To this end, MAD1 localisation to kinetochores was temporally controlled by chemically induced heterodimerisation using the FRB-FKBP12 system[342]. Conditional targeting of MAD1 to kinetochores after metaphase and live monitoring of cyclin B1 showed that MAD1 relocalisation was sufficient to reactivate the SAC after it was initially silenced.

Results and discussion

Constitutive tethering of MAD1 to kinetochores by fusing it to the KMN network component MIS12 prevents SAC silencing in human cells[302]. To examine if MAD1 tethering to kinetochores after SAC silencing is sufficient to reactivate the SAC, we made use of the rapamycin-inducible dimerisation of FRB with FKBP12 (Fig 1A)[342]. MIS12 was fused to FRB and stably expressed in HeLa-FLP-in cells that contained a doxycycline-inducible expression cassette for either wildtype (WT) FKBP-MAD1 or a mutant version (K541/K543A) that perturbs MAD2 binding (MAD1^{AA},[213]) (Fig. 1B and S1). MIS12-FRB could be visualized by virtue of a C-terminal FLAG-tagRFP moiety, while the MAD1 proteins could be visualized via an N-terminal YFP moiety. As expected, 30 minutes of

rapamycin addition to mitotic cells caused accumulation of both FKBP-MAD1 variants on kinetochores (Fig. 1C). In the absence of rapamycin, metaphase kinetochores were devoid of FKBP-MAD1 (1C).

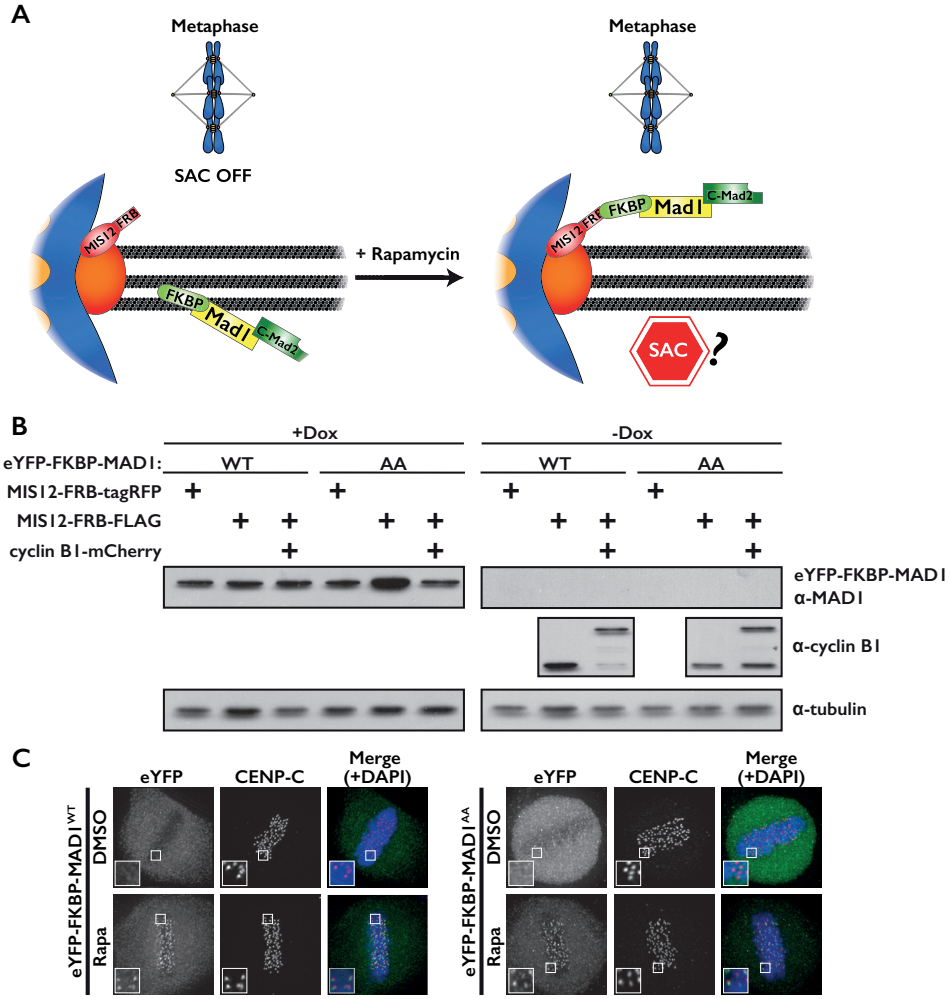

Figure 1. Conditional tethering of MAD1 to kinetochores in human cells. A) Schematic representation of the experimental system to conditionally relocalise MAD1 to kinetochores. B) Immunoblots of tubulin, cyclin B1 and eYFP-FKBP-MAD1 (anti MAD1) from mitotic lysates of various cell lines used in this study. Doxycyline (+Dox) was added sixteen hours prior to harvesting. C) Immunostainings of eYFP-FKBP-MAD1 (eYFP, detected with anti-GFP antibody) and kinetochores (CENP-C) in HeLa FLP-in cells expressing MIS12-FRB-FLAG and induced to express eYFP-FKBP-MAD1 (WT, left, or AA, right) by addition of doxycycline for 4 hours, and treated with DMSO or rapamycin (rapa) for 30 min in combination with MG132.

To verify that conditional tethering of MAD1 to kinetochores could delay anaphase onset like previously shown for direct fusion of MAD1 to MIS12[302], we added rapamycin to a population of cells in G2 phase and monitored mitotic progression by live

cell differential interference contrast (DIC) imaging. As shown in Fig 2A, progression through mitosis was delayed when cells expressing MIS12-FRB and FKBP-MAD1^{WT} were treated with rapamycin. In contrast, mitotic progression occurred with normal timing in the absence of rapamycin (Fig 2A, DMSO) or when rapamycin was added to cells expressing the FKBP-MAD1^{AA} mutant.

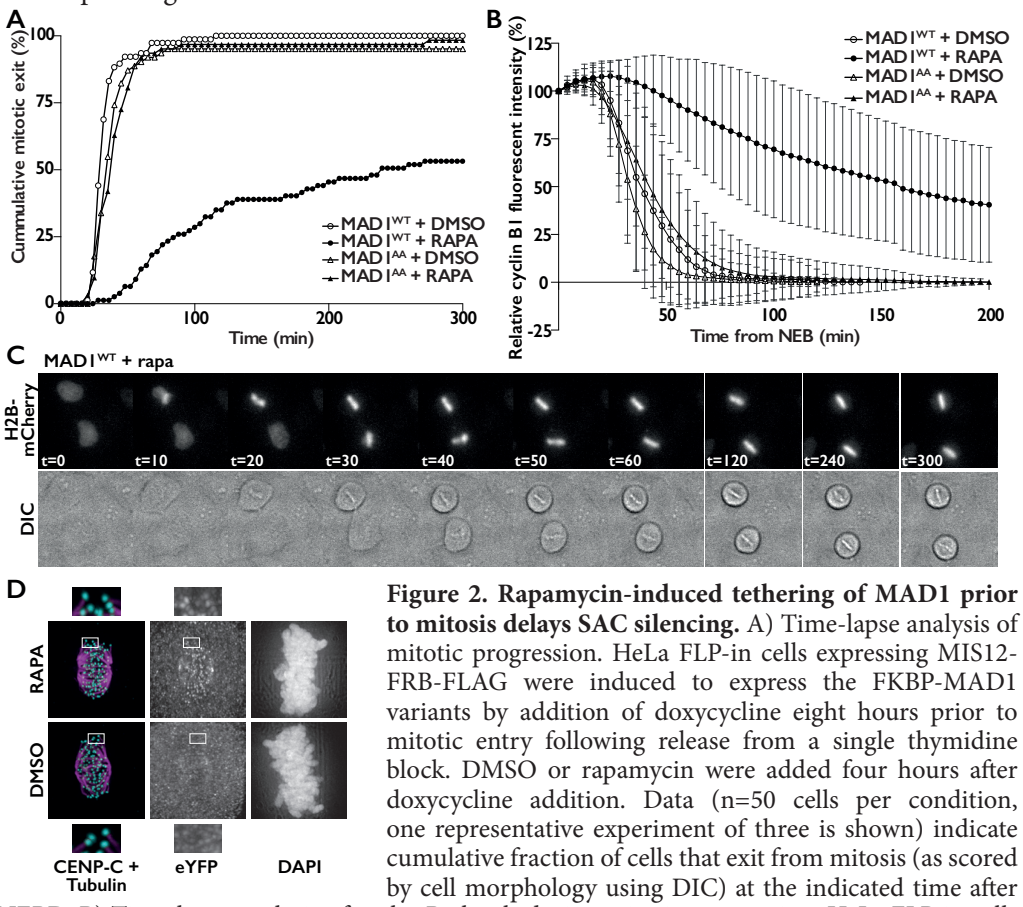

Figure 2. Rapamycin-induced tethering of MAD1 prior to mitosis delays SAC silencing. A) Time-lapse analysis of mitotic progression. HeLa FLP-in cells expressing MIS12-FRB-FLAG were induced to express the FKBP-MAD1 variants by addition of doxycycline eight hours prior to mitotic entry following release from a single thymidine block. DMSO or rapamycin were added four hours after doxycycline addition. Data (n=50 cells per condition, one representative experiment of three is shown) indicate cumulative fraction of cells that exit from mitosis (as scored by cell morphology using DIC) at the indicated time after NEBD. B) Time-lapse analysis of cyclin B1 levels during mitotic progression. HeLa FLP-in cells expressing MIS12-FRB-FLAG and cyclin B1-mCherry were induced to express the FKBP-MAD1 variants by addition of doxycycline eight hours prior to mitotic entry following release from a single thymidine block. DMSO or rapamycin was added four hours after doxycycline addition, after which cells were monitored for cyclin B1-mCherry fluorescence every 5 minutes. Data (n=40 cells per condition, one representative experiment of two is shown) represent the level of mCherry fluorescence relative to the level at NEBD. C) Time-lapse analysis of mitotic progression of FLP-in HeLa cells expressing MIS12-FRB-FLAG, induced to express FKBP-MAD1^{WT} by addition of doxycycline for eight hours following release from a single thymidine block and infected with a H2B-mCherry BacMam virus. DMSO or rapamycin were added four hours after doxycycline addition, after which cells were monitored for morphology (DIC, single plane) and chromosomes (H2B-mCherry, max projection) every 10 minutes. D) Immunostainings of cold-stable tubulin, kinetochores (CENP-C) and eYFP-FKBP-MAD1 (eYFP) of HeLa cells expressing MIS12-FRB-FLAG and eYFP-FKBP-MAD1^{WT} and treated with rapamycin (rapa) for 30 min in combination with MG132.

These finding were corroborated by monitoring the levels of cyclin B1-mCherry: degradation of cyclin B1 occurred with normal kinetics in the three control conditions but was strongly inhibited in rapamycin-treated cells expressing FKBP-MAD1^{WT} (Fig 2B). This implied that the observed mitotic delays were due to persistent inhibition of the APC/C by the SAC. SAC activity under these conditions was not due to destabilisation of kinetochore-microtubule interactions: Rapamycin-treated FKBP-MAD1^{WT} cells were able to rapidly align their chromosomes and remained arrested in mitosis without loss of metaphase plate integrity (Fig. 2C and S2) and the amount and appearance of cold-stable microtubules at metaphase were indistinguishable from control (Fig. 2D).

Thus far, our findings indicate that chemically induced targeting of MAD1 to kinetochores recapitulated published phenotypes of the constitutively kinetochore-tethered MIS12-MAD1 fusion protein[302]. To examine if MAD1 can be recruited to kinetochores in metaphase, we allowed cells to reach metaphase before adding rapamycin. To this end, cells were treated with the proteasome inhibitor MG132 for 30 minutes after which rapamycin was added for an additional 20 minutes. Live cell and immunofluorescence imaging showed that MAD1 was efficiently recruited to metaphase kinetochores under these conditions (Fig. 3A-C). Moreover, endogenous MAD2 accumulated on metaphase kinetochores of rapamycin-treated cells expressing FKBP-MAD1^{WT} (Fig. 3C).

To time the speed with which MAD1 could be recruited to kinetochores in metaphase, we followed MG132-treated cells by time-lapse imaging. Kinetochores were monitored by imaging MIS12-FRB-tagRFP and cells were determined to be in metaphase when all kinetochores had aligned on the cell's equator. Clear MAD1 kinetochore binding could be seen 10-15 minutes after addition of rapamycin to metaphase cells, as evidenced by accumulation of YFP signals to MIS12-tagRFP-positive kinetochores (Fig. 3A). This timing was comparable for the two MAD1 variants. The induced heterodimerisation was relatively slow compared to the speed with which two soluble proteins can be induced to interact, and this may be due to the geometry or microtubule occupancy of the metaphase kinetochore.

Like induced recruitment before mitosis (Fig. 1 and 2), kinetochore recruitment of MAD1 in metaphase did not affect chromosome alignment (Fig. 3B and S3), indicating that conditional targeting of MAD1 in metaphase did not perturb kinetochore-microtubule interactions. In support of this, BUB1 and BUBR1 - proteins that accumulate on kinetochores in the absence of interkinetochore tension[205, 332, 343-347] - were undetectable at metaphase kinetochores to which MAD1 was chemically recruited (Fig 3C). Together, these data show that MAD1 can be recruited within 15 minutes to metaphase kinetochores without affecting chromosome-spindle attachments. This therefore permitted examination of the direct effects of kinetochore MAD1 on SAC activity after metaphase.

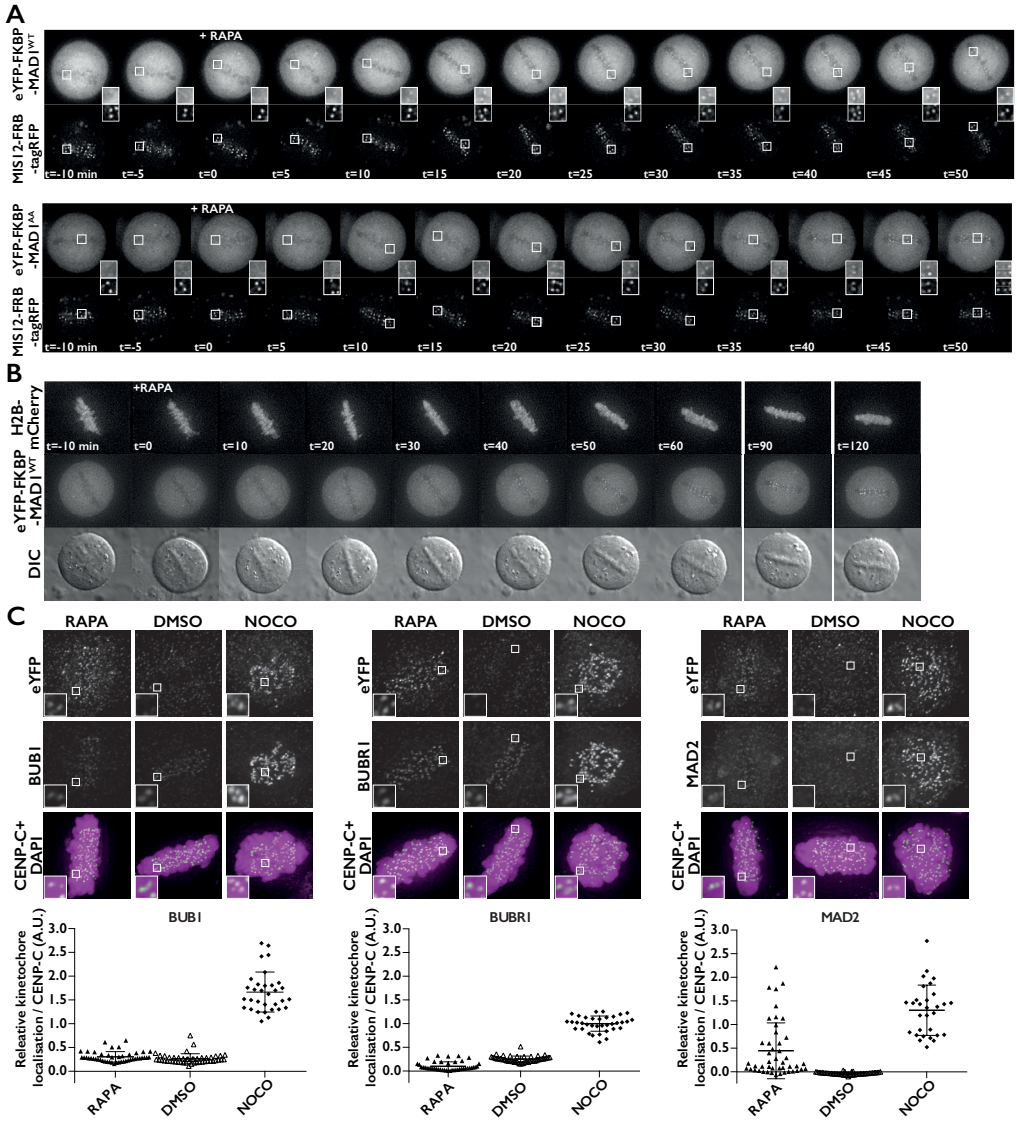

Figure 3. FRB-MAD1 can be recruited to metaphase kinetochores without affecting chromosome alignment. A, B) Time-lapse analysis of MAD1 recruitment (A) and chromosome alignment (B). HeLa FLP-in cells expressing MIS12-FRB-tagRFP (A) and MIS12-FRB-FLAG (B) were induced to express the eYFP-FKBP-MAD1 variants by addition of doxycycline for four hours. MG132 was added for 45 minutes and metaphase cells were selected for time-lapse imaging. In A) DMSO or rapamycin were added as indicated and cells were imaged 5 minutes. In B) HeLa FLP-in cells were infected with H2B-mCherry BacMam virus for 24 hours and treated as in A). Metaphase cells were selected and imaged every 10 minutes. Shown are single plane images of DIC and eYFP and max projections of H2B-mCherry. C) Upper panels: Immunostainings of BUB1 (left), BUBR1 (middle) and MAD2 (right) in combination with kinetochores (CENP-C) and eYFP-FKBP-MAD1 (eYFP) of HeLa FLP-in cells expressing MIS12-FRB-FLAG and induced to express eYFP-FKBP-MAD1^{WT} by addition of doxycycline for four and a half hours. MG132

for 30 minutes and DMSO or rapamycin were added for 20 minutes after cells had reached metaphase. Lower graphs: Quantifications of the corresponding immunostainings. Each dot represents total kinetochore intensity of a single cell (arbitrary units as a ratio over CENP-C). Averages and standard deviation are indicated.

To be certain that the SAC was silenced by the time we forced MAD1 accumulation on kinetochores, we continuously monitored cyclin B1 degradation. Rapamycin was added during the time-lapse experiment at the height of a mitotic wave in the population that occurred roughly ten hours after release from a thymidine block, when most cells were still in prometaphase. The reasoning was that in at least a fraction of the cells this would allow MAD1 to reach significant levels at kinetochores during degradation of cyclin B1 and before anaphase initiation. In all control situations (FKBP-MAD1^{WT}/DMSO, FKBP-MAD1^{AA}/DMSO and FKBP-MAD1^{AA}/rapa), cyclin B1 was degraded with comparable kinetics, and anaphase was initiated when most cyclin B1 was degraded (Fig 4). As expected, however, rapamycin addition to cells expressing FKBP-MAD1^{WT} resulted in three different outcomes. First, cyclin B1 degradation continued as normal, indicating that FKBP-MAD1^{WT} either did not efficiently target to kinetochores in these cells or that it accumulated too late to prevent anaphase onset. Second, cyclin B1 degradation never started, indicating that MAD1 was targeted before the SAC was silenced, similar to rapamycin addition before mitotic entry (Figs 1 and 2). Third, in roughly one third of the cells (a similar fraction as cells showing significant MAD2 relocalisation (Fig. 3C)), cyclin B1 degradation started but was subsequently abrogated (Fig. 4). This behaviour was never seen in any of the control situations and showed at single cell level that relocalisation of MAD1 to kinetochores was able to reactivate the SAC after it had initially been silenced. This re-establishment of the SAC nevertheless still depended on MPS1 activity as addition of the MPS1 inhibitor reversine[240] lifted the re-instated block on cyclin B1 degradation and caused cells to initiate anaphase (Fig. 4B and S4) without affecting FKBP-MAD1 levels (Fig S4). It may be of interest to note that all cells that re-stabilised cyclin B1 after rapamycin addition did so with at least 20% of cyclin B1 left. This may indicate that in this cell line a significant amount of cyclin B1 is needed to either maintain the mitotic state and/or support SAC re-activation, in agreement with recent reports[186, 348].

Our data show that forced localisation of MAD1 to metaphase kinetochores is sufficient to re-activate functional SAC signalling after initial silencing. This implies that MAD1 removal is a key step in SAC silencing. Inhibition of pathways that recruit MAD1 (e.g. MPS1, RZZ, BUB1) combined with activation of pathways that displace MAD1 (e.g. dynein, spindly, kinetochore phosphatases[89, 90, 173, 292, 293, 299, 344, 349, 350]) will thus be required to maintain the silenced state until anaphase. Key unresolved issues are the nature and spatiotemporal regulation of these pathways, and their relation to

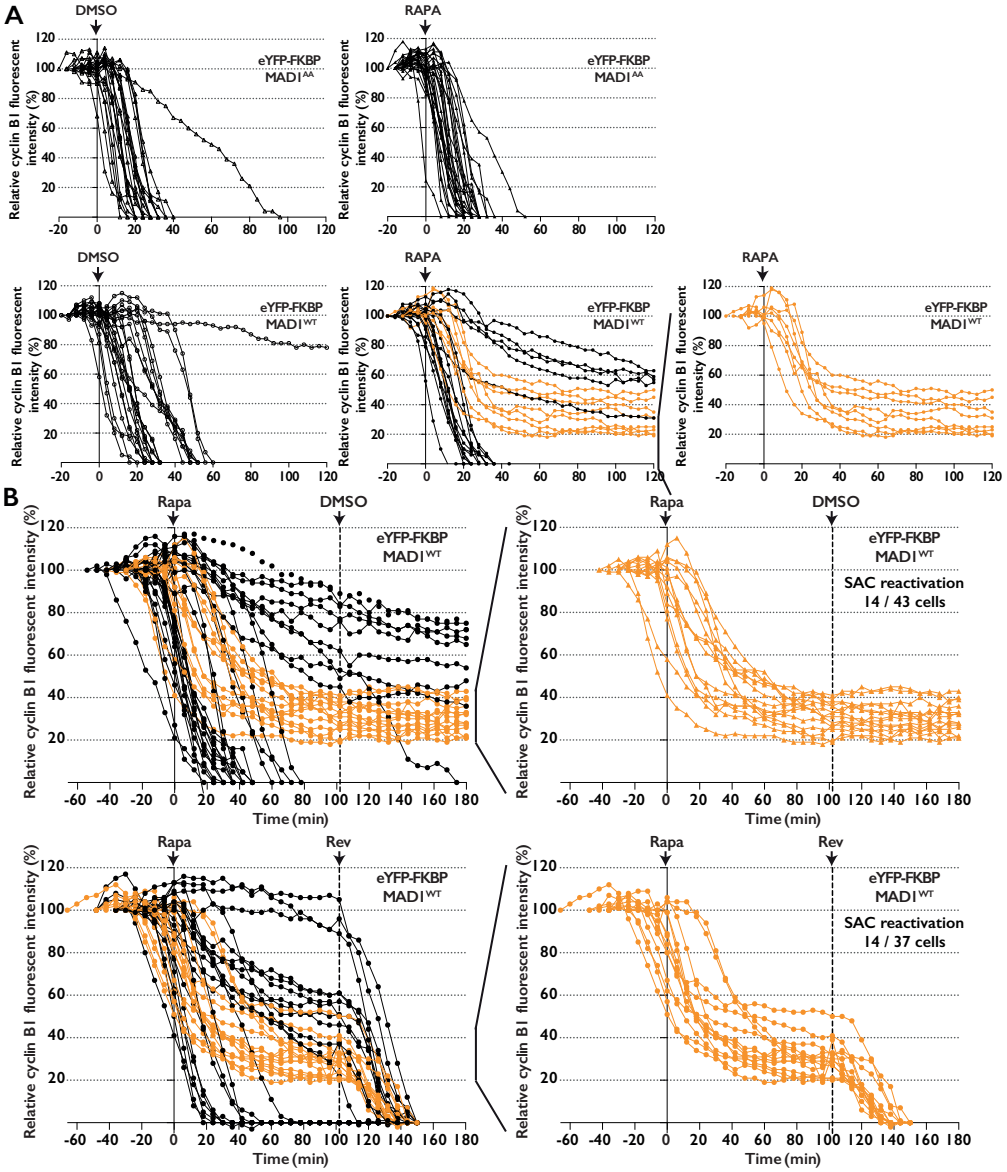

Figure 4. MAD1 recruitment to metaphase kinetochores re-activates the SAC. A, B) Time-lapse analysis of cyclin B1-mCherry. HeLa FLP-in cells expressing MIS12-FRB-FLAG and cyclin B1-mCherry were induced to express the FKBP-MAD1 variants by addition of doxycycline immediately following release from a single thymidine block and imaging started 8 hours after that. Rapamycin/DMSO were added during mitotic wave, after which cells were monitored for cyclin B1-mCherry fluorescence every 5 minutes. Fluorescent intensity on y-axis is relative to intensity at NEBD. In B, 500 nM reversine was added 102 minutes after rapamycin. In A and B, a proportion of cells showed cyclin B1 stabilisation after initial decline only in FKBP-MAD1^{WT} cells treated with rapamycin (orange traces). Those traces are also separately depicted in right graphs. Experiments were performed 4 (A) or 2 (B) times, and one representative experiment is shown in each graph.

kinetochore-microtubule interactions. An intriguing player in this is MPS1. Persistent MPS1 localisation to metaphase kinetochores causes persistent MAD1 kinetochore binding[280], so MPS1 itself needs to be removed from kinetochores at metaphase to allow MAD1 removal and SAC silencing. At the same time, MPS1 remains active and able to contribute to SAC signalling, since SAC re-activation by conditional MAD1 tethering can be reverted by the MPS1 inhibitor reversine (Fig. 4B). This implies that at least part of the SAC signalling pathways that contribute downstream of (or in parallel to) MAD1 kinetochore binding are still operational at metaphase. How some aspects of MPS1 function are maintained so as to assure SAC reactivation if required but some are repressed so as to allow MAD1 removal is an interesting challenge for further research.

Acknowledgments

We thank Stephen Taylor, Klaus Hahn, Lukas Kapitein and Susanne Lens for providing reagents, and the Kops and Lens lab members for fruitful discussions. This study was supported by funds from the European Research Council (ERC-StG KINSIGN) and the Netherlands Organisation for Scientific Research (NWO-Vici 865.12.004).

Methods

Cell culture and reagents

HeLa FLP-in cells (gift from S. Taylor, University of Manchester, England, UK) stably expressing a TetR, were cultured in DMEM (4.5 g/L glucose, Lonza) supplemented with 9% Fetal Bovin Serum (Tetracyclin-approved, Lonza), 50 μg/ml penicillin/streptomycin (Gibco) and 2 mM Ultraglutamine (Lonza). All HeLa FLP-in cell lines stably carrying doxycycline-inducible eYFP-FKBP-MAD1 constructs were transfected with pcDNA5/FRT/TO (Invitrogen) and pOG44 (Invitrogen) plasmid carrying FLP-recombinase. Selection and maintenance of stable cells was done in medium supplemented with 200 μg/ml hygromycin B (Roche) and 4 μg/ml blasticidin (PAA Laboratories). HeLa FLP-in cell lines stably expressing MIS12-FRB constructs were transfected with Fugene HD (Roche) and stable lines were selected for using 2 μg/ml puromycin (Sigma). The HeLa FLP-in cell lines expressing cyclin B1-mCherry were transfected with pcDNA3-cyclin B1-mCherry and stable cell lines were selected using 100 μg/ml Zeocin (Invivogen). The reagents thymidine (2mM), reversine (500 nM), nocodazole (830 μM), MG132 (10 μM) and doxycycline (1 μg/ml) were purchased from Sigma-Aldrich and used at final concentrations indicated. Rapamycin (100 nM) was purchased from LC-Laboratories.

Plasmids

To create pcDNA5-eYFP-FKBP-MAD1^{WT} and –MAD1^{AA} constructs, FKBP12 (a gift from

Lukas Kapitein) was PCR amplified, ligated into pcDNA5-LAP-MAD1 using HindIII sites and the sequence was verified. MIS12-FRB-tagRFP (MIS12-FRB-FLAG-tagRFP-IRES-PURO) and MIS12-FRB-FLAG (MIS12-FRB-FLAG-IRES-PURO) were constructed as follows: FRB was amplified from GFP-FRB (Gift of Klaus Hahn) and inserted into pc3-FLAG-tagRFP using EcoRI/ClaI sites to create pc3-FRB-FLAG-tagRFP. MIS12 was amplified from pcDNA3-MIS12-MPS1^{280} and inserted (AscI/NheI) into pIRES-PURO (a gift of Susanne Lens). FRB-FLAG-tagRFP was then amplified from pc3-FRB-FLAG-tagRFP and inserted (NheI/NotI) into pMIS12-IRES-PURO. pcDNA3-cyclin B1-mCherry plasmid was created by inserting a HindIII-NotI fragment of pcDNA5-cyclin B1-mCherry into pcDNA3. The neomycin selection gene of pcDNA3 was subsequently replaced with zeocin using NotI/MluI.

Immunofluorescence

HeLa FLP-in cells were plated on 12 mm round coverslips (No 1.5) and induction of eYFP-FKBP-MAD1 was done for 4.5 hours. Cells were pre-extracted using 37°C PEMT (100 mM PIPES (pH 6.8), 1 mM MgCl2, 5 mM EGTA, 0.2% Triton X-100) for 1 minute after which cells were fixed in 4% paraformaldehyde/PBS for 15 minutes. Coverslips were blocked in 3% BSA/PBS for 1 hour and primary antibody incubations were done overnight at 4°C. Coverslips were washed three times in PBS/0.1% TX-100 and subsequently incubated with secondary antibodies plus DAPI for 1 hour at room temperature. Coverslips were washed twice in PBS and mounted using ProLong Gold antifade (Molecular Probes). Image acquisition was done on a DeltaVision RT system (Applied Precision/GE Healthcare) with a 100x 1.40 numerical aperture (NA) UPlanSApo objective (Olympus) and for deconvolution SoftWorx (Applied Precision/GE Healthcare) was used. Image analysis and quantification was done using ImageJ and image preparation for figures was done using Photoshop and Illustrator CS5 (Adobe Systems). All graphs were created in Graphpad Prism 6.0d (GraphPad Software, La Jolla California USA).

The following primary antibodies were used for immunofluorescence imaging: GFP (custom rabbit polyclonal, 1:10.000), GFP (Abcam, mouse monoclonal 1:1000), BUB1 (Bethyl, A300-373A, 1:1000), BUBR1 (Bethyl, A300-386A, 1:1000), MAD2 (custom rabbit polyclonal antibody, 1:1000) and CENP-C (MBL Life Science, polyclonal Guinea pig, PD030, 1:2000). Secondary antibodies used for immunofluorescence were highly crossed absorbed anti–guinea pig Alexa Fluor 647, anti–rabbit and anti–mouse Alexa Fluor 488 and 568, anti-rat Alexa Fluor 568 (Molecular Probes).

Live cell imaging

Differential Interference Contrast (DIC) microscopy was performed on an Olympus IX81 inverted microscope equipped with a 10x 0.30 NA objective lens (Olympus) and Cell^M software. Time-lapse imaging of cells plated in a 12 well plate, was done at 37°C and 5% CO_2 concentration. Images were acquired every 5 minutes at 2x2 binning and analysis of time-lapse movies was done using ImageJ software where the time between nuclear envelope breakdown (NEBD) and

anaphase-onset was determined.
For live cell fluorescent imaging of cyclin B1-mCherry degradation above described system was used. Imaged were acquired every 5 minutes 1x1 binning (1024x1024 pixel). Sample illumination was kept to a minimum to prevent perturbing cell viability.
Live cell imaging of eYFP-FKBP-MAD1 was performed on a personal DeltaVision system (Applied Precision/GE Healthcare) equipped with a Coolsnap HQ2 CCD camera (Photometrics) and Insight solid-state illumination (Applied Precision/GE Healthcare). Images were acquired every 5 minutes using a 100x 1.4 NA UPlanSApo objective (Olympus) at 2x2 binning. 12 μm thick optical sections were acquired at 4 μm steps and YFP illumination was set to 100 ms and 50% neutral density (ND) filter, mCherry illumination was set to 150 ms and 50% ND. For H2B-mCherry live cell imaging the mCherry illumination was set to 50 ms and 50% ND. Images were deconvolved using standard settings in SoftWorx (Applied Precision/GE Healthcare). For imaging analysis Image J was used and figure preparation was done in Illustrator CS5 (Adobe).

Immunoblotting

Cells were blocked in thymidine for 20 hours and released for 16 hours in presence of nocodazole and doxycycline when indicated. Mitotic cells were collected by shake-off and cells were lysed in 2x Laemmli sample buffer. Cell lysates were boiled for 5 minutes and separated on a 10% SDS-PAGE gel. Proteins were transferred to nitrocellulose membranes and membranes were blocked in 5% milk / TBS-0.1% Tween-20 for 30 minutes. The following primary antibodies were used: anti-tubulin (clone B-5-1-2; Sigma; T5168, 1:10.000), anti-MAD1 (Fig. 1B and S1B: M-300; Santa Cruz; sc-67337 1:1000; Fig. S1A: Sigma M-8069, 1:1000) and anti-cyclin B1 (GNS1; Santa Cruz; sc-245, 1:1000). Detection of proteins was done with HRP-conjugated secondary antibodies (Bio-Rad) and chemiluminescence. Adobe Photoshop and Illustrator were used to create the figure.

Supplementary material

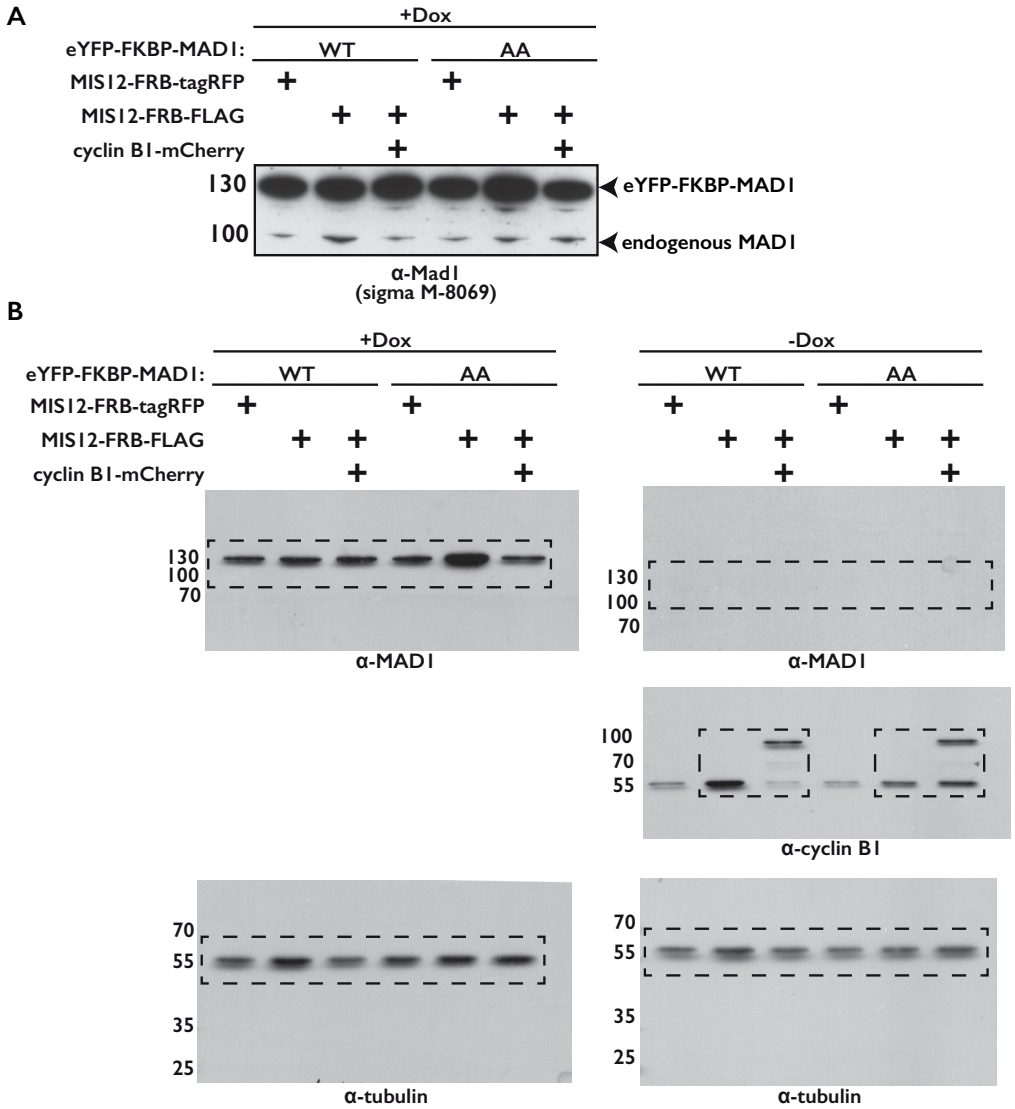

Supplemental Figure 1. Immunoblots of lysates from various FKBP-MAD1 cell lines. A) Long-exposure immunoblot of eYFP-FKBP-MAD1 (anti-MAD1, Sigma M-8069) from mitotic lysates of indicated cell lines. B) Full size immunoblots of experiment in 1B. Marks indicate crop lines used in Figure 1B. Endogenous MAD1 is not visible because of high overexpression of exogenous MAD1 and short exposure time.

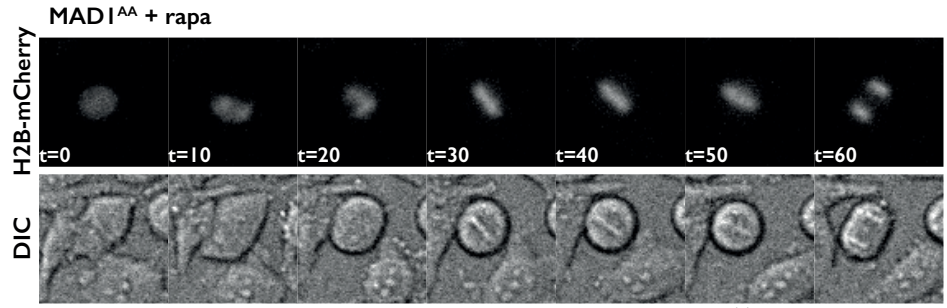

Supplemental Figure 2. Rapamycin-induced tethering of MAD1^{AA} prior to mitosis. Time-lapse analysis of mitotic progression of FLP-in HeLa cells expressing MIS12-FRB-FLAG, induced to express FKBP-MAD1^{AA} and infected with a H2B-mCherry BacMam virus 24 hours. Cells were treated as described in Figure 2A. Depicted are single plane DIC and max projection stills of H2B-mCherry.

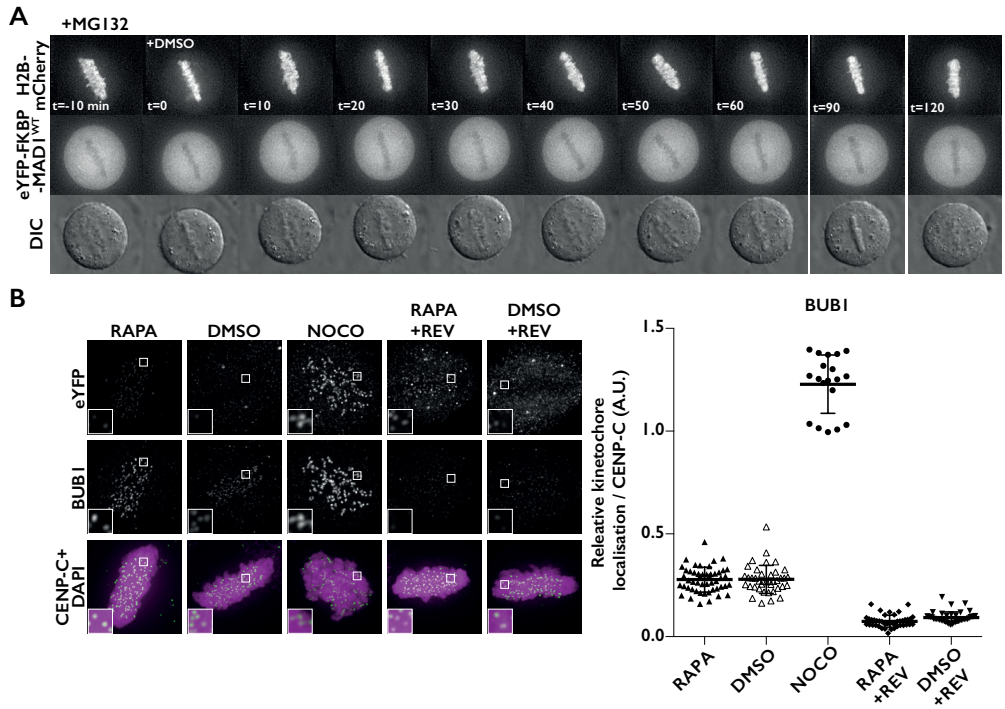

Supplemental Figure 3. FRB-MAD1 can be recruited to metaphase kinetochores without affecting chromosome alignment. A) Stills from time-lapse analysis of chromosome alignment in FKBP-MAD1^{WT} cells. Cells were treated as described in Figure 3B. B) Immunostainings of BUB1 in combination with kinetochores (CENP-C) and eYFP-FKBP-MAD1 (eYFP) of HeLa FLP-in cells expressing MIS12-FRB-FLAG and induced to express eYFP-FKBP-MAD1^{WT} by addition of doxycycline for four and a half hours. MG132 for 30 minutes and the inhibitors were added for 20 minutes after cells had reached metaphase. Addition of DMSO or rapamycin in combination with reversine was done simultaneously for 20 minutes. Graph indicates quantification of the corresponding immunostaining. Each dot represents total kinetochore intensity of a single cell (arbitrary units as a ratio over CENP-C). Averages and standard deviation are indicated.

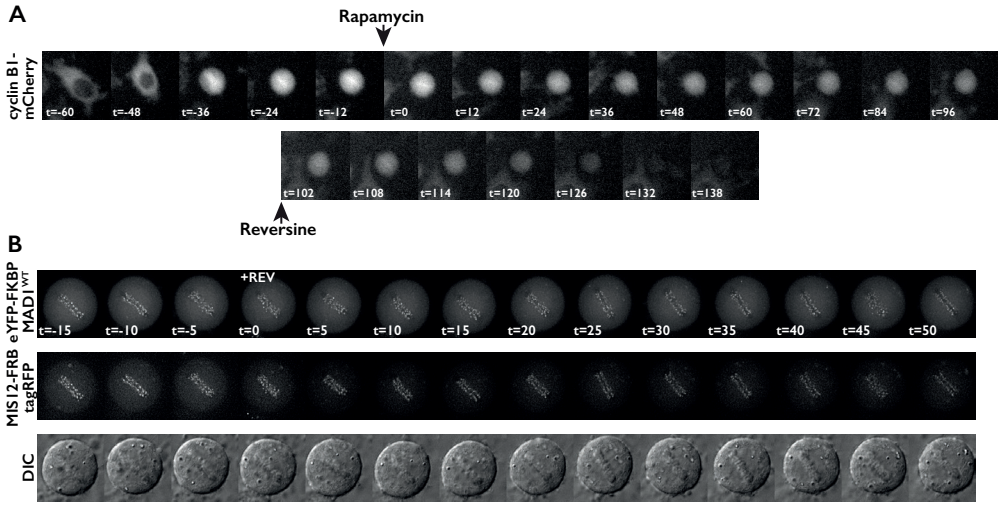

Supplemental Figure 4. MAD1 recruitment to metaphase kinetochores re-activates the SAC in an MPS1-dependent manner. A) Stills from time-lapse analysis of HeLa FLP-in cells expressing cyclin B1-mCherry and induced to express eYFP-FKBP-MAD1^{WT}. Experimental conditions are as described for Figure 4B. Indicated are the time of rapamycin addition (t=0 min) and time of 500 nM reversine addition (t=102 min). B) Stills of time-lapse analysis of FKBP-MAD1 during metaphase arrest before and after reversine addition. Cells were treated exactly as in figure 4B.

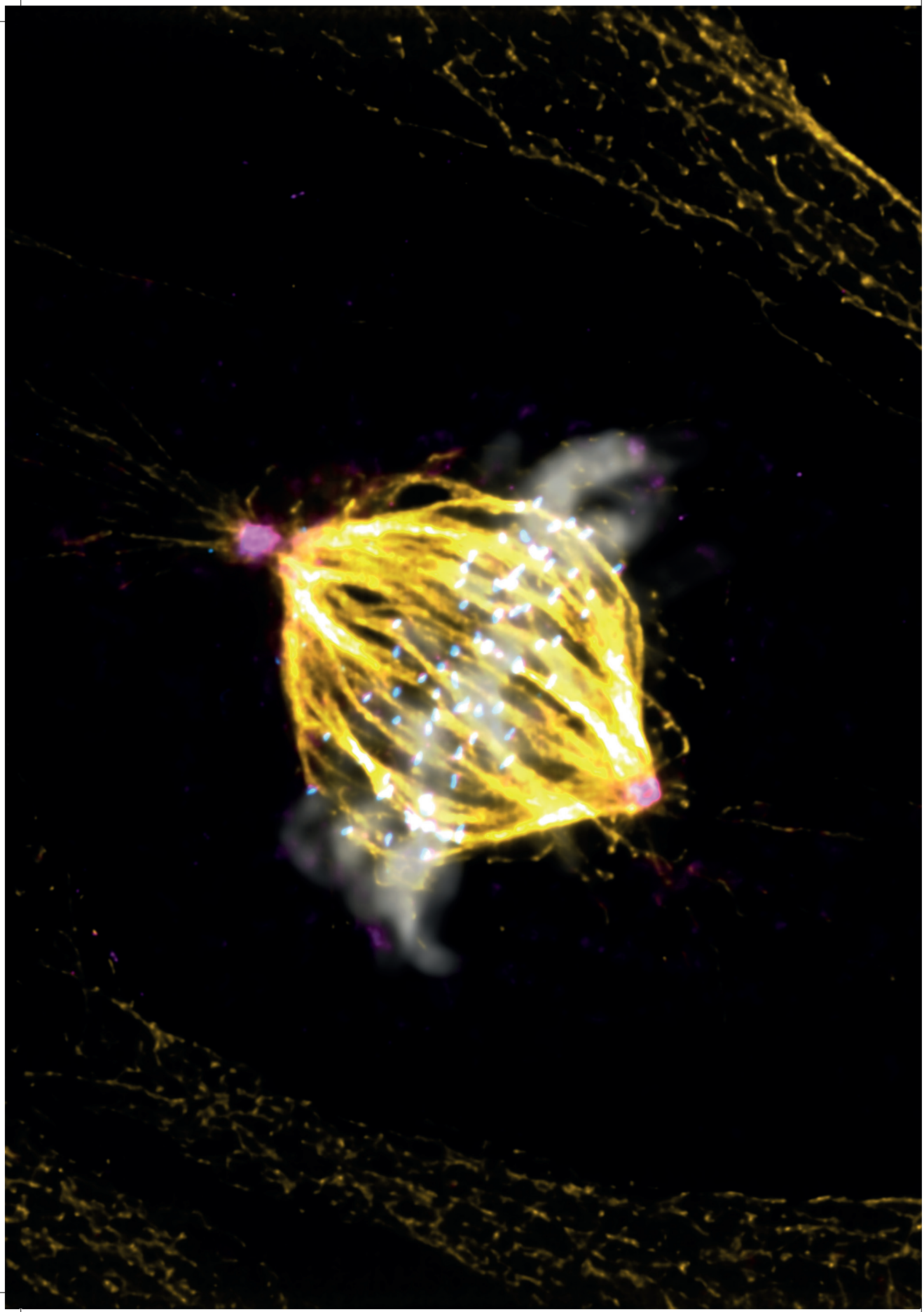

Chapter 3

Kinetochore-microtubule attachment is sufficient to satisfy the human spindle assembly checkpoint

Banafsheh Etemad[1], Timo E.F. Kuijt[1], and Geert J.P.L. Kops[1,2,3,4]

[1]Hubrecht Institute-KNAW (Royal Netherlands Academy of Arts and Sciences), Utrecht, The Netherlands, [2]Molecular Cancer Research, [3]Center for Molecular Medicine, and [4] Cancer Genomics Netherlands, University Medical Center Utrecht, Utrecht, The Netherlands.

Nature Communications (2015) **6**:8987

Summary

The spindle assembly checkpoint (SAC) is a genome surveillance mechanism that protects against aneuploidisation. Despite profound progress on understanding mechanisms of its activation, it remains unknown what aspect of chromosome-spindle interactions is monitored by the SAC: kinetochore-microtubule attachment or the force generated by dynamic microtubules that signals stable biorientation of chromosomes? To answer this, we uncoupled these two processes by expressing a non-phosphorylatable version of the main microtubule-binding protein at kinetochores (HEC1-9A), causing stabilisation of incorrect kinetochore-microtubule attachments despite persistent activity of the error-correction machinery. The SAC is fully functional in HEC1-9A-expressing cells, yet cells in which chromosomes cannot biorient but are stably attached to microtubules satisfy the SAC and exit mitosis. SAC satisfaction requires neither intra-kinetochore stretching nor dynamic microtubules. Our findings support the hypothesis that in human cells the end-on interactions of microtubules with kinetochores are sufficient to satisfy the SAC without the need for microtubule-based pulling forces.

Introduction

Error-free chromosome segregation in human cells requires prior biorientation of all chromosomes and satisfaction of the SAC[351, 352]. Despite profound insights into the molecular mechanisms of SAC signalling gained in recent years[353], a fundamental question remains unresolved: What defect in spindle assembly is 'sensed' by the SAC?: Lack of kinetochore-microtubule attachment, absence of the force generated by dynamic microtubules that signals stable biorientation of chromosomes, or both? Although various studies have addressed this[187, 298, 341, 345, 354-359] a consensus has not been reached[360-362]. This may in part be due to variations in experimental model systems and/or to approaches that have not undisputedly allowed for a way to maintain chromosome-spindle attachments while preventing biorientation, without affecting the SAC machinery. Moreover, distance between sister kinetochores ('tension') was often used as a proxy for a state of stable biorientation required to satisfy the SAC, but recent findings indicate that this may not be a valid assumption[110, 117]. These studies have inspired current models that invoke tension within a kinetochore, generated by microtubule pulling forces, as the signal that satisfies the SAC.

In human cells, iterative rounds of error-correction are required to achieve biorientation after kinetochores initially acquire microtubule connections in early prometaphase[107, 125]. Every round of correction prevents subsistence of non-bioriented kinetochores through microtubule-detachment[363]. Non-bioriented but stably attached kinetochores are therefore non-existent in human cells. The kinase Aurora B achieves error-correction by decreasing affinity for microtubules of the main microtubule-binding complex KMN at kinetochores through multi-site phosphorylation[54]. Hampering Aurora

B activity through chemical inhibition gives rise to stably attached, non-bioriented kinetochores[346] and could potentially be used to study whether the SAC is able to 'sense' lack of biorientation. However, recent evidence of direct Aurora B engagement in SAC signalling renders approaches such as these inconclusive[270, 343, 364-367]. A key target of Aurora B is the HEC1 protein that receives multiple phosphorylations in its N-terminal tail. A non-phosphorylatable HEC1 tail mutant, HEC1-9A, has an increased affinity for microtubules and causes persistent kinetochore-microtubule interactions[52, 72, 73, 368]. We thus reasoned that expression of HEC1-9A would enable the maintenance of stable attachments in the absence of biorientation without affecting kinetochore composition and signalling, and thus provide a tool to understand what state of chromosome-spindle interactions satisfy the SAC.

Results

The SAC is satisfied in HEC1-9A-expressing cells with monopolar spindles

We used our previously published HEC1 reconstitution system in which GFP-HEC1 variants are expressed from a conditional promoter in an isogenic background of HeLa-FlpIn cells[255]. This allowed equal expression of RNAi-resistant mutants in a doxycycline-inducible fashion while depleting endogenous HEC1 by siRNA (**Sup. Figure 1A and B**). A tail-deletion mutant (HEC1-Δ80) and a tail mutant containing phosphomimetic substitutions of the Aurora B phosphorylation sites (HEC1-9D) were used as controls[70, 369]. Expression of GFP-HEC1 variants after siRNA-mediated depletion of endogenous HEC1 resulted in equal levels of GFP-HEC1 at kinetochores (**Sup. Figure 1C and D**). As expected, cells expressing the HEC1 variants displayed chromosome alignment defects and segregation errors, phenotypes previously reported by others[70, 73, 142, 368, 369] (**Sup. Figure 1E and F**).

To inhibit biorientation, we prevented spindle bipolarisation by treating cells with the Eg5 inhibitor STLC[370]. As expected, STLC-treated cells expressing HEC1-WT, -9D and -Δ80 accumulated a marker for unattached chromosomes, MAD2, at their kinetochores, due to either frequent destabilisation of kinetochore-microtubule interactions by the Aurora B kinase (HEC1-WT) or inherently low affinity of kinetochores for microtubules (HEC1-9D and -Δ80) (**Figure 1A-D**). As a result, the SAC was persistently activated in these cells, as evidenced by time-lapse imaging (**Figure 1E**). In contrast, monopolar HEC1-9A-expressing cells were able to form stable kinetochore-microtubule attachments, as shown by the presence of cold-resistant microtubules (**Sup. Figure 2A, B**) and loss of MAD2 from virtually all kinetochores (**Figure 1B-D**). This was not due to diminished Aurora B activity, as various proteins that rely on Aurora B for kinetochore localisation, including MAD2, BUB1 and BUBR1[343], bound kinetochores when microtubules were depolymerized by nocodazole, with equal efficiency as HEC1-WT cells (**Figure 2A-D; Sup. Figure 4A, B**). Strikingly, the vast majority of monopolar HEC1-9A-expressing

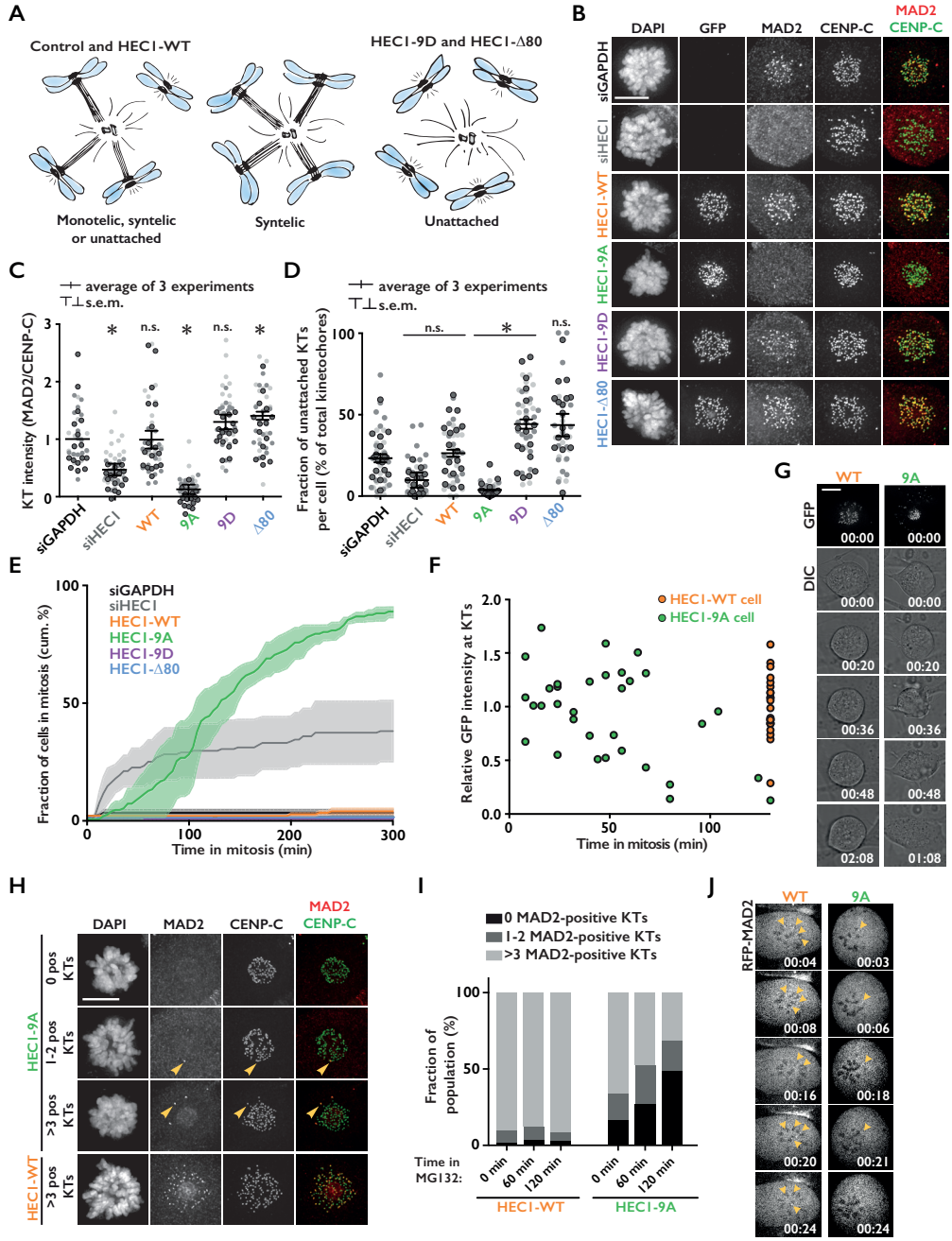

Figure 1. Monopolar HEC1-9A cells satisfy the SAC. A) Cartoons illustrating the experimental set-up that uncouples stable attachments from biorientation. Cells expressing HEC1 variants and forced to be monopolar, as a consequence of chemical inhibition of Eg5 by STLC, will have various states of kinetochore-microtubule attachments, as listed below drawings. **B, C)** Immunofluorescent labelling (B) and quantification (C) of indicated proteins in STLC-arrested cells. Cells were treated with MG132 for two hours prior to fixation. Quantification is normalized

to the kinetochore intensity of CENP-C and is the average-fold change of three experiments (± s.e.m.) normalized to the values of control cells. Each dot represents one cell. The data points of individual experiments (n = 49) are depicted in different shades of grey. Quantifications were subjected to unpaired Student's t-test against the values measured for control cells. *P < 0.01. **D**) Quantification of the number of MAD2-positive kinetochores as a percentage of the total kinetochores per cell. Conditions and representation as in (B). **E)** Time-lapse analysis of mitotic arrest in STLC-treated cells. Shown is the average of three experiments (solid lines) ± s.e.m. (transparent area). **F, G)** Time-lapse single cell analysis (F) and representative stills (G) of HEC1-WT and HEC1-9A monopolar cells. For each cell, the total GFP-kinetochore level was measured at mitotic entry, normalized against the average level measured in HEC1-WT cells and plotted in (F). Filming started approximately one hour after release from RO. 21 HEC1-WT, and 33 HEC1-9A cells were followed in two independent experiments. **H, I)** Representative images (H) and quantification (I) of the number of MAD2-positive kinetochores in HEC1-WT and -9A monopolar cells in time. Cells entered mitosis in the presence of STLC and subsequently treated with MG132 for the duration of the indicated time. Data are the average of two experiments (n = 65). Arrowheads in (H) indicate MAD2-positive kinetochores in HEC1-9A cells that point away from the centrosome and move to the periphery or out of the chromatin pack. **J)** Representative stills from live analysis of HEC1-WT and HEC1-9A expressing RFP-MAD2. Arrowheads indicate MAD2-positive kinetochores. Filming started one hour after release from RO Scale bars, 5 μm.

cells exited mitosis within hours of nuclear envelope breakdown, showing that the SAC had been satisfied in these cells (**Figure 1E**). Accordingly, phosphorylation of the SAC scaffold KNL1 on one of its MELT motifs was undetectable at kinetochores of monopolar HEC1-9A-expressing cells, illustrating diminished signalling by the critical SAC kinase MPS1 (**Sup. Figure 2C, D**), a hallmark of a silenced SAC[150]. To rule out that differences in ectopic HEC1 expression and/or HEC1 depletion, obscured in bulk analyses such as immunoblotting, could account for different SAC responses in our time-lapse experiments, we directly correlated GFP-HEC1 kinetochore levels to duration of mitosis by single cell analyses. As seen in Figure 1F and G, monopolar HEC1-9A cells exited mitosis within 100 minutes, while all cells expressing HEC1-WT at kinetochores to levels comparable to HEC1-9A remained arrested for the duration of the experiment. Moreover, expression of HEC1-9A while retaining endogenous HEC1 resulted in a similar, albeit less severe phenotype (**Sup. Figure 3A**), showing a dominant effect of HEC1-9A on SAC silencing. Similar data were obtained in non-transformed RPE-1 cells (**Sup. Figure 3B-E**).

HEC1-9A binds microtubules tighter than metaphase HEC1-WT[140, 141, 369] and this could conceivably affect SAC silencing in unnatural ways. To exclude this, we constructed cell lines expressing HEC1-8A/S15D or -8A/S55D, two recently described HEC1-8A/1D mutants that have microtubule-binding properties similar to those of HEC1-WT[140, 141, 369] but are, like HEC1-9A, refractory to Aurora B activity (**Sup. Figure 2F**). When forced to form only non-bioriented attachments, cells expressing either of these mutants exited mitosis with a rate close to that of HEC1-9A expressing cells (**Sup. Figure 2G, H**).

Although HEC1-9A cells were not significantly slower in progressing through

mitosis (**Sup. Figure 2E**), monopolar HEC1-9A cells exited more slowly than their bipolar counterparts (**Figure 1E** vs. **Sup. Figure 2E**). Analysis of the number of MAD2-positive kinetochores in monopolar HEC1-9A cells over time showed that these kinetochores progressively obtained stable attachments, and the timing of removal of MAD2 from all kinetochores correlated well with observed exit rates (**Figure 1H, I**, compare to **Figure 1E**: ~50% had exited mitosis at 120 min when ~50% of the cells had no more detectable MAD2 at their kinetochores). The relatively slow exit of monopolar HEC1-9A cells is thus likely due to slow microtubule capture, possibly because of unfavourable orientation of the unattached kinetochore of a monotelic attached pair (Arrowheads in **Figure 1H**). These results were confirmed with live imaging of single cells constitutively expressing RFP-MAD2: monopolar HEC1-WT cells maintained multiple MAD2-positive kinetochores in mitosis when filmed ~30 minutes after mitotic entry, while HEC1-9A cells had 1-2 MAD2-positive kinetochores that became gradually attached (**Figure 1J**). Together, these data show SAC silencing in cells with stably attached, non-bioriented kinetochores.

The SAC is fully proficient in HEC1-9A-expressing cells

Some recent studies hinted at a role for HEC1 tail phosphorylation in the SAC[266, 371], while others and we showed that MPS1 localisation and SAC activity are normal in cells expressing HEC1-Δ80[255, 369, 372]. We thus wished to verify that the SAC was fully functional in cells expressing HEC1-9A, especially because a weakened SAC could potentially have difficulty preventing mitotic exit when only few kinetochores are signalling. The following analyses showed that the SAC in our HEC1-9A cells was maximally proficient. First, the SAC proteins MAD2, BUBR1 and BUB1 localized at normal levels to kinetochores of nocodazole-treated cells, independent of the expressed HEC1 variant (**Figure 2A-D**; **Sup. Figure 4A, B**). Second, all cells maintained long mitotic arrests when spindle microtubules were depolymerized by nocodazole (**Figure 2E**). Third, a similar long arrest in nocodazole was maintained by all cell lines when the SAC was artificially weakened by addition of a low dose of the MPS1 inhibitor reversine, previously used by us and others to uncover subtle SAC deficiencies including those as a result of incomplete HEC1 depletion[208, 270, 364] (**Figure 2F**). Fourth, similar exit rates were observed for HEC1-WT and HEC1-9A-expressing cells after nocodazole-arrested cells were forced to exit mitosis by addition of reversine, showing that efficiency of SAC silencing was unaffected (**Figure 2G**). Finally, MAD2-positive kinetochores in STLC-treated HEC1-9A cells recruited similar levels of MAD2 as those of HEC1-WT cells (**Sup. Figure 4C, D**). Since MAD2 levels correlate with strength of the SAC signal[188], this showed HEC1-9A kinetochores are capable of maximal SAC signalling when their kinetochores are unattached. This was further supported by our previous observation that monopolar HEC1-9A cells (23/23 cells) exited mitosis only after attachment of all kinetochores (**Figure 3D**).

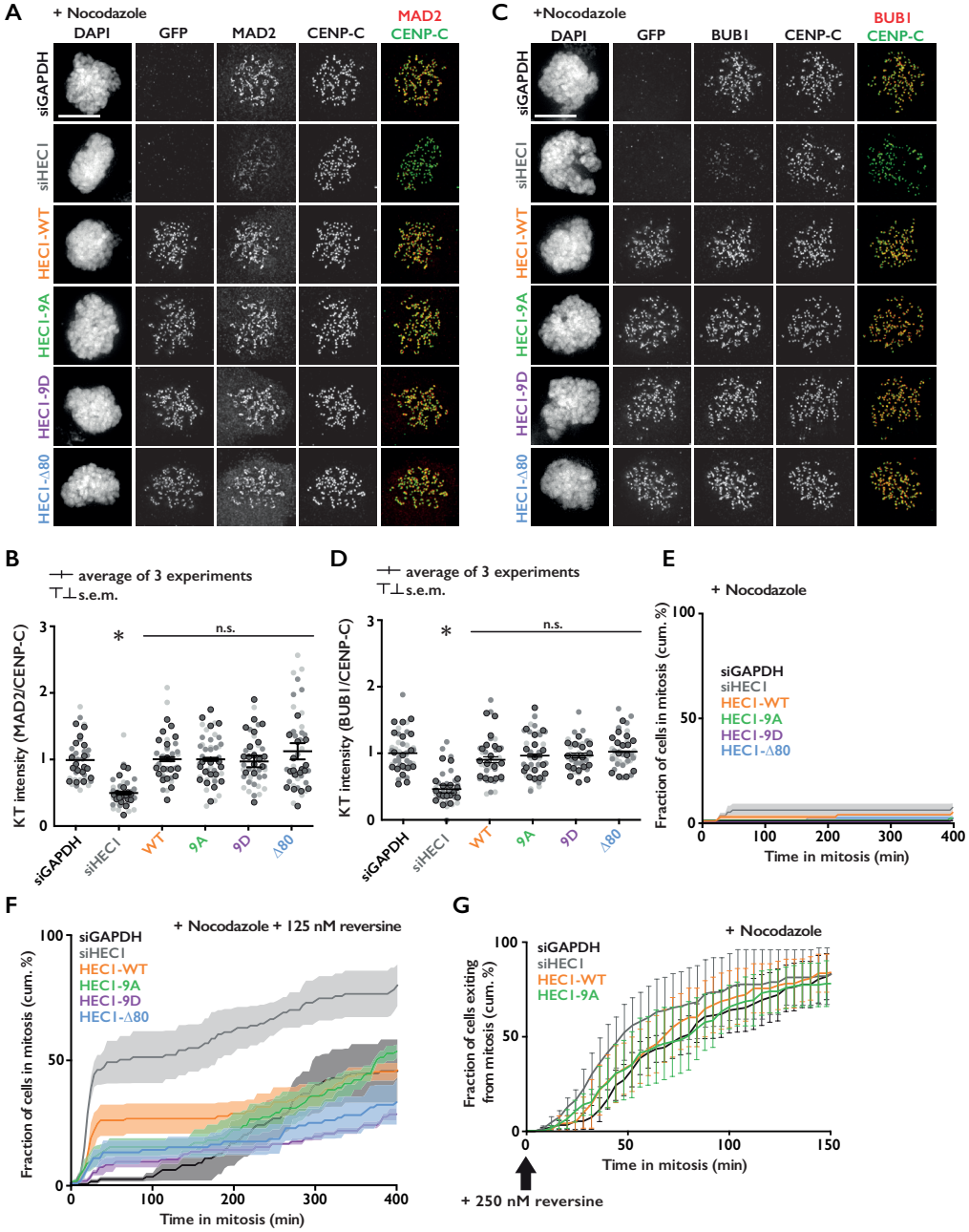

Figure 2. HEC1-9A cells have a fully functional SAC. A-D) Immunofluorescent labelling (A, C) and quantification (B, D) of indicated proteins in nocodazole-arrested HeLa cells expressing mutant versions of HEC1. Channel colours of merged images match those of the labels. Quantification is normalized to the kinetochore intensity of CENP-C and is the average fold-change of three experiments (± s.e.m.) normalized to the values of siGAPDH-transfected cells. Each dot represents one cell. The data points of three independent experiments are depicted in

different shades of grey. A total of at least 47 cells were measured per mutant in (B) and 44 in (D). For statistical analysis, an unpaired Student's *t*-test was performed against the measured values of siGAPDH-transfected cells. **P* < 0.01. **E, F)** Quantification of time-lapse analysis of duration of mitotic arrest in nocodazole-treated cells expressing HEC1 variants as indicated. Cells in (F) were treated with an additional 125 nM dose of reversine before mitotic entry. Data are the average of three experiments (solid line) ± s.e.m. (transparent area) for at least 78 cells in (E) and 81 cells in (F). **G**) Quantification of time-lapse analysis of nocodazole-arrested cells treated with an additional 250 nM dose of reversine after mitotic entry. Representation as in (E, F). At least 92 cells were followed per mutant. Scale bars, 5 μm.

No role for microtubule-based pulling forces in SAC silencing in HEC1-9A cells

Individual kinetochores deform upon microtubule attachments; the distance between inner- and outer kinetochore components increases as a result of forces imposed by dynamic microtubules[110, 112, 373] (**Figure 3A**). This phenomenon, referred to as intra-kinetochore stretching, has been correlated to mitotic exit, and as such has been put forth as the primary signal that satisfies the SAC[110, 117]. To examine if SAC silencing in monopolar HEC1-9A cells correlated with intra-kinetochore stretching, we measured the distance between the inner- and outer kinetochore in our cell lines, using antibodies against CENP-C and the N-terminus of HEC1 (GFP) (HEC1(N)) (see cartoon in **Figure 3C** and Experimental procedures section for details on method and the various technical controls). As a control, we measured the CENP-C to HEC1(N) distance of unattached chromosomes (nocodazole-treated cells) and of bioriented and congressed chromosomes (in MG132-treated cells). In agreement with published measurements[110, 373], we observed an increased distance of ~25 nm between CENP-C and HEC1(N) of both HEC1-WT and -9A-expressing cells when kinetochores of bioriented chromosomes were compared to those of unattached ones. Unexpectedly, we observed only a small, non-significant difference between CENP-C and HEC1(N) in monopolar HEC1-9A expressing cells when compared to HEC1-WT monopoles (**Figure 3B, C**), despite removal of MAD2 (**Figure 1B-D**) and SAC silencing (**Figure 1E**). Furthermore, inhibiting microtubule dynamics in monopolar cells by addition of 1 μM Taxol[110] did not prevent kinetochore-MAD2 removal and mitotic exit of the HEC1-9A cells (**Sup. Figure 5A, B**). These data show that the SAC can be satisfied without substantial intra-kinetochore stretch. We furthermore found no evidence of a role for such stretch in the efficiency of SAC silencing: monopolar HEC1-9A cells did not take significantly longer than bipolar control cells to exit mitosis after attachment of the final kinetochore (**Figure 3D**). These observations imply that microtubule attachment per se is sufficient to silence the SAC and that full intra-kinetochore stretch and pulling forces from microtubules are not a prerequisite

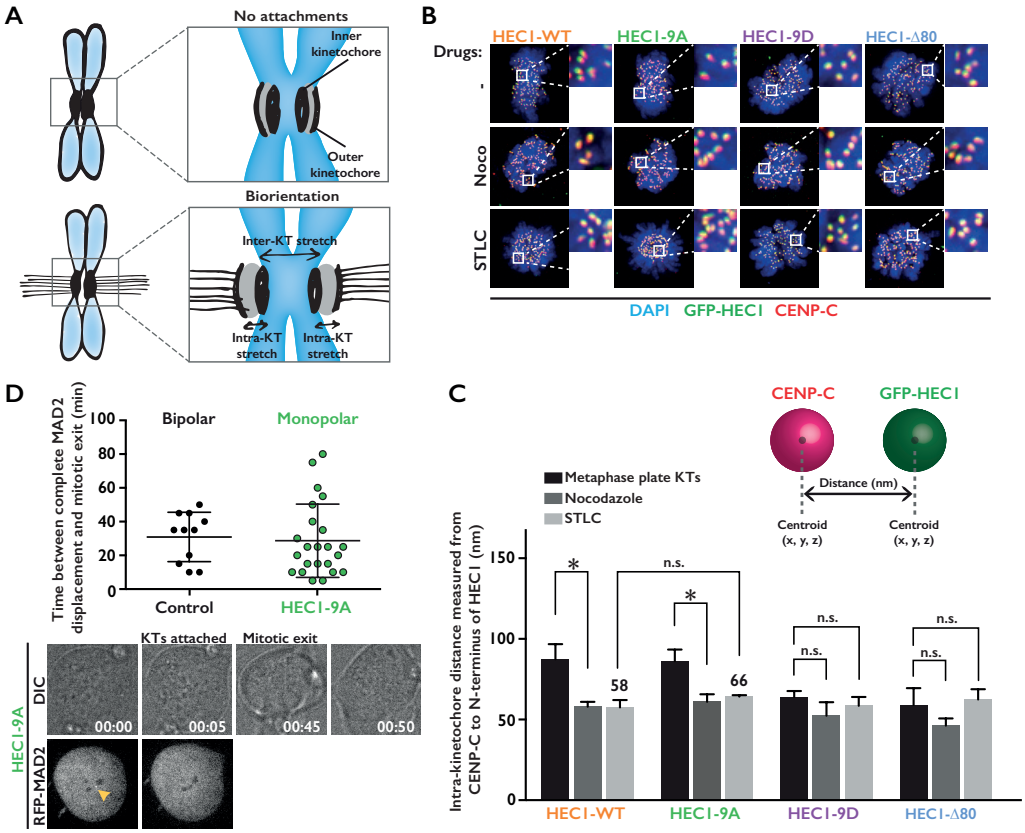

Figure 3. Intra-kinetochore stretch is reduced in HEC1-9A monopolar cells. A) Cartoons illustrating the concept of kinetochore distances in attached or unattached states. Relative to unattached chromosomes (upper drawing), sister kinetochores of bioriented chromosomes (bottom drawing) are positioned further away from one another and experience stretch within individual kinetochores. **B, C)** Representative images (B) and quantification (C; average of three experiments ± s.e.m.) of the distance between HEC1(N) and CENP-C in fixed cells (illustration in (C)). Cells were treated with nocodazole or STLC prior to mitotic entry, after which they were treated with MG132 for two hours before fixation. At least 147 kinetochores were measured for each mutant. **D)** Quantification (upper panel) and representative images (lower panel) of time-lapse single cell analysis of bipolar control cells or monopolar HEC1-9A cells expressing RFP-MAD2. Cells were released from RO and imaging was initiated after mitotic entry. Data are the average of two experiments ± s.d.

Discussion

Here we have shown that formation of stable kinetochore-microtubule attachments, irrespective of kinetochore orientation and stretching, is sufficient to satisfy the SAC in human cells. Although full intra-kinetochore stretch is not required for SAC silencing in our system, we cannot rule out that the small, statistically insignificant ~8 nm increase in the distance between CENP-C and HEC1(N) that we observed in

monopolar HEC1-9A compared to HEC1-WT is sufficient to silence the SAC or that more significant stretch occurs between proteins others than those measured. Given the presented evidence however, we favour the interpretation that stretch may not play a significant role, at least in human cells. This interpretation is perhaps not universally applicable to all eukaryotes, as putting distance between Mps1 and Spc105 was recently proposed to be a main mechanism for SAC silencing in *S. cerevisiae*[297].

What then, if any, is the role of biorientation in SAC silencing? We propose that tension, either within kinetochores or between kinetochores, promotes SAC silencing indirectly by promoting stabilisation of kinetochore-microtubule attachment[362]. Stable microtubule binding in turn inhibits SAC signalling in a number of ways. Microtubules promote Dynein-dependent stripping of Spindly and/or other SAC components[89, 90, 374], and directly displace the critical SAC kinase MPS1[265, 266]. Microtubule engagement could in addition promote biochemical changes in the kinetochore that initiate SAC silencing, such as those elicited by the SAC silencing phosphatases PP1 and PP2A-B56[150, 290]. In agreement with the possibilities that microtubules regulate the balance of kinase/phosphatase signalling at kinetochores is our observation that the PP1 target KNL1 is efficiently dephosphorylated in monopolar HEC1-9A cells. Our ability to uncouple stable attachment from biorientation now provides the tool to interrogate the various ways in which microtubules impact on the SAC signalling system.

Acknowledgements

We thank Jennifer DeLuca and Susanne Lens for reagents. We thank Jennifer DeLuca for sharing data prior to publication, and the Kops, Lens and Biggins labs for discussions. This study was supported by funds from the Netherlands Organisation for Scientific Research (NWO-Vici 865.12.004) and the Dutch Cancer Society (KWF-UU2009-4516).

Material and methods

Cell Culture and transfection. HeLa and RPE1 FlpIn cells were respectively grown in DMEM and DMEM/F12 supplemented with 8% FBS (Lonza), penicillin/streptomycin (50 μg/ml), Ultra-glutamine (Sigma; 2mM), blasticidin (4 μg/ml) and hygromycin for HeLa (200 μg/ml) or puromycin for RPE1 (1.6 μg/ml). 293Ts were grown in DMEM supplemented with 8% FBS (Lonza), penicillin/streptomycin (50 μg/ml) and Ultra-glutamine (Sigma; 2mM). Plasmids were transfected using Fugene HD (Roche) for HeLa or Lypofectamin LTX (Invitrogen) for RPE1 according to the manufacturer's instructions. To generate stably integrated HeLa and RPE1 FlpIn cell lines, pCDNA5-constructs were co-transfected with pOG44 recombinase in a 1:9 for HeLa and 1:5 ratio for RPE1[327]. Constructs were expressed by addition of 1 μg/ml doxycycline for 24h. siHEC1 (custom; Thermo Fisher Scientific; 5'-CCCUGGGUCGUGUCAGGAA-3') and siGAPDH (Thermo Fisher Scientific; D-001830-01-50) were transfected using HiPerfect (Qiagen) according to manufacturer's instructions.
Cells expressing RFP-MAD2 were obtained through lentiviral transduction and subsequent selection with puromycin (1.6 μg/ml).

Plasmids. pCDNA5-pEGFP-HEC1 constructs and cloning strategies are described in[73, 255]. For generation of stable RPEs, the HEC1 variants were subcloned to pCDNA5-pEGFPAID-puro (a kind gift from Andrew Holland[375]) with SnaBI/ApaI. tagRFP-MAD2 was PCR-ed with primers overlapping the pLV-CMV vector and inserted using the Gibson Assembly strategy[376].

Knockdown and reconstitution of HEC1. To knockdown and reconstitute HEC1 in HeLa FLpIn cell lines, cells were transfected with 120 nM HEC1 or mock siRNA for 16h after which cells were arrested in early S phase for 24h by addition of thymidine (2 mM). Subsequently, cells were released from thymidine and transfected again with 40 nM siRNA. 8-10 h after the release, cells were treated with doxycycline (1 μg/ml) and arrested for a second time in S phase for 14-16 h. Finally, cells were released from thymidine, treated with the indicated drugs (STLC at 20 μM, nocodazole at 3.3 μM, Taxol at 1 μM, reversine at 125 nM, RO at 5 μM) and used for experiments. For immunofluorescence imaging, cells were treated with proteasome-inhibitor MG132 (5 μM) for 120 minutes prior to fixation.

Live cell imaging and immunofluorescence. Live imaging of single cells and H2B-mCherry expressing cells was performed on a personal DeltaVision system (Applied Precision/GE Healthcare) equipped with a CoolSnap HQ2 CCD camera (Photometrics) and Insight solid-state illumination (Applied Precision/GE Healthcare). Cells were plated in 8-well plates (μ-Slide 8 well, Ibidi), treated as described above and imaged in a heated chamber (37°C and 5% CO^2) using a 60×/1.42 NA or 100×/1.4 NA UPlanSApo objective (Olympus) at 2×2 binning. Images were acquired every 4 minutes and deconvolved using standard settings in SoftWorx (Applied Precision/GE Healthcare) software. Multiple z layers with 0.20 μm intervals were acquired and projected to a single layer by maximum intensity projection. DIC images were single layer images.

Images for intra-kinetochore measurements were acquired with 0.10 µm intervals.
Live imaging of single cells expressing RFP-MAD2 was performed on a Leica DMI6000 Ultraview VoX Spinning Disk Microscope (PerkinElmer). Images were acquired every 3-5 minutes with a Hamamatsu Orca R2 camera using a 100x/1.4 NA objective and Velocity 3D Image Analysis Software. Multiple z layers with 1 µm intervals were acquired and DIC images were obtained as a reference.
For other live cell imaging experiments, cells were plated in 24-well plates (Corning Incorporated), and subjected to DIC microscopy on an Olympus IX81 inverted microscope equipped with a 10×/0.30 NA CPlanFLN objective lens (Olympus), Hamamatsu ORCA-ER camera and processed by Cell^M software (Olympus). The cells were kept in a heated chamber (37°C and 5% CO^2) and images were acquired every 4 minutes at 2×2 binning. For fluorescent imaging of H2B, cells were transduced 24 hours prior to imaging with Baculovirus carrying H2B-mCherry under the control of a CMV promoter.
For fixed cell immunofluorescence microscopy, cells plated on round 12-mm coverslips (No. 1.5) were pre-extracted with 37°C 0.1% Triton X-100 in PEM (100 mM Pipes (pH 6.8), 1 mM MgCl2, and 5 mM EGTA) for ±45 s before fixation (with 4% paraformaldehyde, 0.1% Triton X-100, 100 mM Pipes, pH 6.8, 1 mM MgCl2, and 5 mM EGTA) for 5-10 min. For cold-shock experiments, cells were placed on ice and treated with ice-cold media for 9 minutes prior to pre-extraction and fixation. Coverslips were washed twice with cold PBS and blocked with 3% BSA in PBS for 16 h at 4°C, incubated with primary antibodies for 16 h at 4°C, washed 4 times with PBS containing 0.1% Triton X-100, and incubated with secondary antibodies for an additional hour at room temperature. Coverslips were then washed twice with PBS/0.1% Triton X-100, incubated with DAPI for 2 min, washed again twice with PBS and mounted using Prolong Gold antifade (Molecular Probes). All images were acquired on a deconvolution system (DeltaVision Elite; Applied Precision/GE Healthcare) with a 100×/1.40 NA UPlanSApo objective (Olympus) using SoftWorx 6.0 software (Applied Precision/GE Healthcare). Images are maximum intensity projections of deconvolved stacks. Images of cold-shock experiments are sum projection images.

Image quantification. Analysis of live cell imaging experiments was carried out with ImageJ software. Time in mitosis was defined as the time between nuclear envelope breakdown and anaphase-onset or cell flattening.
For quantification of immunostainings, all images of similarly stained experiments were acquired with identical illumination settings. Selection of cells was based on Cells expressing comparable levels of exogenous protein were selected for analysis and analysed using ImageJ. An ImageJ macro was used to threshold and select all centromeres and all chromosome areas (excluding centromeres) using the DAPI and anticentromere antibodies channels as described previously. This was used to calculate the relative average kinetochore intensity of various proteins ((centromeres–chromosome arm intensity (kinetochore localized protein of interest))/(centromeres–chromosome arm intensity (CENP-C))). A similar method was used to measure total spindle tubulin after cold-shock experiments.

Intra-kinetochore distance measurements. Cells were treated, fixed, stained and imaged as described above. Analysis was performed with the ImageJ plugin "Object counter 3D" on deconvolved, non-projected images. In this manner, coordinates (x, y, and z) of the centre of mass of the GFP (-HEC1) and CENP-C signals were identified and used accordingly to calculate the distance between the inner (CENP-C) and outer kinetochore (GFP) independent of direction of kinetochore stretching. To correct for chromatic aberrations, GFP was stained with two secondary antibodies with different fluorophores in each individual cell line. For each experiment, the distance between the two fluorophores was measured for 25 kinetochores in 5-7 cells, averaged and used to correct the position of the CENP-C signal in the intra-kinetochore measurements.

Immunoblotting. Cells were treated as described above and entered mitosis in the presence of nocodazole. Mitotic cells were isolated by mitotic shake off and lysed in Laemmli lysis buffer (4% SDS, 120 mM Tris (pH 6.8), 20% glycerol). Lysates were processed for SDS-PAGE and transferred to nitrocellulose membranes for immunoblotting. Immunoblotting was performed using standard protocols. Visualisation of signals was performed on a scanner (Amersham Imager 600) using enhanced chemiluminescence.

Antibodies. The following primary antibodies were used for immunofluorescence imaging: CENP-C (polyclonal Guinea pig, 1:2,000; MBL), α-TUBULIN (mouse monoclonal, 1:10,000; Sigma-Aldrich), γ-Tubulin (rabbit polyclonal, 1:500; Sigma-Aldrich), HEC1 (mouse monoclonal 9G3, 1:2,000; Abcam), GFP (custom rabbit polyclonal raised against full-length GFP as antigen[251], 1:10,000), GFP (mouse monoclonal, 1:1,000; Roche), MAD2 (custom rabbit polyclonal raised against full-length 6×His-tagged MAD2 as antigen[252], 1:2,000), BUBR1 (rabbit polyclonal, 1:1,000; Bethyl), BUB1 (rabbit polyclonal, 1:1,000; Bethyl).
Secondary antibodies were highly crossed absorbed goat anti-guinea pig Alexa Fluor 488 and 647, goat anti–rabbit Alexa Fluor 488, 568 and 647, and anti–mouse Alexa Fluor 488 and 568 (Invitrogen Molecular Probes).

Supplementary material

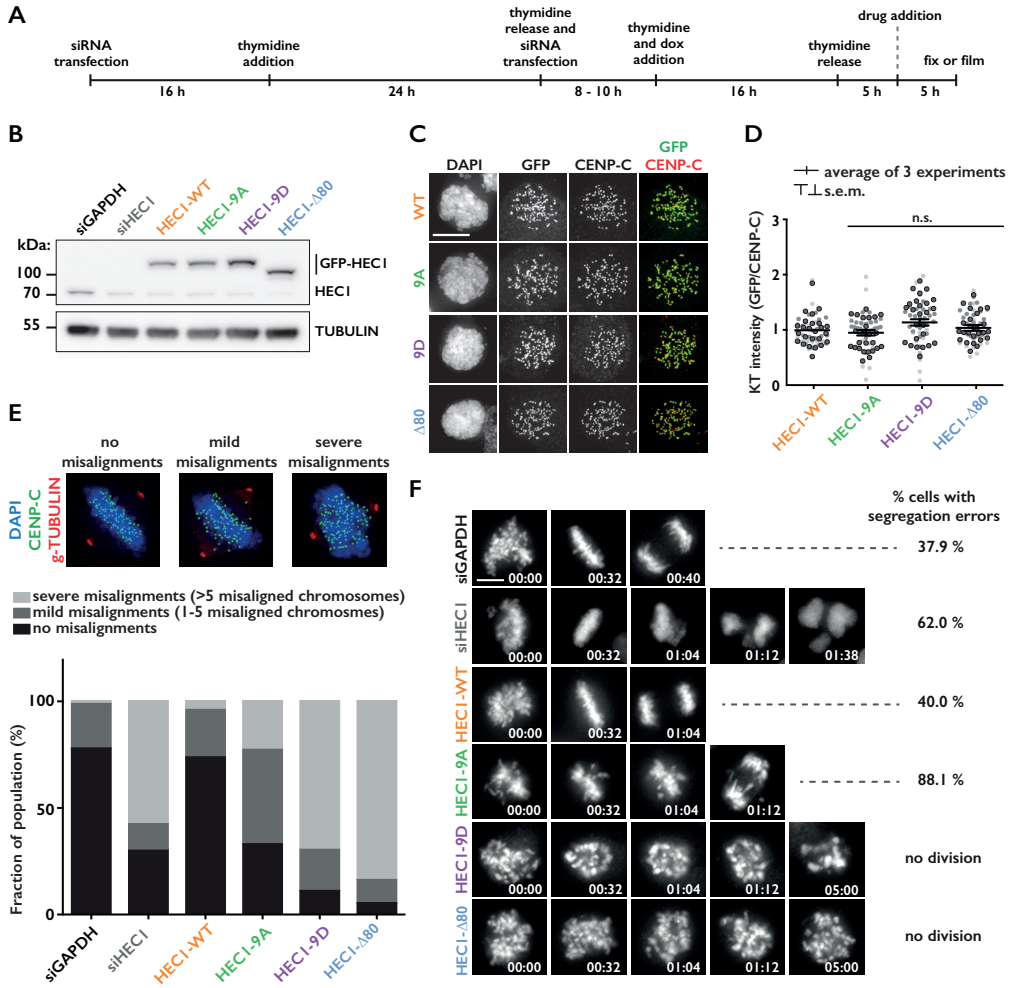

Supplementary Figure 1. Characterisation of cells expressing variants of HEC1. A) Scheme of workflow used throughout this paper. Exceptions are indicated. **B)** Immunoblot showing HEC1 knock down and expression of siRNA-resistant GFP-tagged versions of HEC1 in a mitotic population. **C)** Immunofluorescent labelling of indicated proteins in nocodazole-arrested cells. Channel colours of merged images match those of the labels. **D)** Quantification of the kinetochore intensity of GFP in (C) normalized to the kinetochore intensity of CENP-C. Each dot represents one cell. The data points of three independent experiments are depicted in different shades of grey. Also shown is the average fold-change of three experiments (± s.e.m.) normalized to the average values of HEC1-WT. A total of at least 63 cells were measured per mutant. For statistical analysis, an unpaired Student's t-test was performed against the measured values of HEC1-WT expressing cells. *P < 0.01. **E)** Alignment assay of cells expressing mutant versions of HEC1 as indicated. Top panel shows examples of the scored categories. Alignment status was scored only in cells with centrosomes that lay in the same plane. (f) Representative stills from movies of cells co-expressing variants of HEC1 and mCherry-H2B. At least 50 cells were scored per condition in two independent experiments. Scale bars, 5 μm.

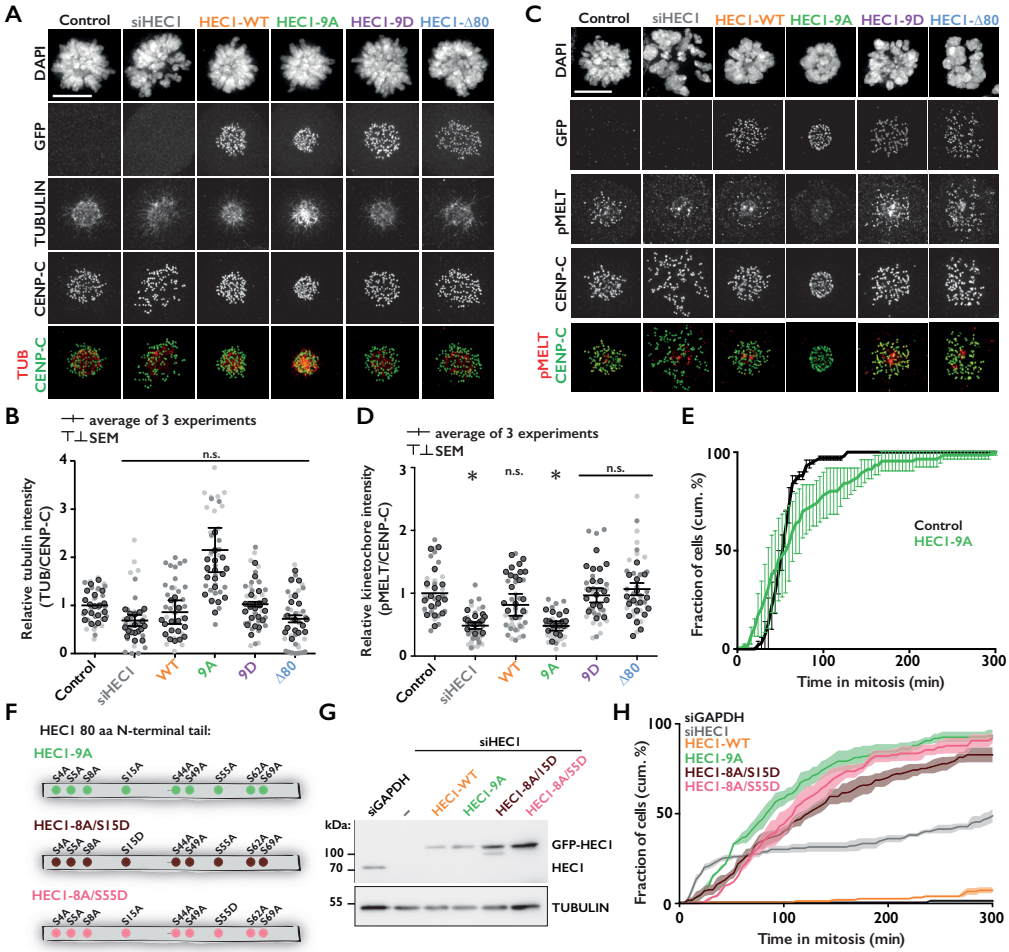

Supplementary Figure 2. Characterisation of attachments in monopolar HEC1-9A expressing cells. A-D) Immunofluorescent labelling of indicated proteins in STLC-arrested cells (A, C) and quantification thereof (B, D). To visualize stable microtubules in (A, B) cells were cold-treated prior to fixation. Channel colours of merged images match those of the labels. Quantification is normalized to the kinetochore intensity of CENP-C and is the average fold-change of three experiments (± s.e.m.) normalized to the values of control cells. Each dot represents one cell. The data points of three independent experiments are depicted in different shades of grey. A total of at least 45 cells were measured per mutant in (B) and 47 in (D). **E)** Time-lapse analysis of control and HEC1-9A expressing cells going through mitosis with bipolar spindles. Data are the average of two experiments ± s.e.m. (error bars) for at least 97 cells. (F) Cartoon of the N-terminal tail of HEC1 showing the mutated residues in the indicated variants of HEC1. **G)** Immunoblot showing HEC1 knock down and expression of siRNA-resistant GFP-tagged versions of HEC1. **H)** Time-lapse analysis of cells expressing indicated HEC1 mutants. Cells entered mitosis in the presence of STLC. Data are the average of three experiments (solid line), ± s.e.m. (transparent area) for at least 130 cells. All quantifications were subjected to unpaired Student's t-test against the measured values of siGAPDH-transfected cells. *P < 0.01. Scale bar, 5 μm.

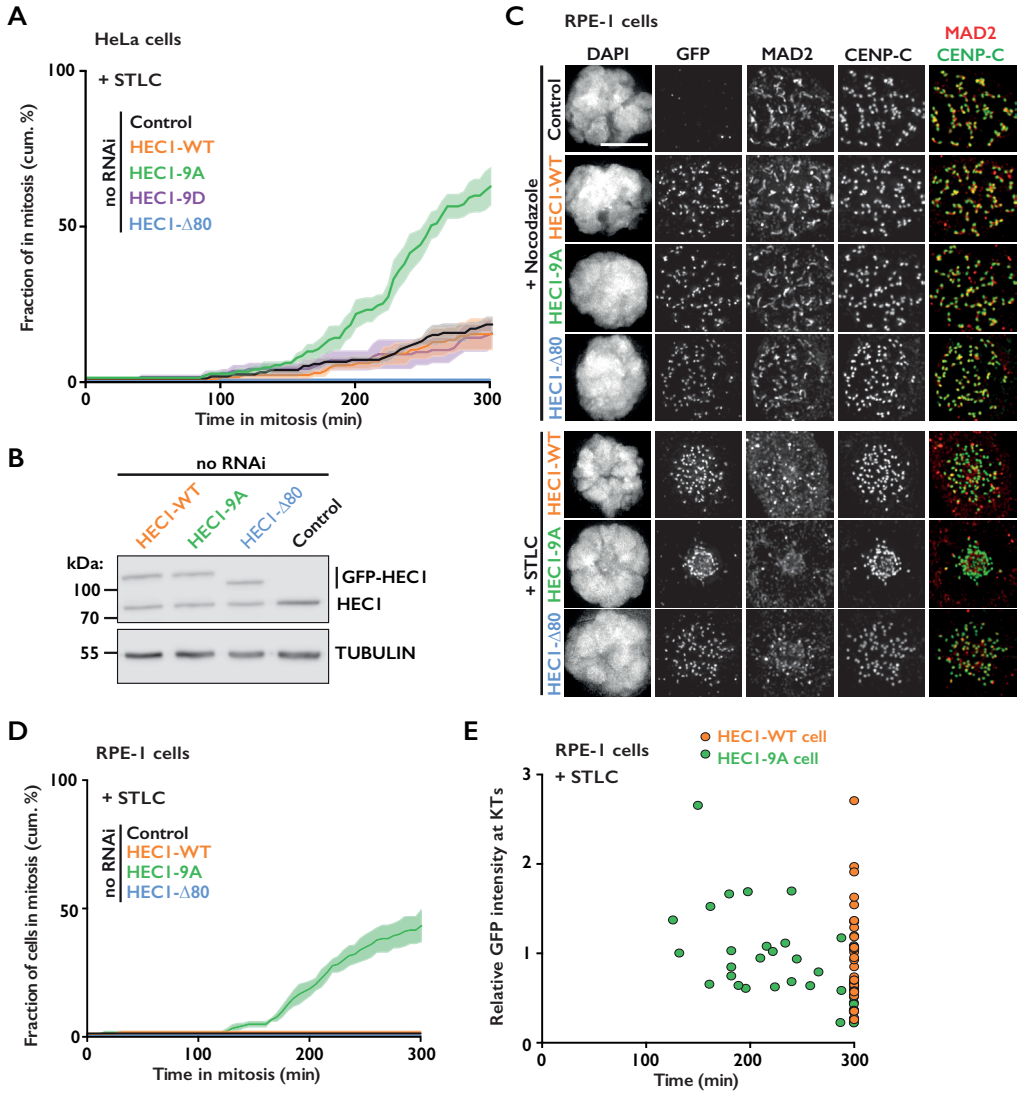

Supplementary Figure 3. Characterisation of HEC1-9A expressing RPE-1 cells. A) Time-lapse analysis of duration of mitotic arrest in STLC-treated HeLa cells overexpressing HEC1 variants as indicated. **B)** Immunoblot showing HEC1 expression in a mitotic population of RPE-1 cells. Lower band represents endogenous HEC1, upper one is the tagged mutant version. **C)** Immunofluorescent labelling of indicated proteins in nocodazole- and STLC-arrested cells. Cells were treated with MG132 for 2 hours prior to fixation. Channel colours of merged images match those of the labels. Scale bar, 5 μm. **D)** Time-lapse analysis of duration of mitotic arrest in STLC-treated RPE-1 cells overexpressing HEC1 variants. **E)** Time-lapse single cell analysis of HEC1-WT and HEC1-9A expressing RPE-1 treated with STLC plotted against the total GFP-kinetochore levels. The total GFP-kinetochore level of analysed cells was measured at mitotic entry and normalized against the average level measured in HEC1-WT cells. Data are from two independent experiments. Each dot represents one cell. For HEC1-WT 34 cells were imaged, for HEC1-9A 42 cells. Data in (A) and (D) is the average of three experiments (solid line) ± s.e.m. (transparent area) for at least 144 cells in (A) and 180 cells in (D).

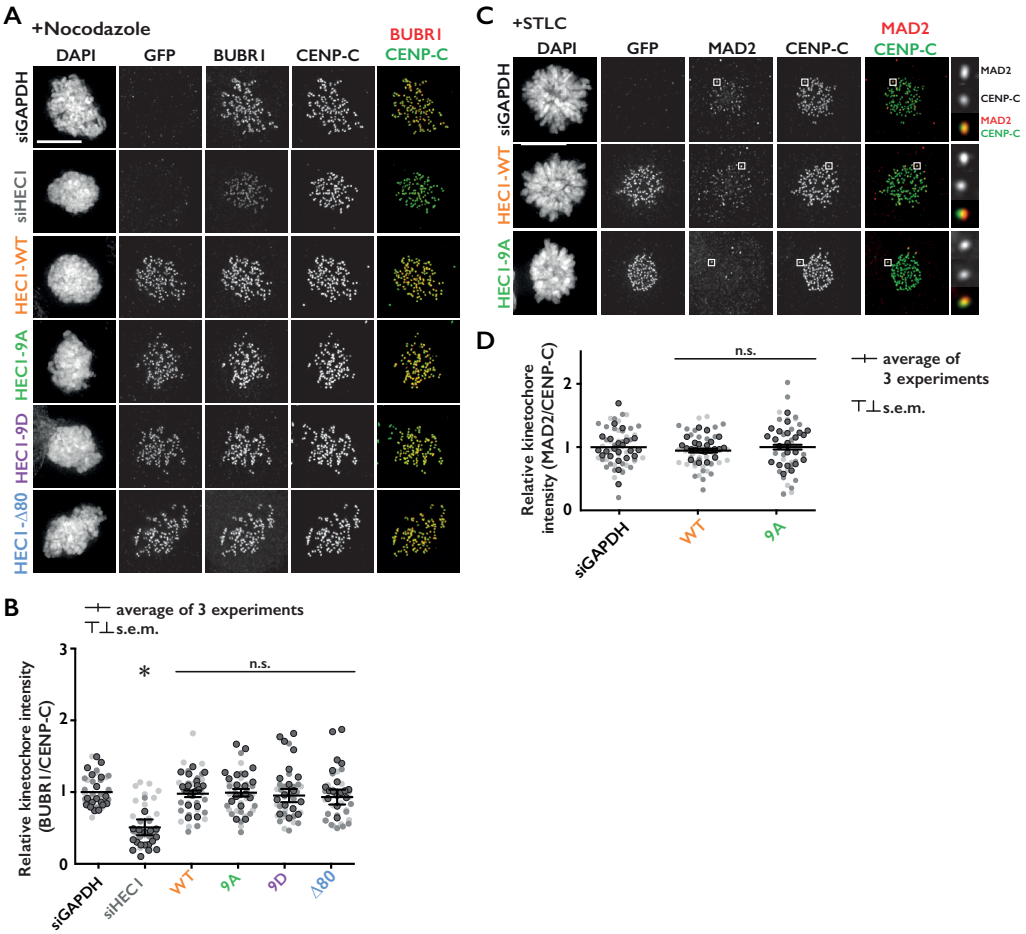

Supplementary Figure 4. SAC protein levels of cells expressing HEC1 variants. (A-D) Immunofluorescent labelling of indicated proteins in nocodazole- (A, B) and STLC-treated cells (C, D). Channel colours of merged images match those of the labels. In (C, D) cells entered in the presence of STLC and were subsequently treated with MG132 for two hours prior to fixation. MAD2 and CENP-C levels were measured on kinetochores positive for this protein. Quantification is normalized to the kinetochore intensity of CENP-C and is the average fold-change of three experiments (± s.e.m.) normalized to the values of control cells. The data points of three independent experiments are depicted in different shades of grey. A total of at least 50 cells was measured per mutant in (B) and 57 kinetochores in (D). Quantifications were subjected to unpaired Student's t-test against the measured values of siGAPDH-transfected cells. *P < 0.01. Scale bars, 5 μm.

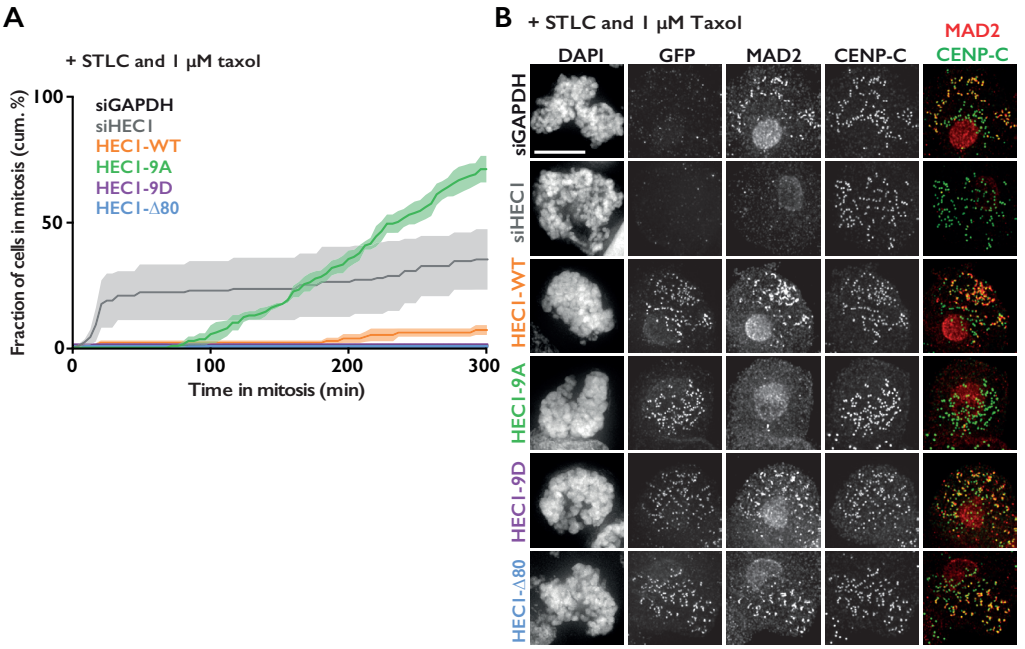

Supplementary Figure 5. Microtubule based pulling forces have no role in SAC silencing in HEC1-9A cells. A) Time-lapse analysis of duration of mitotic arrest in cells treated with STLC and Taxol prior to mitotic entry. Data are average of three experiments (solid line) ± s.e.m. (transparent area) for at least 100 cells per mutants. **B)** Immunofluorescent labelling of indicated proteins. Cells entered in the presence of STLC and Taxol and were subsequently treated with MG132 for 2.5 hours. Channel colours of merged images match those of the labels. Representative images of two experiments. Scale bar, 5 μm.

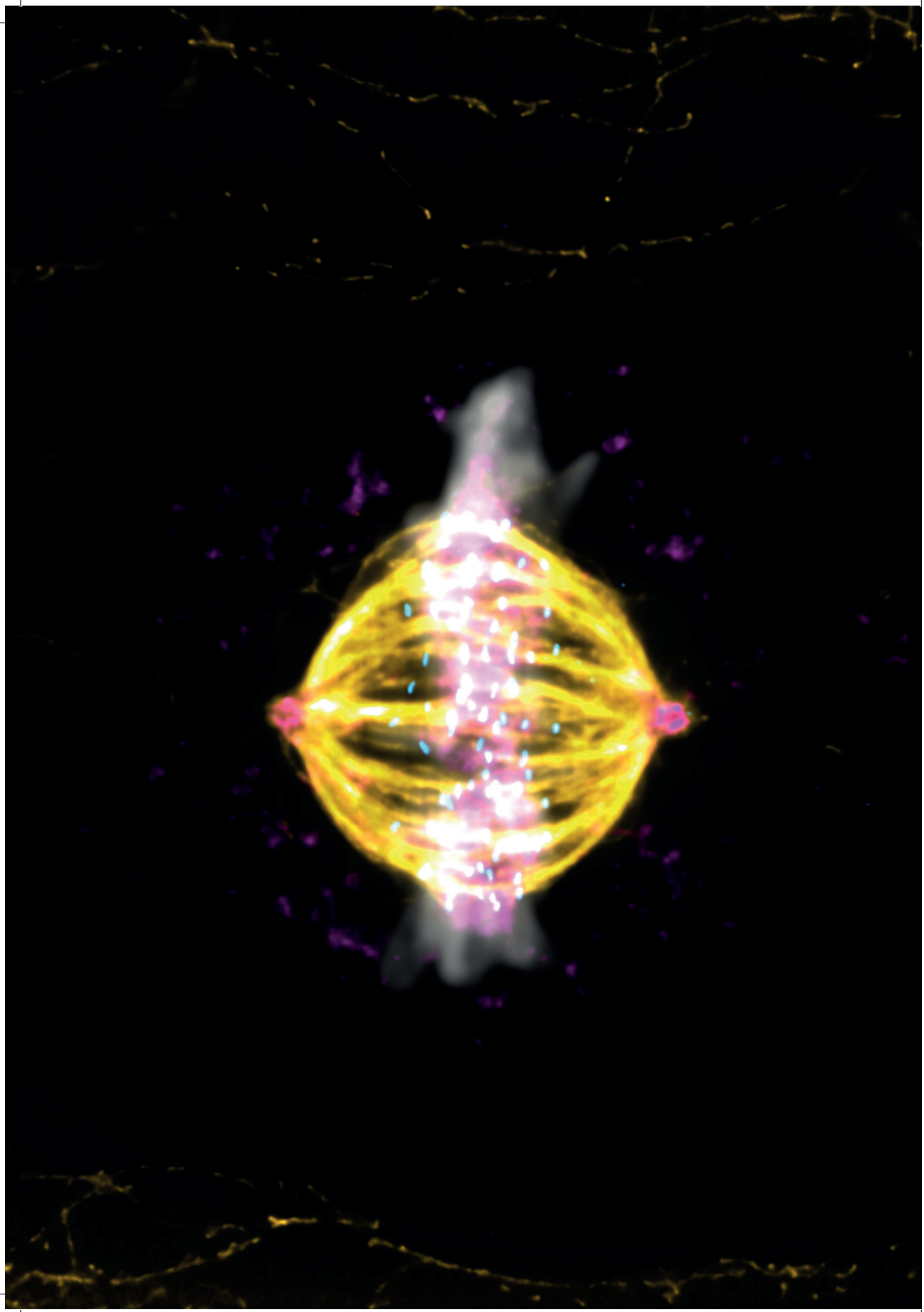

Chapter 4

A biosensor for the mitotic kinase MPS1 reveals spatiotemporal activity dynamics and regulation

Timo E. F. Kuijt[1], Sonja Weterings[1], Bas Ponsioen[2,3], Ana F. Bolhaqueiro[1], Debbie Staijen[1] and Geert J.P. L. Kops[1*]

[1]Oncode Institute, Hubrecht Institute-KNAW and University Medical Centre Utrecht, Utrecht, 3584 CT, the Netherlands, [2]Cancer Genomics Netherlands, UMC Utrecht, 3584CG Utrecht, The Netherlands, [3]Molecular Cancer Research, Centre for Molecular Medicine, UMC Utrecht, 3584CG, Utrecht, The Netherlands.

Manuscript under revision at Current Biology

Abstract

Accurate chromosome segregation during cell division critically depends on error correction of chromosome-spindle interactions and the spindle assembly checkpoint (SAC). The kinase MPS1 is an essential regulator of both pathways, ensuring full chromosome biorientation before anaphase onset. To understand when and where MPS1 activation occurs and how its activity is modulated during mitosis we developed MPS1sen, a sensitive and specific FRET-based biosensor for MPS1 activity. By placing MPS1sen at different subcellular locations, we show that MPS1 activity initiates in the nucleus ~9-12 minutes prior to nuclear envelope breakdown (NEB) in a kinetochore-dependent manner, and reaches the cytoplasm at the start of NEB. Soon after initiation, MPS1 activity increases with switch-like kinetics, peaking at completion of NEB. We further show that timing and extent of pre-NEB MPS1 activation is regulated by Aurora B and PP2A-B56. MPS1 activity declines in prometaphase as a result of formation of kinetochore-microtubule attachments, reaching low but still detectable levels at metaphase. Finally, leveraging the sensitivity and dynamic range of MPS1sen, we show deregulated MPS1 activity dynamics in colorectal cancer cell lines and tumour organoids with diverse genomic instability phenotypes.

Introduction

Whole chromosome imbalances are common causes of developmental defects and are hallmarks of cancer cells[377, 378]. They are caused by errors in chromosome segregation during cell divisions[16, 379]. Accurate chromosome segregation requires biorientation of all chromosomes before the onset of anaphase. This is achieved by efficient correction of erroneous kinetochore-microtubule attachments and a robust response of the spindle assembly checkpoint (SAC) to lack of such attachments[352, 380]. Central to regulation of these processes is the mitotic kinase MPS1[381].

During prophase, MPS1 kinase translocates to the nucleus and localises to kinetochores by virtue of binding the outer kinetochore protein dimer HEC1/NUF2[69, 248, 255, 265, 266, 381, 382]. This interaction is promoted by the kinases Aurora B and cyclin B1/CDK1[255, 270, 364, 383]. Clustering on kinetochores allows MPS1 trans-autoactivation, after which it dissociates. Subsequent continuous MPS1 rebinding and dissociation at kinetochores occurs with fast kinetics and is important for its function[224, 253, 259, 260, 280, 344]. Once active, MPS1 coordinates events to promote error-correction and the SAC.

In human cells, the SAC is activated by default in early mitosis and requires silencing before cells can proceed to anaphase. The SAC is generated by unattached kinetochores where the scaffolding proteins KNL1, BUB1 and MAD1 facilitate the assembly of an inhibitor of anaphase known as the mitotic checkpoint complex (MCC)[193, 194, 219, 352, 384]. MPS1 controls MCC production through a cascade of multi-site phopshorylations of KNL1, BUB1 and MAD1[208, 231, 233, 235, 236, 322]. Simultaneously, MPS1 promotes efficient

chromosome biorientation. It drives corona-assembly to facilitate initial microtubule capture[76, 79], recruits the kinesin CENP-E to kinetochores to facilitate chromosome congression[224], regulates Aurora B activity to ensure error-correction[278, 385], and regulates the SKA-complex to modulate stability of kinetochore-microtubule interactions[239]. In addition to these activities, MPS1 has also been implicated in chromosome condensation[386], centrosome duplication[250], and G2 DNA damage signalling[387].

The activity of MPS1 during mitosis is countered by several mechanisms. PP1- and PP2A-B56 family phosphatases can dephosphorylate MPS1 substrates as well as directly inactivate MPS1[150, 173, 292-295]. Local MPS1 activity at kinetochores is furthermore reduced by progressive end-on microtubule attachments that obstruct the MPS1 binding sites on the HEC1/NUF2 dimer[265, 266]. At metaphase low levels of MPS1 and some of its substrates remain on kinetochores, suggesting MPS1 might still be active[269, 295, 388].

Given its central role in coordinating essential mitotic processes, much can be learned about maintenance of chromosomal stability from studying mechanisms and dynamics of MPS1 activation prior to and during mitosis and of subsequent MPS1 inactivation. FRET-based biosensors have uncovered localised regulation of kinase activity and greatly increased our understanding of signalling pathways in single cells. Biosensors for Aurora B and PLK1 kinases, for example, revealed an activity gradient from mitotic centromeres and its mechanistic underpinnings[139 389], and mechanisms of kinase regulation in G2[390], respectively. Inspired by these studies, we set out to develop a FRET-based biosensor specific for MPS1 kinase, the results of which are described in this report.

Results

MPS1sen is a specific biosensor for MPS1 kinase

To study spatiotemporal activity dynamics of MPS1, we modified an existing PLK1 biosensor with the substrate sequence LLLDS(pThr)LSINW, previously shown to be also targeted by MPS1 kinase during mitosis[391, 392]. Substrate consensus motifs for MPS1 and PLK1 kinases are similar in some positions (e.g. negative charges at -2 or -3 relative to phosphorylated S/T) but also have distinct features[393, 394], which we utilized to increase specificity for MPS1 kinase. We introduced a Glycine at position -1, an additional negative charge at -3 and an Alanine at +2, creating the substrate sequence LLEDG(pThr)LIANW (**Fig. 1A**). We furthermore exchanged CyPet for the high quantum yield mTurquoise2 donor[395] to enhance the dynamic range of MPS1sen.

A prominent pool of active MPS1 is located at the outer kinetochore where it binds to the HEC1/NUF2 components of the NDC80 complex[265, 266, 382]. To verify MPS1sen specificity, we placed it close to the MPS1 activation site by fusion to the N-terminus of SPC24 (hereafter named MPS1sen-KT) and monitored FRET (mTurquoise2/YPet ratio after mTurquoise excitation) in mitotic HeLa cells treated with the spindle poison

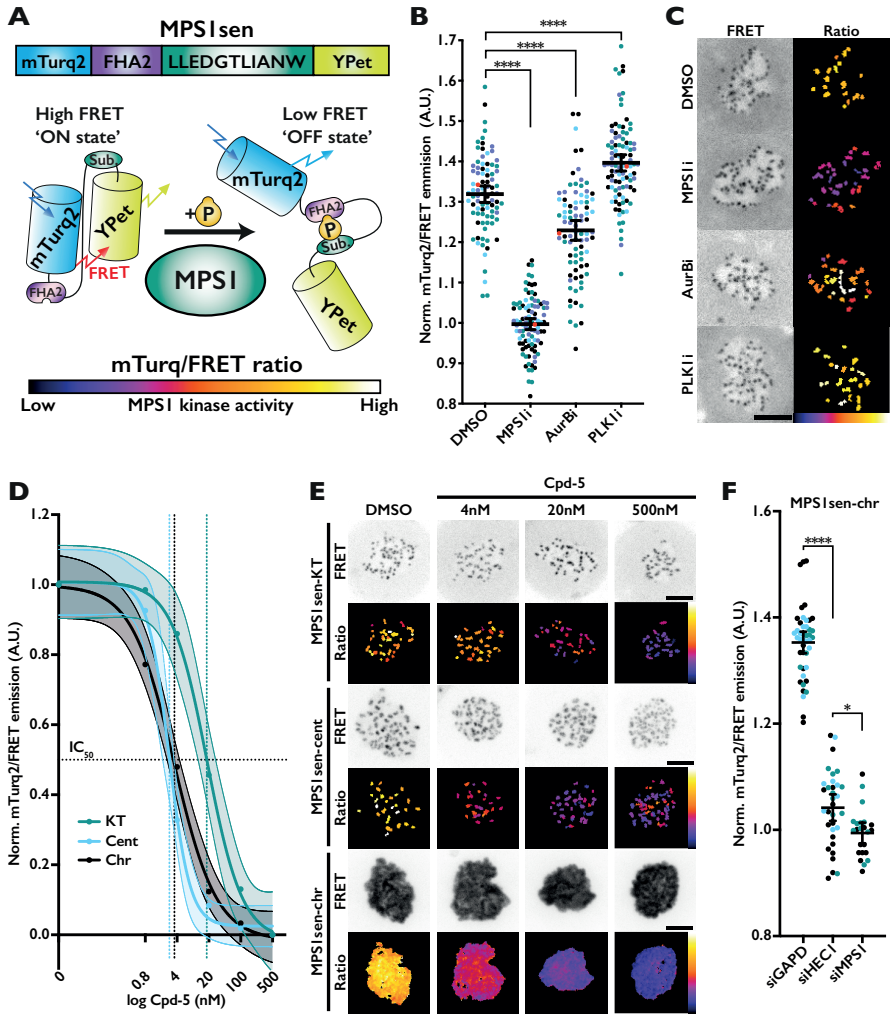

Figure 1. MPS1sen is a specific sensor for MPS1 kinase activity and originates from kinetochores. (**A**) Cartoon of MPS1sen design. MPS1sen FRET decreases by increasing phosphorylation of the substrate sequence. The pseudo-coloured calibration bar represents low (dark purple) to high (yellow/white) MPS1 activity as applied to FRET ratio images in this work. (**B, C**) HeLa cells stably expressing MPS1sen-kinetochores (-KT), arrested in prometaphase (Noco) for 1 hr. and treated with indicated inhibitors for 45 min (+MG-132). (**B**) Representative images of data shown in (C) where the max. projected FRET (YFP) channel and object ratio (pseudo-coloured) images are scaled identically for direct comparison. (**C**) Quantification of MPS1sen-KT (local ratio), normalized to MPS1i (500 nM Cpd-5) condition. Each data point represents multiple kinetochores per cell. Data point colours indicate individual repeats of experiment (N=4), red symbol indicates data point used as representative image (B). (**D**) MPS1sen-KT, centromeres (-cent) or chromatin (-chr) expressing cells, arrested in mitosis with Noco and subsequently treated with MG-132 + Cpd-5 for 45-60 min before imaging. FRET ratio per MPS1sen location were normalised and plotted on Y-axis and MPS1i concentrations were converted to log scale (X-axis). 5-fold serial dilutions of Cpd-5 were freshly prepared for each individual repeated (KT N=4, cent N=2, chr N=3). (**E**) Images from cells quantified in (D), scaled to compare, scalebar =

5 µm. (**F**) HeLa cells expressing MPS1sen-chr treated with indicated siRNAs for 48 hrs., data is extracted from **FigS3A** at timepoint 30 min. post NEB. In (C,D,F) the mean and 95% Confidence Interval (CI, range indicating true population mean with 95% certainty) are indicated.

nocodazole. MPS1sen-KT showed a robust FRET signal, which was abolished upon inhibition or depletion of MPS1 by the small molecule inhibitor Cpd-5[396] (**Fig. 1B,C**) or by RNAi, respectively (**Fig. S1A,B**). Importantly, despite similarity in consensus substrate sequences and overlapping localization[393, 394, 397], inhibition of PLK1 with BI-2536[398] did not reduce FRET and if anything even increased it, further validating specificity of MPS1sen (**Fig. 1B,C**). Furthermore, when cells were treated with the Aurora B inhibitor ZM447439[343], we observed a slight but significant reduction of FRET. This is in line with the known role of Aurora B in promoting MPS1 activity[255, 270, 364], and thus further illustrates the ability of MPS1sen to report on MPS1 activity states. MPS1sen-KT showed similar dynamic range in non-transformed RPE-1 cells and responded similarly to inhibition of Aurora B or PLK1 in these cells (**Fig. S1C,D**). Taken together, we conclude that MPS1sen is a highly specific reporter for MPS1 activity with a dynamic range that enables it to detect subtle changes in MPS1 activity.

MPS1 activity originates at kinetochores

To examine if MPS1 activity can be detected beyond the kinetochore, we placed MPS1sen at centromeres or chromatin by fusing it to CENP-B (MPS1sen-cent) or Histone H2B (MPS1sen-chr), respectively. In agreement with reported MPS1 substrates at these locations[278 386], both MPS1sen-cent and MPS1sen-chr revealed substantial activity that was sensitive to treatment with MPS1 inhibitor (**Fig. 1D,E**). The MPS1 activity reported on by these probes originated from kinetochores, as evidenced by strong reduction of FRET signals in mitotic cells from which the MPS1 kinetochore receptor HEC1 was depleted by RNAi (**Fig. 1F**). If active MPS1 reaches distant sites by diffusion of active kinase molecules from kinetochores, we reasoned that this should result in local concentration differences of active MPS1. In support of this hypothesis, full inhibition of MPS1 at kinetochores required 500nM of Cpd-5 (IC50 18nM) while at more kinetochore-distal locations 100nM Cpd-5 sufficed (IC50 2-3nM) (**Fig. 1D,E**). Although differences in phosphatase activities at these various sites may exist, our data are consistent with a model in which MPS1 is activated at the outer kinetochore by binding the NDC80 complex and subsequently diffuses to distant sites.

Kinetochore-microtubule interactions regulate MPS1 activity throughout the cell

We and others have shown that formation of end-on kinetochore-microtubule attachments disrupt the MPS1-HEC1/NUF2 interaction and can silence the SAC in the absence of tension[265, 266, 399-401]. Our MPS1 sensor allowed us to examine how MPS1

substrate phosphorylation is affected by various kinetochore-microtubule attachment configurations. To this end, we modulated kinetochore-microtubule attachments using various perturbations in cells expressing MPS1sen-KT. In these cells mCherry-BUB1[388] was expressed from the endogenous locus as an second, independent readout for MPS1 activity. While unattached kinetochores in nocodazole-treated cells displayed high MPS1 activity, stably bioriented kinetochores at metaphase in MG132-treated cells showed low activity that was further reduced by addition of Cpd-5 (**Fig. 2A-B, S2A**). This is in agreement with residual BUB1/BUBR1 and MPS1 localisation on metaphase kinetochores[265, 269, 388], and shows MPS1 has detectable activity in metaphase. In STLC-treated cells with a mixture of (transient) attached and unattached kinetochores, MPS1 activity was high but reduced compared to nocodazole-treated cells. To directly compare attachment states in single cells, we inhibited the kinesin CENP-E, generating bioriented chromosomes at the metaphase plate and unattached chromosomes near centrosomes. Unaligned kinetochores retained high MPS1 activity while bioriented kinetochores had MPS1 activity indistinguishable from metaphase kinetochores in MG132-treated cells (**Fig. 2A-B, S2A-B**). Similar results were obtained in RPE-1 cells (**Fig. S2G**). Interestingly, while MPS1 activity modulations by attachment states were generally similar on centromeres, chromatin and kinetochores, MPS1 activity was substantially lower on unaligned centromeres/chromosomes compared to kinetochores in CENP-E-inhibited cells (**Fig. 2C-D, S2C-H**). Whether this reflects differences in local phosphatase activities or in ability of MPS1 to diffusion to more distant sites as microtubules transiently attach to kinetochores is unknown. Taken together, MPS1 activity is regulated by kinetochore-microtubule interactions and chromosome biorientation throughout the cell.

Switch-like activation of MPS1 in the nucleus in prophase

In previous studies, activity biosensors revealed that nuclear translocation of cyclin B/CDK1 in prophase does not restrict CDK1 activity solely to the nucleus[402] and that PLK1 activity is restricted to the nucleus in G2-phase[391]. MPS1 localises to the cytoplasm in interphase and translocates to the nucleus upon mitotic entry[244, 258]. To visualise the spatial dynamics of MPS1 activation, we expressed MPS1sen without specifying its subcellular localisation and co-expressed mScarlet-NLS to accurately monitor nuclear envelope breakdown (NEB). MPS1 activity became apparent in the nucleus roughly 10 minutes before completion of NEB, while phosphorylation of the cytoplasmic pool of MPS1sen was delayed by several minutes (**Fig. 3A,B and Supplemental Movie 1**). Phosphorylation of this pool tracked leakage of mScarlet NLS from the nucleus as NEB commenced. These data agree with a recent observation that MPS1 kinetochore localisation correlates with nuclear import of cyclin B[244].

To more accurately visualise pre-mitotic activation of MPS1, we next wished to tether MPS1sen in the nucleus. Unfortunately, MPS1sen-KT levels were very low in early prophase due to ongoing outer-kinetochore assembly[403]. We thus opted to use

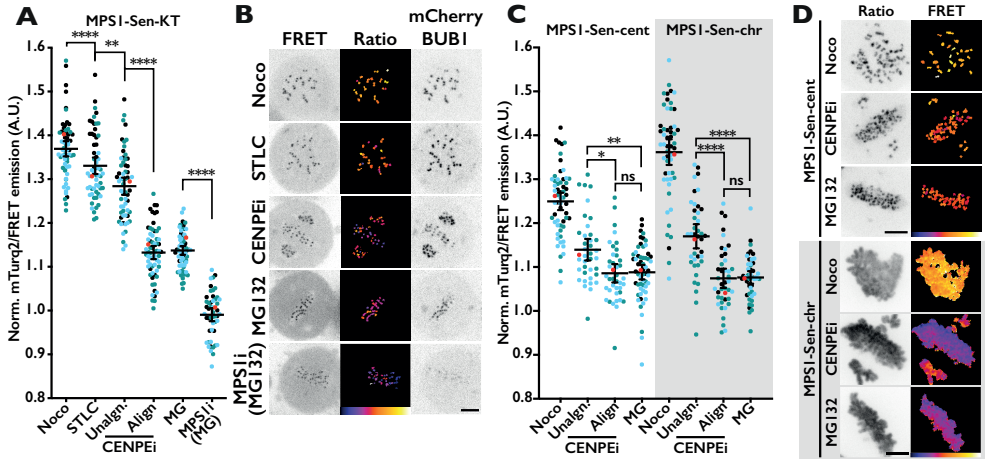

Figure 2. Kinetochore-microtubule interactions regulate MPS1 activity throughout the cell. (**A, C**) HeLa cells expressing MPS1sen biosensor arrested in mitosis using indicated compounds for 45 min after which FRET was measured (MPS1i + MG132 are metaphase-arrested to which 500 nM Cpd-5 was added). Ratio were normalised to Noco + MPS1i condition. In CENP-E-inhibited cells, FRET ratios were computed after which aligned vs. unaligned FRET ratio were calculated. Each data point represents multiple kinetochores/ centromeres/chromosomes per cell and the mean ±95%CI are indicated. Colours of data points represent data from independent repeats of experiment (N=3), red symbol indicates data point used in (B, D, F). (**B, D)** Representative images of data quantified (A) MPS1sen-kt, (C) MPS1sen-cent and MPS1sen-chr. Images are equally scaled for comparison per biosensor location, scalebar = 5 µm.

MPS1sen-chr, as it is stably bound to chromatin throughout the cell cycle. To further ensure that MPS1sen-chr correctly reports on kinetochore-derived Mps1 activity (**Fig. 1F, and 2C,D**), we mutated the substrate sequence, inhibited MPS1 or depleted HEC1 or MPS1, all of which prevented any FRET ratio change (**Fig. 3C, S3A**). By contrast, MAD2 depletion to inhibit the SAC had little impact (**Fig. S3A**). During an unperturbed mitosis, MPS1 activation was detectable 9-12 minutes before full NEB (monitored by mScarlet-NLS (**Supplemental Movie 2**)), rapidly increased thereafter, and peaked around completion of NEB (**Fig. 3C**). This switch-like activation was more rapid than that of PLK1[391] and resembled the activation kinetics of cyclin B1/CDK1[402]. As cells progressed from prometaphase to metaphase, MPS1 activity decreased and the FRET ratio returned to pre-mitotic levels as cells exited mitosis (45-60 minutes after NEB) (**Fig. 3C**).

Timing of prophase MPS1 activation is regulated by PP2A-B56

Our data shows that MPS1 activation starts in prophase and is maximal by the time of full NEB (**Fig. 3A-C**), consistent with a prominent role for CDK1 in MPS1 activation [247, 266, 270, 383]. We next wished to investigate which other activities regulate prophase MPS1

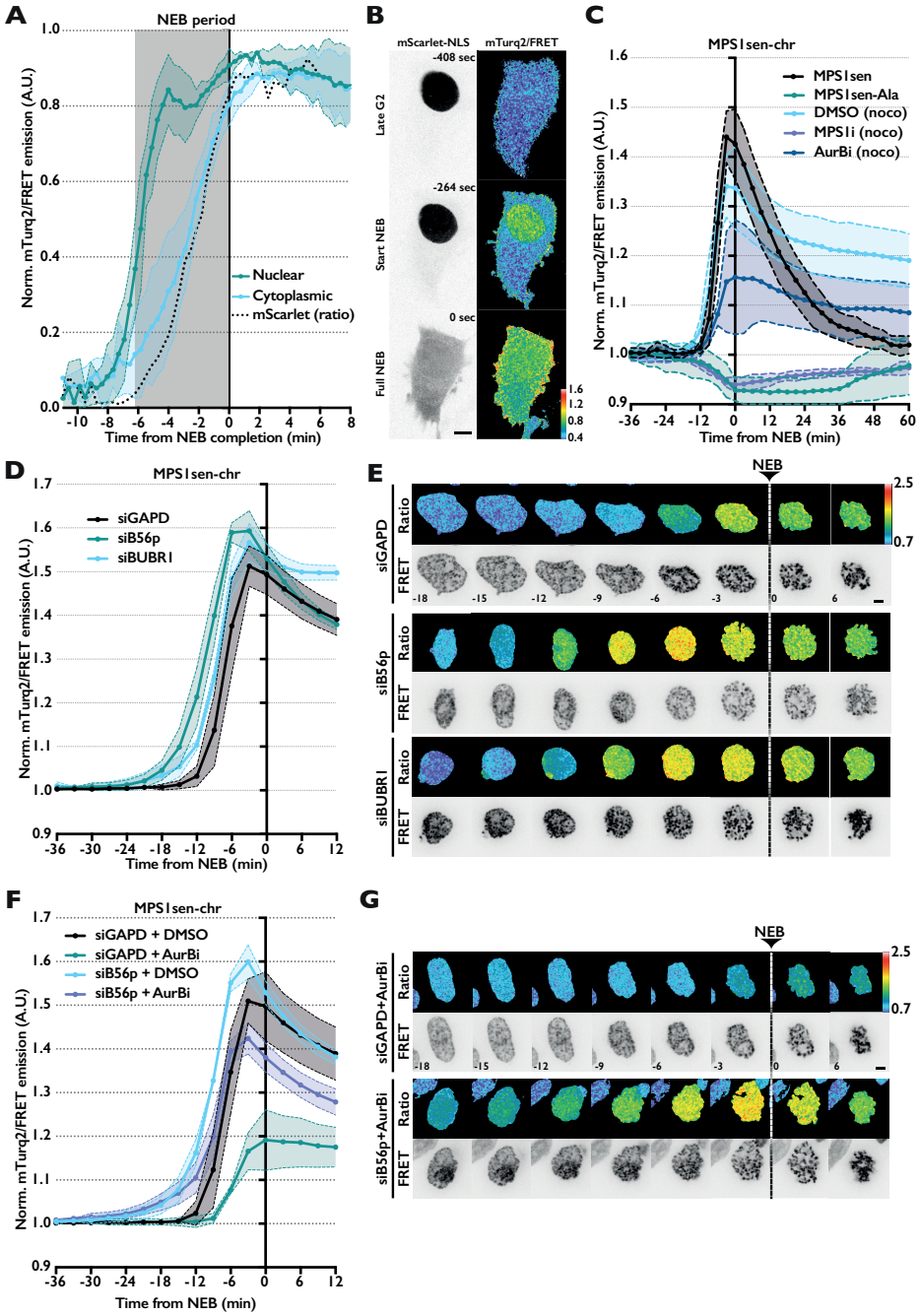

Figure 3. Switch-like activation of MPS1 in the nucleus in prophase and PP2A-B56 regulates timing of prophase MPS1 activation. (**A**) FRET quantification (mean ±95% CI, N≥3) of HeLa cells expressing cytoplasmic-MPS1sen (on 1 replicate +P2A-mScarlet-NLS) were arrested overnight in G2 by RO-3306. Cells were released from G2-block in 6.6 μM Noco while imaging continuously (±20s) imaging. (**B**) Still from **Supplemental Movie 1** showing MPS1sen nuclear

FRET ratio change at 168 seconds before full NEB. (**C**) FRET quantification (mean ±SD, N≥3) of HeLa cells expressing H2B-MPS1sen or H2B-MPS1sen-Ala progressing through unperturbed mitosis (from 16 hrs. thymidine release). In addition, HeLa cells expressing H2B-MPS1sen (with or without P2A-mScarlet-NLS, see **Supplemental Movie 2**) progressed to in the presence of Noco and proTAME (to delay exit of MPS1i cells) and treated with indicated inhibitors. Normalization was performed at t=-51 min relative to NEB on the population average of each condition. (**D,F**) FRET quantification (mean ±SD, N≥3) of HeLa cells expressing H2B-MPS1sen, depleted for indicated proteins for 16 hrs., followed by 24hr thymidine block and released for 7 hrs. before imaging at which point 6.6 μM nocodazole was added. Data was processes as described for (C) with exception of no P2A-mScarlet-NLS being present in these experiments. In (F) cells were imaged in presence of 2 μM ZM447439 (AurBi) or solvent (DMSO). (**E, G**) Representative images of data quantified in (D, F) t=0 is first frame after full NEB, images scaled equally, scalebar = 5 μm. In (E) premature MPS1 activation and elevated MPS1 activity around NEB is shown. In (G) depletion of B56p (pool of siRNA to all isoforms) plus Aurora B inhibition allows efficient MPS1 activation but does not restore timing of MPS1 activation. Images in (G) are scaled identically to (E) for direct comparison.

activation dynamics. In agreement with a reported role for Aurora B in promoting MPS1 activity[240, 270], inhibition of Aurora B strongly reduced activation speed of MPS1 and reduced maximum MPS1 activity during prometaphase (**Fig. 3C**). Aurora B activity is regulated by the phosphatase PP2A-B56[143, 144, 150], and PP2A-B56 can directly inactivate MPS1[294]. Strikingly, RNAi of B56 (all isoforms[143]) not only elevated MPS1 activity during early mitosis but also advanced the onset of MPS1 activation by up to 18 minutes (**Fig. 3D-G, FigS3F**). These effects were in part mimicked by depletion of the PP2A-B56-binding protein BUBR1 (**Fig. 3C,D, S3E**), suggesting a role for this interaction in MPS1 activity regulation. To further examine the mechanism by which PP2A-B56 stimulated late G2 MPS1 activity, we inhibited Aurora B in B56-depleted cells. We reasoned that if PP2A-B56 acted on MPS1 solely by modulating Aurora B-dependent phosphorylation, Aurora B inhibition should fully revert the effects of B56 depletion. Remarkably, while inhibition of Aurora B partly restored the extent of MPS1 activation at NEB in the absence of B56, it had no effect on the advanced moment of activation (**Fig. 3F,G, S3G**). Together, these data suggest PP2A-B56 directly counters MPS1 activation in late G2, and additionally indirectly modulates MPS1 peak activity near NEB by dampening Aurora B.

MPS1 activity is deregulated in colorectal cancer

Our data shows that MPS1sen is a specific biosensor for MPS1 kinase activity capable of detecting relatively subtle changes to MPS1 activity dynamics. Cancer cells are marked by extensive aneuploidies that are caused by chromosomal instability (CIN). The molecular causes for CIN are likely related to pathways generating, regulating or monitoring correct attachments of kinetochores to spindle microtubules[16, 404]. Since MPS1 is at the heart of these processes, we wished to explore if MPS1sen would be

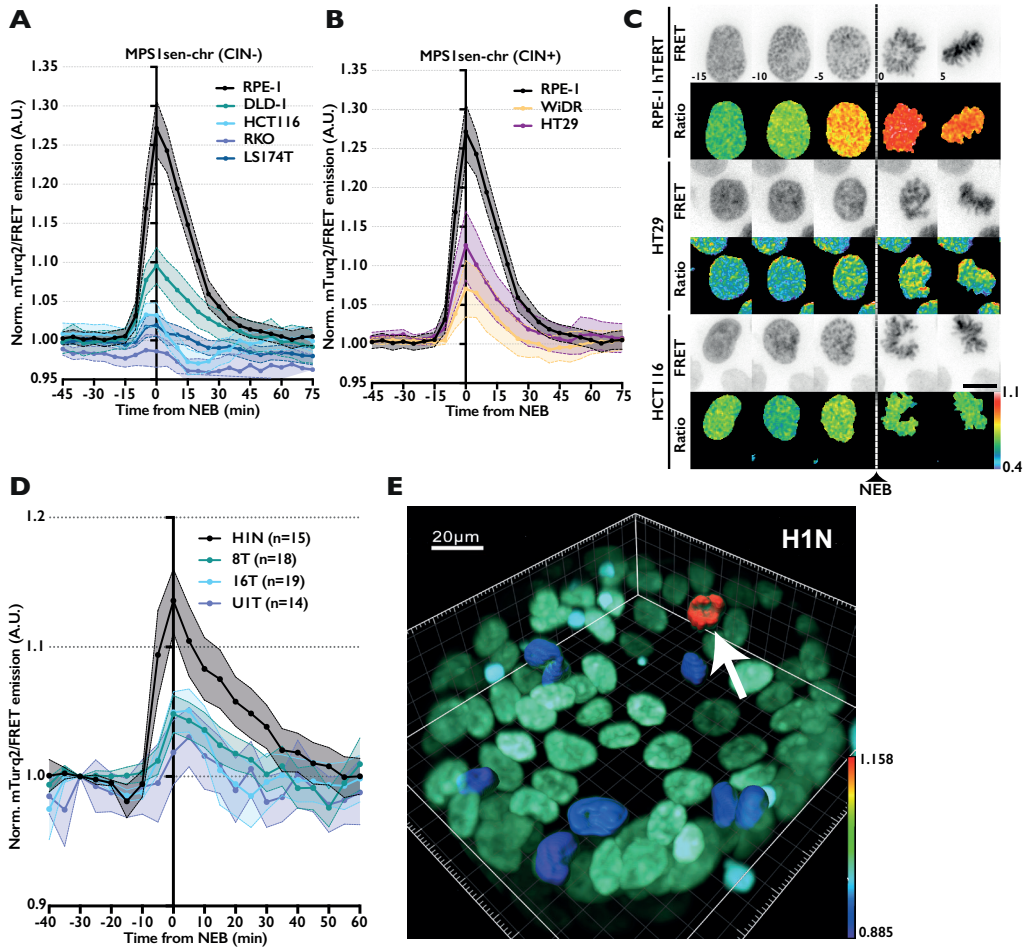

Figure 4. MPS1 activity is deregulated in CRC cells and patient-derived stem cell cultures. (**A, B**) FRET quantifications (mean ±95%CI) of CRC cells and RPE-1 (N=3) stably expressing MPS1sen-Opti-chr. Cells were thymidine synchronized (16 hrs.) and released (7 hrs.) before imaging unperturbed mitotic progression. Cell lines in (A) are classified as CIN- (all N=2, except HCT116 N=3) and cell lines in (B) are CIN+ (HT29 N=3, WiDR N=2), RPE data is same in both graphs. Ratios were calculated using custom ImageJ code and normalised on population average of each cell line at t=-51 min. (**C**) Images (mTurq2/FRET ratio and FRET channels) RPE-1, HT29 and HCT116 cells expressing MPS1sen (from data presented in A,B), scaled identically for direct comparison, scalebar = 5 µm. (**D**) FRET quantifications (mean ±SEM, N≥2) of human colon patient-derived organoids (PDOs) expressing MPS1sen-chr. Organoids were imaged every 5 min. for 16 hrs., and data was normalised at t=-30 min before NEB. (**E**) 3D volume image of human colon PDO H1N, from data quantified in (D). Chromatin in all cells (Turquoise-coloured) is rendered as an overlay of mTurq2 and FRET. Chromatin of cells that divide during the time-lapse (Blue, Red) is 3D-rendered and colour-coded by mTurq2/FRET ratio, ranging from 0.885-1.158. The red cell (white arrow) is undergoing NEB and has a ratio of 1.158. The blue cells are in interphase and have a mean mTurq2/FRET ratio of ~0.9. Scalebar represents 20µm, grid represents 10 µm.

useful to assess if alterations to its activity are apparent in cancer cells. We selected a panel of colorectal cancer (CRC) cell lines in which aneuploidy levels and CIN status has been extensively documented[17, 405, 406], and expressed MPS1sen-chr to comparable levels by lentiviral transduction. All of the CRC cell lines showed reduced MPS1 activation levels compared to non-cancerous RPE-1 cells, and no obvious differences were observed between those designated as CIN (high aneuploidy) or MSI/MIN (low aneuploidy) (**Fig. 4A-C**). However, whereas some lines (DLD-1, WiDR, HT29) showed clear, albeit low Mps1 activation (peaking at NEB), others showed very weak (LS174T, HCT116) or no (RKO) MPS1 activity. It thus seems that low MPS1 activity is a shared feature of this panel of cancer lines but that it does not correlate to aneuploidy status. To further validate this, we sought to extend our observations to patient-derived stem cell cultures (organoids) that were recently isolated from patients. These tumour organoids closely resemble the tumour of origin, and that were extensively characterised for CIN status[407, 408]. We introduced MPS1sen-chr into four lines: two non-hypermutated lines with medium CIN, a hypermutated/MSI line with medium CIN and one normal line derived from healthy colon tissue[408]. Strikingly, while MPS1 activation was robust in healthy colon organoids, it was substantially weaker in all tumour lines (**Fig. 4D,E and Supplemental Movie 3-6**). Our data therefore suggest that MPS1 activation is reduced in CRC cells, regardless of their intrinsic forms of genomic instability.

Discussion

In this work we present MPS1sen, an MPS1-specific FRET-biosensor to investigate the activation dynamics and regulation of MPS1 in living cells and tumour organoids. We show MPS1 activation is detected 9-12 minutes before NEB in the nucleus and increases with rapid kinetics to peak around completion of NEB. Pre-mitotic activation of MPS1 is promoted by Aurora B kinase and restricted by PP2A-B56. We furthermore show that MPS1 activity can be detected throughout the cell but originates from kinetochores, where it is modulated by progressive kinetochore-microtubule attachments during prometaphase. Finally, we show that MPS1sen can detect subtle changes in MPS1 activity and provide evidence that MPS1 activity is affected in colorectal cancer cells.

Rapid establishment of the SAC signal ensures the fidelity of chromosome segregation by stabilising cyclin B at the G2/M transition[270]. This requires MPS1 and involves interaction of MAD1 and MAD2 with nuclear pores to generate a kinetochore-independent pool of MCC[221, 277]. We show that MPS1 activation occurs well before full NEB and is restricted to the nucleus, and that MPS1 activity was undetectable in the cytoplasm or nucleus before then, although we cannot exclude existence of very local and/or transient pools of MPS1 activity. As our data indicate that active MPS1 kinase can diffuse from kinetochores, we speculate that MPS1 substrates such as condensin II[386] and nuclear pore-bound MAD complexes[221, 222, 235] can be readily phosphorylated in G2. This would allow unrestrained activation of the SAC in G2, which is further

assisted by nuclear exclusion of the MPS1-inactivating B56 phosphatase[291]. In support of this, chromatin-localised MPS1sen showed a decrease in MPS1 activity after NEB has occurred and depletion of BUBR1, a recruiter of PP2A-B56 to kinetochores, largely prevented 'dampening' of MPS1 activity in prometaphase (**Fig. 3D**). We excluded a role for SAC override in BUBR1-depleted cells playing a role as MAD2 depletion did not affect prometaphase 'dampening' of MPS1 activity but effectively overwrote the SAC.

Activation of MPS1 is regulated by Aurora B and cyclin B/CDK1 during mitosis[267, 270, 383]. How MPS1 activation is coupled to mitotic entry at a molecular level is poorly understood. Our data show that Aurora B not only promotes efficient MPS1 activation but also regulates its timing, and that also PP2A-B56 and BUBR1 play important roles in these events. We can only speculate as to how these factors impact on spatiotemporal MPS1 activation dynamics. Interestingly, advancement of MPS1 activation in B56-depleted cells was unaffected by Aurora B inhibition, showing that at least Aurora B is not downstream of PP2A-B56 in MPS1 regulation. Instead, PP2A-B56 may directly affect MPS1 activity by reverting T-loop phosphorylation[294]. How Aurora B impacts on MPS1 is unknown. Since delay and reductions of MPS1 activation were (partly) prevented by PP2A-B56 depletion, the phosphatase may be downstream of Aurora B. This is consistent with recent finding that kinetochore localisation of MPS1 in Aurora B-inhibited cells can be restored by depletion of B56[294]. It will be of interesting to use MPS1sen to elucidate the exact contributions of regulators to MPS1 activation dynamics.

MPS1 activity is modulated by formation of kinetochore-microtubule attachments, resulting in low but detectable activity in metaphase when the SAC is silenced. This is in line with residual levels of BUB1 (**Fig. 2B** and ref [388]) and KNL1 phosphorylation[265, 388, 409] on metaphase kinetochores, and with observations that targeting of MAD1 to metaphase kinetochores re-elicits an MPS1-dependent SAC response[302, 410, 411] . The reason for residual MPS1 activity in metaphase is unclear. Since we observed an extent of loss of metaphase plate integrity upon MPS1 inhibition (**Fig. S2B,D**), perhaps it functions to maintain correct microtubule dynamics or retain some BUB1-Sgo1 to promote centromeric CPC localisation and thus preserving sister chromatid cohesion[284, 412]. Alternatively or additionally, low metaphase MPS1 activity could aid in fast SAC reactivation upon loss of kinetochore-microtubule attachments.

MPS1sen analyses showed widespread reductions of maximal MPS1 activity in various cancer cultures. Although all analysed tumour organoids are CIN[407, 408] and therefore MPS1 activity status correlates with CIN status in these cultures, it did not so in the cell lines. Since MPS1 may impact DNA damage signalling or centrosome function, it is conceivable that its deregulation impacts the cancer cell phenotype in non-mitotic ways. It therefore remains to be seen to what extent MPS1 activity deregulation is associated with the CIN phenotype, and this is an interesting topic for future studies.

Acknowledgments

We thank M. Lampson (UPen) for sharing reagents and MatLab code. We are thankful to S. Lens (UMC Utrecht) and H. Snippert (UMC Utrecht) for sharing reagents. We thank S. Sonneveld for help with providing code to semi-automate Matlab analysis. We are grateful to members of the S. Lens, A. T. Saurin and Kops lab for fruitful discussions. This study is financially supported the Netherlands Organisation for Scientific Research (NWO/ALWOP.153 G.J.P.L. Kops).

Material and Methods

Plasmids & reagents

MPS1sen was generated by restriction digestion of pIRES-PURO-H2B-mTFP1-Aurora B with BamHI/BspEI (NEB). The MPS1sen substrate sequence (or MPS1sen-Ala) was inserted using synthesized DNA oligo's and validated by Sanger sequencing. mTFP1 was replaced by mTurquoise2 (mTurq2, gift from D. Gadella, Addgene plasmid 36202) by PCR and inserted by restriction digestion (NheI/KpnI). The H2B coding sequence was substituted by restriction digestion with AscI/NheI and PCR amplification of CENP-B (DNA binding domain, 1-158) to generate MPS1sen-cent. N-terminal fusions to MPS1sen were generated by subcloning of a plasmid containing mTFP1-Aurora B-YPet-CAAX[413] (gift from S. Lens) where mTFP1 was replaced by mTurq2 and a multiple cloning site identical to the MCS found in plasmid pDL009-HEC1-Aurora B biosensor (gift from M. Lampson, Addgene plasmid 45239) was inserted. SPC24 coding region was PCR amplified from cDNA to create MPS1sen-KT. To visualize nuclear envelope breakdown, mScarlet (gift from D. Gadella, Addgene plasmid 85054) was amplified by PCR, adding an N-terminal P2A sequence and a C-terminal SV40-NLS sequence. This fragment was inserted by Gibson assembly cloning behind the IRES-PURO of various MPS1sen-plasmids.

To generate lentivirus MPS1sen version, pLV-H2B-mNeon[414] was digested with AscI/NheI and backbone was gel purified. MPS1sen was PCR-amplified and inserted by Gibson assembly cloning. mTurq2 was replaced with a codon-optimized version of Turquoise2GL (kind gift from H. Snippert) to prevent recombination of MPS1sen during production of lentivirus. To reduce Turq2-YPet dimerization, the K206A and V224L 'sticky'-mutations in Turquoise2GL were reverted by site-directed mutagenesis, generating MPS1sen-Opti. CENP-B and SPC24 pLV-MPS1sen-Opti were generated by Gibson assembly. Coding regions of all MPS1sen plasmids were verified by Sanger sequencing.

The following chemicals were used at indicated final concentrations unless state otherwise in figure legends: nocodazole (6.6 μM, Sigma-Aldrich M1404), MG-132 (5 μM, Sigma-Aldrich C2211), thymidine (200 mM, Sigma-Aldrich T1895), ZM-447439 (2μM, Tocris Bioscience 2458), Cpd-5 (500 nM, MPS1 inhibitor[396]), RO-3306 (8 μM, Tocris Bioscience 4181), taxol (1 μM, Sigma T1912), STLC (10 μM, Tocris 1291), CENP-E inhibitor (250nM, GSK923295 Selleck Chem), proTAME (3.3 μM, Boston Chemicals I-440), puromycin (1μg/ml, Sigma, P7255), rutin (16 μM, Thermo Fisher Scientific AC132391000).

The following siRNAs were used at 20nM final concentration unless stated otherwise: siGAPD (ON-TARGETplus Dharmacon D-001830-01-05), siBUBR1-UTR[415] (100nM): GUCUCACAGAUUGCUGCCU, siMPS1[278]: GACAGAUGAUUCAGUUGUA, siMAD2: UACGGACUCACCUUGCUUG siHEC1-UTR (40nM) [399]: CCCUGGGUCGUGUCAGGAA, Pool of siB56[143] B56α: UGAAUGAACUGGUUGAGUA, B56β: GAACAAUGAGUAUAUCCUA, B56γ: UGACUGAGCCGGUAAUUGU, B56δ: GGAAGAUGAACCAACGUUA, B56ϵ: GCACAGCUGGCAUAUUGUA.

The following primary antibodies were used for immunofluorescence: guinea pig anti-CENP-C (1:2000, MBL Life Science PD030), rabbit anti-KNL1- pT943/1155 (custom, described in ref. [208]), rabbit anti-BUB1 (1:2000, Bethyl A300-373 A-1) mouse anti-HEC1 (1:1000, Thermo Fisher Scientific MA1-23308) and secondary antibodies at 1:1000: goat anti-guinea pig Alexa Fluor 647 (Molecular Probes A21450), goat anti-rabbit Alexa Fluor 488 (Molecular Probes A11034), goat anti-rabbit Alexa Fluor 568 (Molecular Probes A11036), goat anti-mouse Alexa Fluor 488 (Molecular Probes A11029), goat anti-mouse Alexa Fluor 568 (Molecular Probes A11031).

Cell culture, organoids & FACS sorting

HeLa FLPin T-Rex, WiDR and HT29 cells were cultured in DMEM - high glucose (Thermo Fisher Scientific, 11965092) supplemented with 10% Tet-free foetal bovine serum (Sigma), penicillin-streptomycin (50 µg/ml, Sigma P0781) Ala-Gln (2 mM, Sigma G8541). RPE-1 hTERT FLPin T-Rex and RKO cells were cultured in DMEM/F12 (Thermo Fisher Scientific) + 10% Tet-free FBS, 50 µg/ml pen/strep and 2mM Ala-Gln. DLD-1 and LS174T cells were cultured in RPMI (Thermo Fisher Scientific) supplemented with 10% FBS, 50 µg/ml pen/strep and 2mM Ala-Gln. HCT116 were cultured in McCoy's 5A (Sigma) medium 10% FBS, 50 µg/ml pen/strep and 2mM Ala-Gln. Cell line identity was verified by microscopic inspection of morphological traits as described in literature. Endogenously tagged HA-mCherry-BUB1 HeLa FLPin T-Rex cell line was described previously[388]. Live-cell imaging was performed in freshly prepared DMEM^{gfp}-2 medium (Evrogen MC102) supplemented with 8% FBS, 2 mM Ala-Gln and rutin (2000x stock in DMSO).

To generate HeLa cells expressing MPS1sen, plasmids were transfected using Fugene HD (Roche) according to manufactures instruction and 24 hrs. after transfection puromycin was added. RPE-1 and CRC cell lines were generated by transduction with lentiviral MPS1sen-Opti. After growing out stable clones expressing MPS1sen(-Opti), cells were FACS sorted to isolate a polyclonal population that expressed mTurq2:YPet at 1:1 ratio. Cells were resuspended after trypsin in DMEM, pelleted at 300xg for 3 min. by centrifugation, washed with 1xPBS0 (-Mg^{2+}/Ca^{2+}) and resuspended in FACS buffer (1xPBS0 + 25mM HEPES pH7.2 + 0.1% EDTA + 0.1% FCS). FACS sorting was performed on a custom BD FACSAria Fusion flow cytometer system. mTurq2 (Ex405nm, Em450/50) was plotted against YPet (Ex488nm, Em549/15) and mScarlet/mCherry (Ex561nm, Em610/20) against autofluorescence (Ex640nm, Em670/30). Sorted cells were collected in cooled DMEM full growth medium (FGM) supplemented with 10% FBS and

10mM HEPES (Sigma).

Cell synchronization was performed by addition of 2 mM thymidine (Sigma) for 20 hrs. and cells were released from thymidine for 7 hrs. before initiating assays. Arresting cells at G2 was performed by addition of 8 μM RO3363 for 17 hrs. and cells were released from CDK1 blocks by washing 2x with DMEM medium while inside the microscope.

Delivery of siRNAs was performed using Lipofectamin RNAiMax (Thermo Fisher Scientific). In brief: cells were plated to 12 well plate in 625μl medium (50% full growth medium + 50% Optimem (Thermo Fisher Scientific). Lipid:siRNA complexed were formed in 123 μl optimem + 0.75μl siRNA (20 μM stock) and 1.25μl RNAiMax, incubated for 10 min. before addition to cells. siRNA was performed for 24 hrs. (siB56) or 48 hrs. (siHEC1, siMPS1, siMAD2, siBUBR1). Cells were arrested in S-phase using thymidine for 20 hrs. before imaging commenced and released 7 hrs. before imaging in imaging medium (see below)

Colon Patient derived organoids (PDOs) were cultured as described previously[408] and tumour PDOs expressing MPS1sen-Opti-chr were generated as described in [414]. Two days before imaging of PDOs, PDOs were dissociated with TrypLE (Thermo Fisher Scientific) and colon PDOs were mechanically dissociated. The PDOs were plated in Matrigel in a pre-warmed 8-well glass bottom μ-slide (Ibidi, #80827). Upon plating, Rock inhibitor (10 μM, Sigma-Aldrich Y-27632) was added to culture medium for 2 days.

Live cell imaging and microscopy

Cells were plated on 96-well glass bottom 1.5H well plates (CellVis) 24 hrs. before imaging. For experiments in which cells were released from G2 by RO-3363 block, medium was replaced by warm DMEM medium twice and image acquisition was initiated directly after or medium replacements were performed in between image acquisition rounds.

Live cell imaging of all cell lines was performed on a Nikon TiE microscope, controlled by NIS Elements software (Nikon V4.56), equipped with a Yokagawa CSU-W1-T2 spinning disk (dual disk), Borealis (Andor), two iXon-888 Ultra EMCCD cameras (Andor), 1x camera relay lens and ILE-400 (Andor) laser emission controller. MPS1sen was excited using a 445nm±5nm laser with 35 - 45 μW at the objective, passing emission light through a 445-561-640 custom dichroic mirror to block excitation light and emission light of mTurquoise2 and FRET (YPet) was split by a 514nm razor edge dichroic mirror (Semrock). Emission light was collected with 490-40nm (Semrock) and 545-50 (Semrock) emission filters. For experiments involving mScarlet, a 561nm laser (100mW rated) was used at the lowest possible intensity and emission was collected with a 609-57nm filter (Semrock). All imaging was performed using a PLANAPO 100x 1.45 NA objective lens (Nikon) and 50μm pinhole disk. For imaging H2B and cytoplasmic MPS1sen camera settings were: 2x2 binning, 10MHz readout speed, gain 1 mode, -80°C cooled EMCCD-chip, 100-150ms exposure time and 3x6μm Z-steps (12μm stack size). For imaging kinetochore or centromere FRET camera settings were 1x1 binning, 1MHz readout speed, gain 2 mode, 300 EM-gain (both channels), -90°C cooled CCD-chip, a 150x150 ROI, 200-300ms exposure and for kinetochore (SPC24) FRET 2x averaging was applied. Z-steps were 0.6μm with a 2.4μm stack size

for kinetochores and 7.8µm stack size for centromere FRET. CENP-E-inhibited cells were imaged with a Z-stack of 19 images to capture both aligned and unaligned objects in the cell.

For imaging PDO, a 30x UPLSAPO silicone objective lens (Olympus) was mounted by using a M25 to RMSA1 adaptor (Thorlabs) and a 15mm parfocal extender (Thorlabs).

Immunofluorescence

HeLa FLPin cells were plated on glass ø10 mm coverslips (#1.5H) >24 hrs. before fixation. Cells were pre-extracted with 37°C PHEM-TX100 (PIPES, HEPES, EGTA, 2 mM MgCl2, 0.2% Triton X-100) for 1 min. at room temperature after which cells were fixed in freshly prepared 4% paraformaldehyde/PBS (pH7.2) for 5 mins. at room temperature. Cells were washed with PBS and blocked in 3% BSA/PBS (blocking buffer) for 30 min. at room temperature. Primary antibody dilutions were made in blocking buffer and coverslips were incubated at 4°C overnight inverted. Next, cells were washed in blocking buffer + 0.1 % Triton X100 followed by 1 hr. incubation with secondary antibodies diluted in blocking buffer. Coverslips were washed in blocking buffer and a final wash step in ddH2O before mounting onto glass slides using Prolong Gold antifade (Thermo Fisher Scientific). Images were acquired on a DeltaVision Elite (GE Healthcare) with a 100x 1.40NA UPlanSApo objective (Olympus) and SoftWorx 6.0 software (GE Healthcare). Images were acquired with 0.15µm Z-intervals and then deconvolved and maximum intensity projections were made using SoftWoRx. Early prometaphase cells were selected based on the mitotic shape of DAPI signal.

Data analysis

Immunofluorescent images were quantified using Fiji[416] as follows: in maximum projected image region of interest (ROI) was drawn to exclude neighbouring cells, a threshold was applied to generate an ROI of the DAPI signal, following a threshold on CENP-C channel to generate an ROI for kinetochore signal. The kinetochore ROI was subtracted from the DAPI after DAPI channel was removed, background was measured in all channels using DAPI-ROI followed by measuring of kinetochore signal in all channels using kinetochore-ROI. The mean background intensity was subtracted from mean kinetochore signal and the kinetochore/CENP-C ratios were computed.

Time-lapse FRET data from H2B and cytoplasmic MPS1sen were sum projected in Z-axis using Fiji and analysed using custom written macro in ImageJ (B. Ponsioen, unpublished). In brief, background was subtracted for each channel over time and background was set to NaN using manual set threshold on the weighted sum of donor/acceptor intensities. Next, donor/acceptor ratio image was calculated and a region of interest (ROI) was manually placed and a thresholding (weighted sum of donor/acceptor) was applied to define pixels for quantification. The pooled donor/acceptor ratios were computed and used for subsequent data normalization. For H2B FRET cells, normalization was applied at t=-51 min. before NEB by computing the population average at this timepoint. For cytoplasmic MPS1sen quantifications a 15x15 pixel ROI was placed in the nucleus or cytoplasm and analysed as described for H2B data. Data was

normalised by setting the first frame to 1 for each cell where the mean FRET ratio of nuclear and cytoplasm was used per cell.

Raw kinetochore/centromere FRET data was processed in Fiji by custom written macro (available upon request) performing in brief the following steps: image masking (nearby cells/aggregates), mean background calculation per channel, mean kinetochore/centromere calculation per channel and saving these parameters to a spreadsheet. FRET ratios were calculated using custom written MATLAB code (kindly provided by M. Lampson, University of Pennsylvania), where adjustments to the script (available upon request) were made to read-out spreadsheet containing parameters calculated in Fiji and generate donor/acceptor FRET images. An additional Matlab script (available upon request) was written (kindly provided by S. Sonneveld) to batch-process all images for a single condition and assemble the FRET ratios in a single spreadsheet file containing either local or object ratios.

Quantification of aligned vs. unaligned in the CENP-E-inhibited conditions was done on the projected image of local FRET. A manual ROI was drawn to select the aligned objects after which the unaligned objects were masked. Next a threshold (Otsu) was applied to create a selection within the ROI and measure the FRET ratio of all aligned objects. Unaligned objects were measured by inverting the ROI and mask the aligned objects after which images were processed with identical steps described for aligned objects.

Organoid data was processed using Imaris XT 9.3.1 (bitplane.com) and the plugin XT Mean Intensity Ratio (open.bitplane.com). The XT Mean Intensity Ratio code was rewritten to run on Matlab Runtime Compiler 8.0 (kindly provided by S. Sonneveld). Image data was duplicated and a background subtraction and gaussian filter were applied. When possible, surface tracking of H2B nuclei was performed semi-automated, in other instances manual ROI were defined using adaptive thresholding. The mTurquoise2 and FRET quantifications were performed on raw imaging data. Mean donor/acceptor ratio per nucleus was computed using XT mean ration intensity and data was exported and normalised to first frame (±45 min before NEB). All FRET data was computed on an HP-Z440 workstation (Xeon 3Ghz E5-1660 v3, 96GB RAM, AMD FirePro W7100).

All statistical analysis was performed using Graphpad Prism (9.0) where normality test was performed (D'Agostino & Pearson) and subsequently One-way Analysis of Variance (ANOVA) with Tukey's multiple comparison test were performed to compare experimental groups when $n \geq 3$ independent replicates were performed. The standard deviation, standard error of the mean or 95% confidence interval of the mean were computed using Graphpad which is indicated in figure legend. The indicated p-values are in GraphPad style (ns $p>0.05$, * $p\leq0.05$, ** $p\leq0.01$, *** $p\leq0.001$, **** $p\leq0.0001$).

Supplementary material

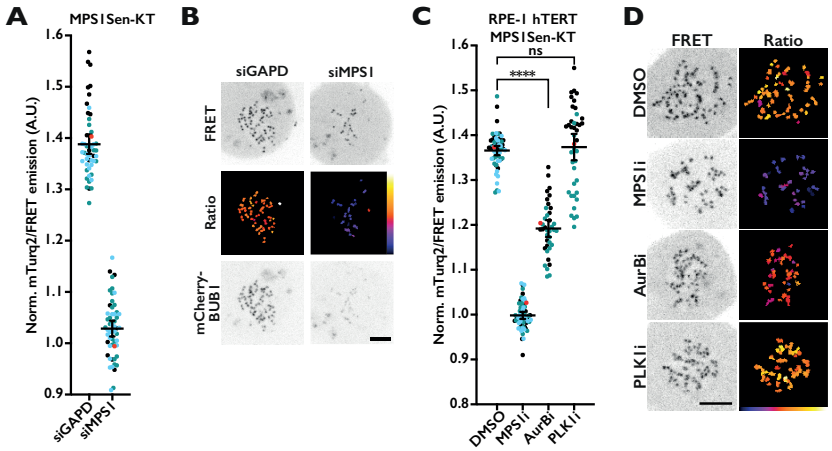

Supplemental Figure 1. MPS1sen is a specific biosensor for MPS1 kinase in human cells. (**A, C**) HeLa cells (A) or RPE-1 cells (C) stably expressing MPS1sen-SPC24. (**A**) Cells depleted of MPS1 by RNAi and thymidine synchronized for 24 hrs., released for 7 hrs., captured in prometaphase using 6.6 μM Noco for 2 hrs. followed by addition MG132 for 30 min. before imaging. (**C**) RPE cells arrested in prometaphase using 6.6 μM Noco for 1 hr., followed by 45 min of treatment with indicated drugs + MG132 before imaging. For (**A, C**), mTurq2/FRET ratio were normalized to MPS1 inhibited condition which for A are omitted from dataset. Data point colours indicate individual repeats of experiments (N≥4), red symbol indicates data point used as representative image shown in (**B, D**). (**B, D**) Representative images of cells quantified in (A, C), scaled equally to allow direct comparison within each experiment.

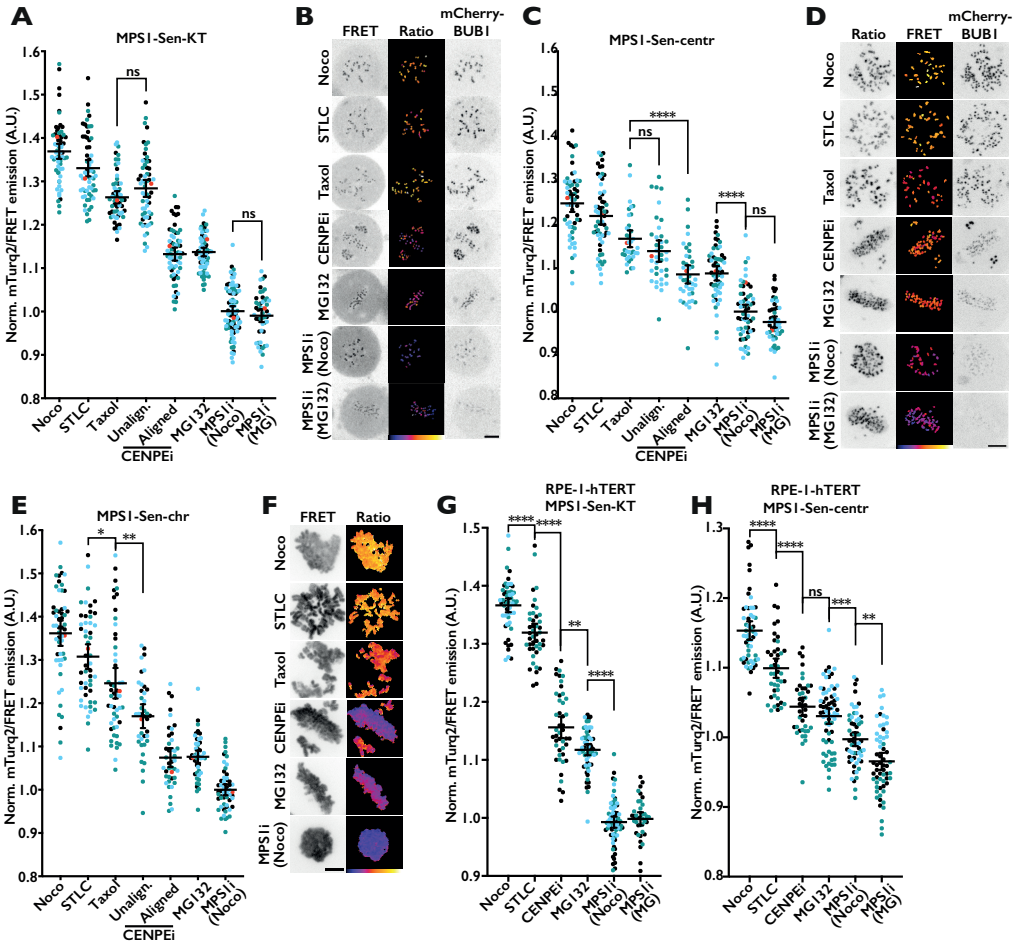

Supplemental Figure 2. Kinetochore-microtubule interactions regulate MPS1 activity throughout the cell. (A-F) extended data set shown in **Fig2**. (**G+H**) FRET quantifications of RPE-1 cells expressing MPS1sen-kt (G) or MPS1sen-cent (H) arrested in mitosis using indicated inhibitors for 1 hr. and treated with additional inhibitors (500 nM Cpd-5 + MG132) for 45 min before imaging. Data point colours indicate individual repeats of experiment (N≥3 or N=2 for Taxol and STLC conditions). Each data point represents multiple kinetochores/ centromeres/ chromosomes per cell and the mean ±95%CI of the population are indicated.

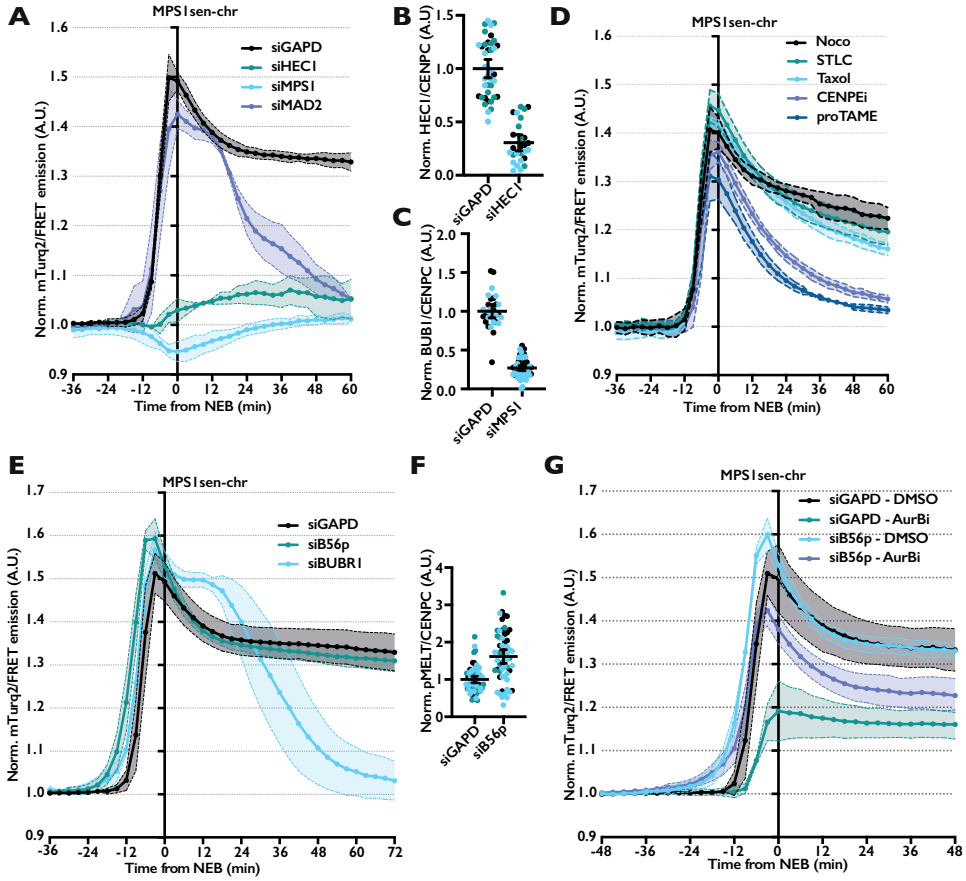

Supplemental Figure 3. Switch-like activation of MPS1 in prophase and PP2A-B56 regulates timing of prophase MPS1 activation. (**A**) FRET quantification (mean ±SD) of HeLa cells expressing MPS1sen-chr, depleted of indicated proteins. Depletion of HEC1 or MPS1 strongly impairs MPS1 activation as measured by MPS1sen-chr. SAC overwrite by siMAD2 does not affect MPS1 activity, in contrast to siBUBR1 (**Fig3D**). (**B,C,F**) From HeLa cells used in (A) or (E), the kinetochore-localization of indicated antigens was quantified by immunofluorescence. Data was normalized to siGAPD and shows the depletion efficiency in independent replicates. (**D, E**) Same data (mean ±SD) as in **Fig2D** and **Fig2G** showing extended FRET measurements in prometaphase. Note in (D) siBUBR1 overwrites the SAC and cells exit from nocodazole.

Supplemental Movie 1. MPS1 activation is restricted to the nucleus during prophase. HeLa cells expressing MPS1sen and IRES-PURO-P2A-mScarlet-NLS, imaged every ±20 from RO-3306 release. Fluorescent channels are mTurq2 (top left), mScarlet (top, right), FRET (YPet, bottom left), smoothed mTurq2/FRET (bottom, right). (https://youtu.be/kfmpvqviDLM)

Supplemental Movie 2. MPS1 activation is initiated before NEB and peaks around completion of NEB. HeLa cells expressing MPS1sen-chr and IRES-PURO-P2A-mScarlet-NLS, imaged every 3 min. from thymidine release (released 7 hrs. before imaging). Fluorescent channels are mTurq2 (top left), mScarlet (top, middle), FRET (YPet, bottom left), smoothed mTurq2/FRET (bottom, middle). Graphs display mTurq2 & YPet intensity traces (top) and normalized mTurq2/FRET ratio calculated from smoothed ratio data and the pooled mTurq/FRET (Bottom). (https://youtu.be/RI9BdfIVSBE)

Supplemental Movies 3-6. MPS1 activity in colon patient-derived tumour and healthy colon organoids. (**Movies 3-6**) Time-lapse movies of colon patient-derived organoids (PDOs) progressing through unperturbed mitosis. Cells were imaged every 5 minutes and analysed in Imaris. Both mTurq2 and FRET channels are visible and cells that were analysed have a pseudo colour coded surface overlay, indicating the mTurq2/FRET ratio. Note that the pseudo colour range varies between movies and cannot be directly compared. **Movie-3:** (https://youtu.be/TuGtjRoosPI), H1N colon PDO cell with robust MPS1 activity during mitotic cell division. **Movie-4:** (https://youtu.be/x7ZWildGeDg), 8T colon PDO 8T (non-hypermutated), **Movie-5:** (https://youtu.be/KtjTEIvkQ-s), 16T colon PDO 16T (non-hypermutated), **Movie-6**: (https://youtu.be/6B-RsV0DMJQ), U1T colon PDO U1T (hyper-mutated, MSI).

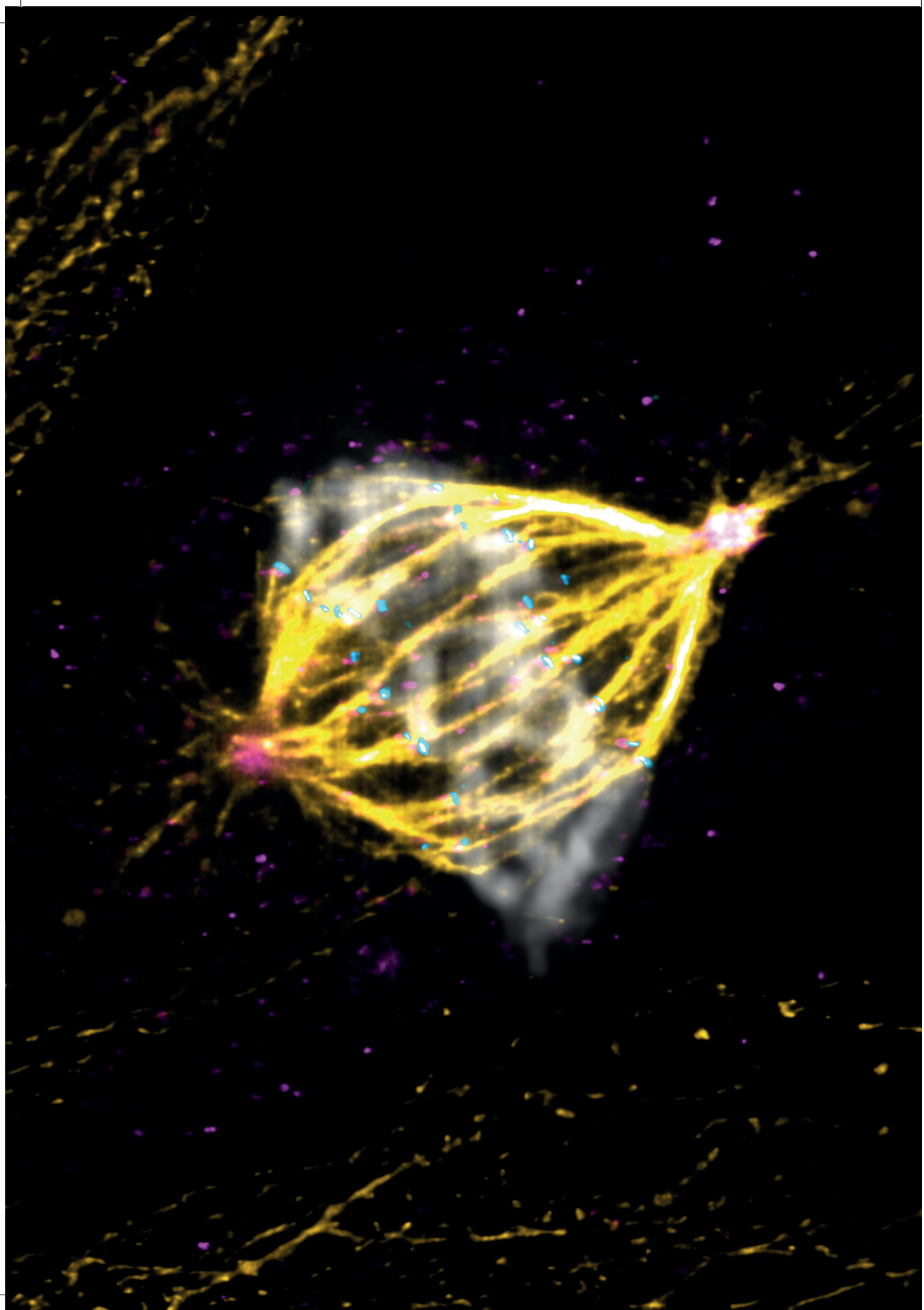

Chapter 5

Discussion

Mechanism of SAC reactivation by Mad1 tethering to metaphase kinetochores

In **Chapter 2** we show that artificially relocalising MAD1 to kinetochores at metaphase suffices to reactivate a SAC signal and halt cyclin B1 degradation. Retargeting MAD1 permits kinetochores to reinitiate the production of MCC. The interaction of MAD1 with MAD2 is essential for this, as a MAD1-mutant deficient in binding MAD2 ($MAD1^{K541/K543A}$) did not reactivate the SAC. Our data, and that of a corroborating study[410], suggest that upstream factors required for the catalysis of MCC are at least partly present on bioriented kinetochores at metaphase. We demonstrate that SAC reactivation induced by relocalising MAD1 to kinetochores at metaphase still depends on MPS1 activity and in **Chapter 4** we show that low levels of MPS1 activity persist on kinetochores at metaphase. Silencing the SAC at kinetochores thus critically depends on separating MAD1:MAD2 from the factors that orchestrate MAD2 activation and MCC assembly and these factors themselves appear to be not fully silenced on kinetochores at metaphase.

Recent studies have revealed that in addition to scaffolding the activation step of MAD2, MAD1 is also a kinetochore-receptor for cyclin B1/CDK1 and this interaction promotes efficient SAC signalling[244-246]. Could our observation, that the SAC is reactivated by targeting MAD1 to metaphase kinetochores, in part be attributed to relocalisation of cyclin B1/CDK1? We think not: Firstly, artificial relocalisation of $MAD1^{K541/K543A}$, did not reinstate the SAC and we assume the MAD1-cyclin B1 interaction is intact in this mutant as cyclin B1 binds near the N-terminus of MAD1[246]. As such, retargeting cyclin B1 alone to kinetochores at metaphase is unlikely to be sufficient for SAC reactivation. We cannot however rule out that cyclin B1/CDK1 activity has a non-essential contribution to SAC reactivation, for instance by acting upstream of MAD2-conversion to its active conformer at the MAD1:MAD2 dimers. Secondly, the activity of MPS1 is promoted by cyclin B1/CDK1[267, 383], therefore we would expect an increase in MPS1 activity upon retargeting of MAD1 and cyclin B1/CDK1. We did not measure an increase of downstream substrates of MPS1 at kinetochores (BUB1 or BUBR1), a finding corroborated by Ballister and colleagues[410]. Further analysis of MPS1 activity would be required to confirm this, for instance by quantifying the phosphorylation status of KNL1 on MELT-motifs[208, 417]. Measuring these sites would have an additional benefit of assessing a second role for CDK1 in the SAC, namely of inactivating the SAC silencing phosphatase PP1, who dephosphorylates the MELTs[150, 418].

It remains unclear what the role of cyclin B1/CDK1 is at kinetochores and investigating this is hampered by the presence of at least one additional cyclin B1 scaffold at kinetochores[246]. The MAD1-cyclin B1 interaction promotes robust SAC signalling as cells are more sensitive to partial MPS1 inhibition if the MAD1-cyclin B1 interaction is perturbed[246]. Although currently unknown, this could involve phosphorylation of MAD2 or CDC20[419]. To investigate how cyclin B1/CDK1 contributes to generating a robust SAC signal, inspiration may be taken from our study. Although our data

suggests that retargeting cyclin B1/CDK1 alone will not suffice for reactivation of the SAC on metaphase kinetochores, our assay enables examination of the cyclin B1/CDK1 contribution. Mutating the cyclin B1-binding site in MAD1 (MAD1-3EK[246]) and subsequently retargeting this MAD1-mutant to kinetochores at metaphase would be a direct way to examine how specifically the MAD1-associated pool of cyclin B1/CDK1 contributes to the SAC at a moment when other pools are already removed. An alternative approach would be to retain high levels of cyclin B1/CDK1 at kinetochores by directly tethering cyclin B1 to kinetochores and monitor mitotic progression. This approach could for instance reveal a role for cyclin B1/CDK1 in regulating stable attachments, a function previously hinted at[420].

Dissecting the regulation of MPS1 and Aurora B activity in response to end-on attachments

In **Chapter 3** we show that SAC satisfaction depends on formation of stable end-on attachments and does not require biorientation-associated inter- or intra-kinetochore stretch. By using a HEC1-mutant (HEC1-9A) we prevent Aurora B from destabilising end-on attachments. In addition, we perturb chromosome biorientation by inducing monopolar spindles, preventing kinetochores from enduring tension. By virtue of these two perturbations, stable kinetochore-microtubule attachments are formed in the absence of inter- or intra-kinetochore stretch. Given that tension is the key ingredient in the models on how Aurora B regulates outer kinetochore substrates including KNL1-pRVSF, an important question that arises from our work is: How is the kinase/phosphatase balance allowed to switch in favour of SAC silencing in the absence of tension?

The Aurora B and MPS1 signalling pathways are intricately linked, both regulating the SAC and kinetochore-microtubule attachment stability. This complicates interpretation of experiments that seek to untangle their roles but in which indirect effects on kinetochore-microtubule attachment stability are induced. Studies investigating SAC signalling use high concentrations of microtubule-depolymerising drugs to uncouple kinetochore-microtubule attachments from SAC silencing mechanisms. This however precludes the investigation of how end-on attachments modulate Aurora B and MPS1 signalling and of proteins that localise only to kinetochores with end-on attachments. Replacement of HEC1 with HEC1-9A in combination with imposing monopolar spindles in cells could be a practical assay to study attachment-dependent mechanisms that regulate Aurora B and MPS1 signalling. In this assay, attachment stability is ensured while leaving the signalling pathways that regulate attachment stability untouched, thus permitting the evaluation of mechanisms that regulate Aurora B and MPS1 activity without the concern of indirect effects through alterations in the attachment status of kinetochores.

Kinetochores that are bioriented and under tension have strongly reduced activity of Aurora B at outer kinetochores[54, 139]. The regulation of Aurora B in response to formation of tension is not clearly understood and several models have been proposed. The spatial separation model proposes that Aurora B activity originates from centromeres and is precluded from reaching the outer kinetochore as inter-kinetochore stretch distances the centromere from the outer kinetochore[139, 152-154]. In this model, Aurora B counteracting phosphatases at the outer kinetochore create a bistable switch for Aurora B activity[389]. Alternative models propose an active pool of Aurora B near the outer kinetochore and stretching within a kinetochore obstructs the binding site of this Aurora B pool[155, 159] or creates an increase in phosphatase activity that counteracts Aurora B signalling[147, 173]. In our HEC1-9A assay, biorientation is precluded and we do not measure significant intra-kinetochore stretching. This raises the question if Aurora B output is reduced by the formation of stable end-on attachments and which mechanisms then modulate Aurora B output at tensionless kinetochores.

It would be interesting to measure Aurora B activity in HEC1-9A cells with stable end-on attachments that are not bioriented and have no tension. If low or no Aurora B activity is measured at the outer kinetochores, it would suggest that tensionless mechanisms at end-on attachments regulate Aurora B activity at kinetochores. The opposite result, if high Aurora B activity were to persist, this would imply that kinetochore stretching (either inter or intra) is needed to regulate Aurora B activity. Aurora B activity can be measured by determining the phosphorylation status of various outer kinetochore substrates. By measuring phosphorylation of CENP-A Serine 7[421], Dsn1 Serine 110[54] (MIS12 complex) and the RVSF-motif in KNL1[54], changes in Aurora B activity could be observed when compared to unattached and metaphase kinetochores. Additionally, placing an Aurora B-specific FRET-biosensor[139] at the outer kinetochore would permit quantification of Aurora B activity closest to the microtubule binding interface of the kinetochore. Ascertaining if stable end-on attachments impact Aurora B activity could provide new insights into which mechanisms regulate Aurora B. Furthermore, as Aurora B acts upstream of MPS1 activation, the cross-talk between these pathways can be further investigated using this approach. We show that MPS1 output is reduced in HEC1-9A cells, as phosphorylation of MELT-motif on KNL1 is nearly absent. This implies either that KNL1-PP1 activity is high (and Aurora B activity is reduced) or reflects a reduction in MPS1 kinase activity. Recent work from our lab and others, showed that the MPS1-binding surfaces in HEC1/NUF2 are obstructed by end-on microtubule attachments[265, 266]. In HEC1-9A cells, MPS1 kinetochore localisation would be obstructed as end-on attachments are rapidly formed. Furthermore, MAD2 is strongly reduced at kinetochores, suggesting dynein-dependent stripping contributes to SAC silencing in our assay. It is unclear if additional mechanisms contribute to SAC satisfaction or if obstructing MPS1-binding sites and stripping of SAC components is sufficient. For instance, end-on attachments could result in a reduction of Aurora B

activity at the outer kinetochore and this would subsequently reduce MPS1 activation[240, 270, 364]. Vice-versa, obstructing MPS1 localisation could alleviate the positive feedback of MPS1 towards Aurora B and reduce the local activity of Aurora B at the outer kinetochore.

The role of PP1 in regulating MPS1 and Aurora B at kinetochores

Several pools of PP1 and B56 phosphatases have been shown to modulate the SAC and error correction activities of MPS1[290, 294, 295], Aurora B[143, 150] and PLK1[390, 409, 422] at kinetochores. In the absence of microtubules, kinetochores are decorated with high levels of BUBR1- and Sgo1-associated B56 complexes which oppose Aurora B[143, 144] activity. In turn, Aurora B inhibits kinetochore-localisation of several PP1 pools. As kinetochore attachments mature, levels of the PP1-scaffolding proteins KIF18A[163] Astrin-SKAP[176, 423] and the SKA complex[97, 100, 166], accumulate at the outer kinetochore. Aurora B inhibits the kinetochore localisation of both Astrin[158, 423] SKA[104, 151, 166, 177] and KIF18A[163-165], thereby precluding these pools of PP1 from localising to kinetochores. In addition, CENP-E[162] and KNL1[147] scaffold PP1 at kinetochores and Aurora B phosphorylates their PP1-binding motifs to preclude PP1 localisation. Our data show that KNL1-PP1 is sufficiently active as MPS1-dependent phosphorylation of MELT-motifs is nearly absent in monopolar HEC1-9A cells. Dissecting the function of these other PP1 pools is hampered by feedbacks that arise when manipulating a given pool. For example, the C-terminal domain (CTD) in Ska1 contains both the PP1- and microtubule-binding sites[104, 151]. The SKA-complex binds microtubules and depletion of Ska1 results in the destabilisation of kinetochore-microtubule attachments[97, 100, 102, 105, 239, 424, 425]. It was shown that deleting the PP1-binding domain (Ska1-ΔCTD) results in a strong metaphase-delay and increased the phosphorylation of a MELT-motif[177]. This suggests that MPS1 activity or substrate phosphorylation (lack of KNL1-PP1 activity) are affected in Ska1-ΔCTD. This phenotype could be rescued by fusing a well characterised PP1-binding motif to Ska1-ΔCTD[177], suggesting this phenotype is not caused by the inability of Ska to bind microtubules. Nevertheless, PP1 might counteract a pathway that destabilises attachments. The SKA-complex in *C. elegans*, for example, was shown to be important for the dephosphorylation of the HEC1-tail[67]. The metaphase-delay and elevated MELT-phosphorylation in cells expressing the Ska1-ΔCTD-PP1 fusion could originate from subtle attachments defects not detected in this study. It thus remains unclear if Ska1-PP1 regulates either Aurora B or MPS1 activity or alternatively act as an activator for other PP1 pools at kinetochores[148]. As both Aurora B and MPS1 regulate kinetochore-microtubule attachment stability independently from each other[239, 240] and MPS1 additionally activates the SAC, it is difficult to discriminate these functions. By ensuring end-on attachments remain stable in cells with monopolar spindles, the function of Ska1-PP1 in regulating attachment stability can be uncoupled from possible other functions.

This approach could be extended to studying the roles of KIF18A-PP1, CENP-E-PP1 and Astrin-PP1, as attachment stability might inadvertently be affected for

when perturbing their interaction with PP1. For instance, perturbing the KIF18A-PP1 interaction was reported to arrest cells at metaphase with fully-functional attachments[426], yet subtle defects in attachment stability could have gone unnoticed in this study. In the case of CENP-E-PP1, congressed chromosomes still require an intact CENP-E-PP1 interaction to maintain stable microtubule-attachment, suggesting this pool of PP1 might oppose attachment-destabilising pathways[162]. Perturbing the Astrin-PP1 interaction destabilised attachments and increased MAD2 localisation at kinetochores[158], it remains unclear if Astrin-PP1 counteracts Aurora B or MPS1. Investigating the role of above-mentioned PP1-scaffolds in monopolar HEC1-9A conditions is only feasible if their kinetochore-localisation is not regulated by inter- and intra-kinetochore stretch.

Is MPS1 active during interphase?

During mitosis, MPS1 regulates kinetochore-microtubule attachments and orchestrates the catalysis of MCC complexes at kinetochores[381]. Mounting evidence shows that low levels of MCC are present during interphase[219, 222, 427], and that MAD1:MAD2 at nuclear pores facilitates interphase-MCC production[221]. Nuclear pore localisation of MPS1 has been described[276], conveniently placing the orchestrator of MCC production in close proximity to MAD1:MAD2 in interphase cells. It was proposed that interphase-MCC (iMCC) is produced in an MPS1-dependent manner[277], however no activity of MPS1 has been shown at nuclear pores. Furthermore, recent work suggests that MPS1 activity is not required for iMCC production as a robust SAC arrest was observed when MPS1 inhibition was combined with perturbing the pathways that disassemble iMCC[222]. It is unclear if MPS1 activity exists during interphase and if this activity is important for iMCC production. In **Chapter 4** we show that MPS1 activity was not detectable until 9-12 minutes before NEB using either nuclear-localised or chromatin-associated MPS1sen. As MPS1 localises to nuclear pores and iMCC is likely produced at this location we sought to measure MPS1 activity near nuclear pores by fusing MPS1sen to Lamin A, Lamin B1, Emerin, NUP85 or fragments of TPR[302] and Lamin B1 receptor. Unfortunately, MPS1sen fusion to these proteins either delocalised the fusion protein or impaired protein expression, precluding us from measuring MPS1 activity at the nuclear pore/lamina. We therefore cannot rule out that a transient pool of active MPS1 exists at the nuclear envelope during interphase.

Interphase-MCC was shown to be important for accumulating sufficient cyclin B1 in G2-phase[222]. However, it is unclear if iMCC is produced only in G2 phase or also at phases of the cell cycle where cyclin B1 is absent. Interestingly, the MCC components C-MAD2 and BUBR1 are repurposed during interphase to regulate insulin receptor (IR) endocytosis[428, 429]. As the APC/C^{CDC20} has several non-mitotic functions[430-433], it is tempting to speculate that iMCC might be repurposed entirely and potentially does not depend on MPS1 activity for its production.

Regulating the timing of MPS1 activation

We show in **Chapter 4** that activation of MPS1 occurs 9-12 minutes before NEB, with switch-like kinetics after which the activity of MPS1 is damped in prometaphase. Aurora B is known to promote MPS1 activation[270, 280, 364] and indeed Aurora B inhibition slightly delayed MPS1 activation and prevented full MPS1 activation in our study. Recent work has demonstrated that the BUBR1 pool of B56 regulates MPS1 directly[290, 294] in addition to regulating Aurora B activity[143, 144, 146, 150]. We found that depletion of all B56 isoforms slightly increased maximum MPS1 activation at onset of mitosis. Similarly, BUBR1 depletion increased pre-NEB activity of MPS1, consistent with a role for B56 in counteracting MPS1 activity. A more striking observation was that BUBR1 or B56 depletion prematurely activated MPS1, shifting MPS1 activation to 15-18 minutes pre-NEB. To determine if premature activation of MPS1 in B56-depleted cells was due to premature Aurora B activity, we inhibited Aurora B in B56-depleted cells. This did not restore timing of MPS1 activation, suggesting that B56 regulates MPS1 activation downstream or independently of Aurora B input (**Figure 1A**). Interestingly, Aurora B inhibition displaces MPS1 from kinetochores in prometaphase and B56 depletion to rescues MPS1 kinetochore localisation[294].

Many questions arise from our observations and the molecular mechanism by with B56 regulates the timing of MPS1 activation remains to be explored. Firstly, it is unclear if premature activation of MPS1 is kinetochore-dependent. HEC1 levels at kinetochores are undetectable until late G2 and HEC1-loading is regulated by cyclin B1/CDK1-depedent phosphorylation of CENP-T[434, 435]. We show that MPS1 activation is strongly impaired by HEC1 depletion, consistent with previous work showing HEC1 is essential for MPS1 activation[255, 265, 266, 371]. By depleting the kinetochore scaffolds of HEC1 (CENP-C and CENP-T) and measuring kinetochore localisation of HEC1 in G2-phase the role of HEC1 at kinetochores in initiating MPS1 activation could be addressed.

Secondly, the finding that BUBR1 depletion also results in premature activation of MPS1 is surprising as BUBR1 localises to the cytoplasm in interphase[344, 436] and interacts with B56 only after NEB[291]. It is therefore unlikely that a kinetochore pool of BUBR1 could regulate MPS1 activation, implying a function for BUBR1 in the cytoplasm. To further investigate this pathway, replacement of BUBR1 with a mutant that cannot bind B56[149] could show that premature activation of MPS1 is regulated by B56 and not through other functions of BUBR1.

Our preliminary data shows that depletion of B56α+ϵ alone suffices to prematurely activate MPS1 (data not shown). During interphase, B56 isoforms were reported to differentially localise to either the nucleus (B56δ/γ) or the cytoplasm (B56α/β/ϵ)[437, 438] and furthermore, B56α was enriched at centrosomes[437, 439]. Loss of cytoplasmic B56 could potentially alleviate inhibition of MPS1, similar to the proposed mitotic function of BUBR1-B56 in opposing MPS1 activity at the kinetochore[239, 290, 294]. Further deconvolving

which B56 isoform specifically regulates the timing of MPS1 activation would simplify future experimental design.

During mitosis, PLK1 regulates the BUBR1-B56 interaction at kinetochores by phosphorylating S676 and T680 on BUBR1[146, 149]. Interestingly, partial inhibition of PLK1 was found to prematurely localise MPS1 in G2-phase[409]. This warrants further inquiry on a putative role of PLK1 in regulating the timing of MPS1 activation. For instance, a complex of PLK1-BUBR1-B56 might regulate either the timing of MPS1 activation or nuclear translocation of MPS1. Therefore, the localisation of MPS1 in interphase should be carefully examined in B56 or BUBR1-depleted cells. Furthermore, centrosomes cluster numerous proteins including PLK1[440], HEC1[434], BUBR1[441], B56α[437, 439], MPS1[250, 274] and low levels of active cyclin B1/CDK1[28, 31]. It is therefore tempting to speculate that either MPS1 nuclear translocation or initial MPS1 activation is regulated at centrosomes. We placed MPS1sen at centrosomes (by fusion to centrin-1) and did not observe significant dynamic activity of MPS1 (data not shown), however we did not specifically investigate MPS1 activation in B56 or BUBR1-depleted conditions.

A model for MPS1 activation at onset of mitosis

Bistable systems have been found to regulate the activation of several mitotic kinases, including Aurora B[389] and cyclin B1/CDK1. In a bistable system[442], the kinase may be found in either an active or inactive state, but no intermediate states are found (**Figure 1B**). Kinase activation is initially inhibited by an inhibitory signal, setting a threshold for the input signal to overcome. When the activation signal surpasses the threshold, a positive feedback loop ensures rapid activation. Bistable systems exhibit hysteresis, where switching the kinase from one state to the other is more difficult than maintaining it in its current state. This allows the input signal to fall below the initial threshold required for activation without switching the kinase off.

We show in **Chapter 4** that activation of MPS1 is initially inhibited by BUBR1-B56 during G2-phase. Once sufficient input signal is generated, MPS1 activation occurs with switch-like kinetics. After NEB, MPS1 activity is dampened by BUBR1-B56. Furthermore, we found that titration of an MPS1 inhibitor generates either predominantly active or inactive MPS1 at kinetochores around the IC50 value. Together, these characteristics are reminiscent of a bistable system. A more thorough investigation is warranted to show MPS1 bistability, similar to experimental designs used to show Aurora B bistability[389]. By inhibiting MPS1 activity with inhibitor concentrations close to its kinetochore-IC50 value, a single concentration might be found in which MPS1 exists in either an active or inactive state, as bistability models predict.

A possible model describing MPS1 activation (**Figure 1C**) could involve initial inhibition by BUBR1-B56, similar to the proposed role of BUBR1-B56 in opposing MPS1 activity during mitosis[294]. A potential trigger for MPS1 activation might be

the phosphorylation of MPS1 by cyclin B1/CDK1, promoting HEC1/NUF2-binding of MPS1[266, 383]. In the nucleus, Aurora B promotes the activation of MPS1 possibly by suppressing the activity of PP1. Cyclin B1/CDK1 and Aurora B jointly promote trans-autoactivation of MPS1 at kinetochores. In a positive feedback loop, MPS1 promotes activity of its own activators, clustering Aurora B at centromeres and sequestering MAD1-cyclin B1/CDK1 to kinetochores. This mechanism ensures the rapid and switch-like activation of MPS1 during prophase. After NEB, this positive feedback loop switches to negative feedback as MPS1 recruits BUBR1 to the kinetochores and the antagonising phosphatase B56 is indirectly recruited by cyclin B1/CDK1[146, 330] and PLK1[149, 291, 443].

An important constraint in studying MPS1 signalling is the uncertainty of which phosphatase opposes MPS1. Both B56[290, 294] and PP1[229, 295] have been proposed to perform this function. Both phosphatases have also been reported to regulate Aurora B activity[143, 444], further complicating interpretation of experimental data. Additionally, a study in yeast suggested that an interaction between PP1 and B56 occurs[445], potentially explaining why both PP1[229, 295] and B56[290, 294] phosphatases can regulate MPS1. Resolving the specificity of these phosphatases is a challenging future undertaking, but is needed to interpret the various effects seen upon their depletion/delocalization.

Unravelling the mechanism by which Aurora B promotes MPS1 activation would also aid in understanding how MPS1 activation occurs. Recent work has established a recurring mechanism in which Aurora B phosphorylates the R/K-V-S-F-motif to preclude PP1-binding on numerous proteins[178]. An untested hypothesis we put forward is one where Aurora B phosphorylates ARHGEF17 on its PP1-binding motif KVSF (amino acids 374-377)[178], to disrupt PP1-binding and thereby permit MPS1 kinetochore clustering and auto-activation. This would be consistent with a role of both Aurora B[255, 270, 364] and ARHGEG17[269] as upstream regulators of MPS1 kinetochore-localisation. Alternatively, Aurora B-dependent regulation of KIF18A-PP1 and or Ska1-PP1 could regulate either MPS1 localisation or activation.

Multiplexing kinase sensors to dynamically monitor cross-talk and feedback loops

Complex signalling pathways with crosstalk and several layers of feedback generate a graded signal and thereby regulate chromosome alignment and SAC signalling during mitosis. Inhibition of a single kinase can impact multiple pathways and interpreting the results can be complex. Common strategies utilise antibodies to probe the phosphorylation state of a known kinase substrate and use this mark to infer the activity status of the kinase. Changes in substrate phosphorylation can reflect modulation of kinase activity or result from a change in opposing phosphatase activity. By selectively inhibiting both kinase and phosphatase it is possible to delineate the signalling pathway. The ability to measure multiple such substrates within a single cell would allow correlation of dynamic changes across several pathways, while avoiding adverse effects induced by

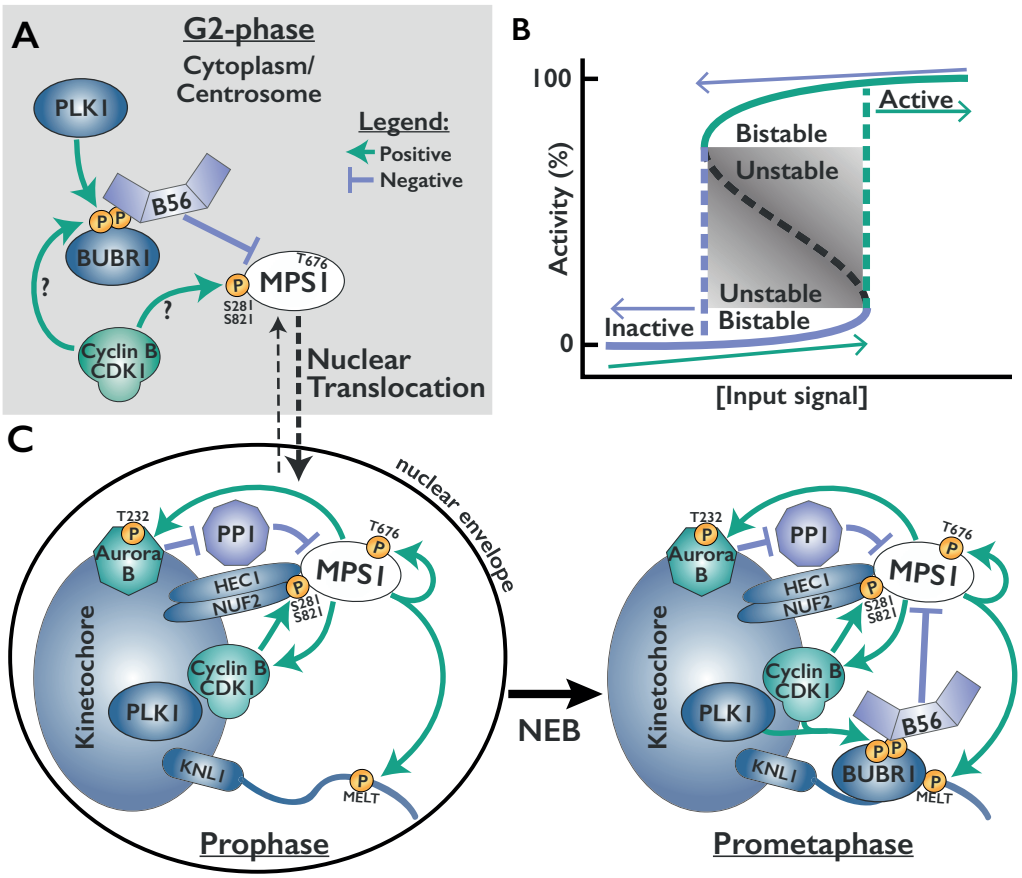

Figure 1. Model of MPS1 activation. (**A**) Model for MPS1 inhibition in G2-phase (grey panel). Colours represent positive signal (green) or negative signal (purple). BUBR1-B56 restricts MPS1 activation in the cytoplasm or at centrosomes (or prevents nuclear translocation). The BUBR1-B56 interaction might be promoted by cyclin B1/CDK1 and PLK1. An unknown mechanism directs MPS1 nuclear translocation, potentially cyclin B1/CDK1 directs this critical step. (**B**) Graph of a bistable kinase system. A negative signal (purple arrow, bottom) keeps the system inactive. To breach the negative signal, a high input signal is required (green arrow, bottom). Once this threshold is reached, the system rapidly switches to an active state. In the active state, the system is tolerant to a reduction in input signal (purple arrow, top) without switching off, this is the bistable zone. A further decrease of the input signal switches the system off and no intermediate activity state is stable. (**C**) Model for regulation of MPS1 activity at prophase (left) and prometaphase (right). Cytoplasmic/centrosome is described in (**A**). once MPS1 translocates in the nucleus, cyclin B1/CDK1 phosphorylates MPS1 to promote its kinetochore localisation. Aurora B enhances MPS1 activation, possibly by inhibiting PP1 localisation at kinetochores (we speculate Aurora B regulates ARHGEF17-PP1 binding, not shown). MPS1 trans-autoactivates and subsequently phosphorylates MELT-motifs, however in prophase BUBR1 remains in the cytoplasm. The positive feedback loop that allows rapid MPS1 activation is repressed with the recruitment of BUBR1-B56 to kinetochores in prometaphase. BUBR1-B56 either impinges Aurora B or MPS1 activity, reducing their kinetochore signalling.

experimental variation. For instance, the recently developed method to sequentially probe epitopes in single cells by iterative indirect immunofluorescence imaging (i4)[446], would be interesting to apply in researching mitotic signalling pathways if quantitative measurements are feasible. Nevertheless, measuring substrate phosphorylation provides a static image of dynamic signalling pathways.

FRET biosensors provide a dynamic readout of signalling pathways and allow interrogation of activity at locations where no known substrates have been identified. Recent advances in fluorescent protein engineering have yielded a method to generate single colour FRET biosensors, given that FRET is quantitatively measured using fluorescent lifetime imaging microscopy (FLIM). By substituting the fluorescent acceptor for a non-emitting version in biosensors (e.g. ShadowG[447] or Y[448]), only a single fluorescent channel is required for quantification[448, 449]. As biosensors specific for Aurora B, PLK1, CDK1 and now MPS1 are available, it would be highly informative if two signalling pathways could be monitored nearly simultaneously in live cells. For instance, simultaneously monitoring the signal output of MPS1 and Aurora B during nuclear envelope breakdown could reveal an initial change in one pathway to which the second pathway responds. By specifically altering the localisation of one counteracting phosphatase (e.g. BUBR1-B56 or KNL1-PP1) the changes in both signalling pathways could be observed. By correlation changes in two pathways, subtle dynamics behaviour such as delayed-responses or oscillations in signal output preceding the establishment of an equilibrium state could be observed. Such observations could greatly enhance our understanding of signalling pathways and provide new insight to refine *in silico* models. It goes without saying that converting biosensors would require extensive testing to ensure the specificity and dynamic range of the sensors is maintained. But if achieved, multiplexing live kinase sensors could provide unprecedented insights into regulation of the mitotic programs.

Concluding remarks

The work presented in this thesis contributes to improved understanding of the fundamental aspects of SAC signalling and silencing. We reveal that the removal of MAD1 from kinetochores is the key step in SAC silencing and definitively show that SAC satisfaction requires end-on attachments but not tension. Our work additionally provides a novel instrument to advance our understanding of MPS1 regulation and we uncover a regulatory mechanism that governs the timing of MPS1 activation. Developing novel instruments to measure and manipulate activities and interactions at subcellular locations, including the kinetochore, will greatly increase our understanding of the molecular orchestration of complex signalling pathways.

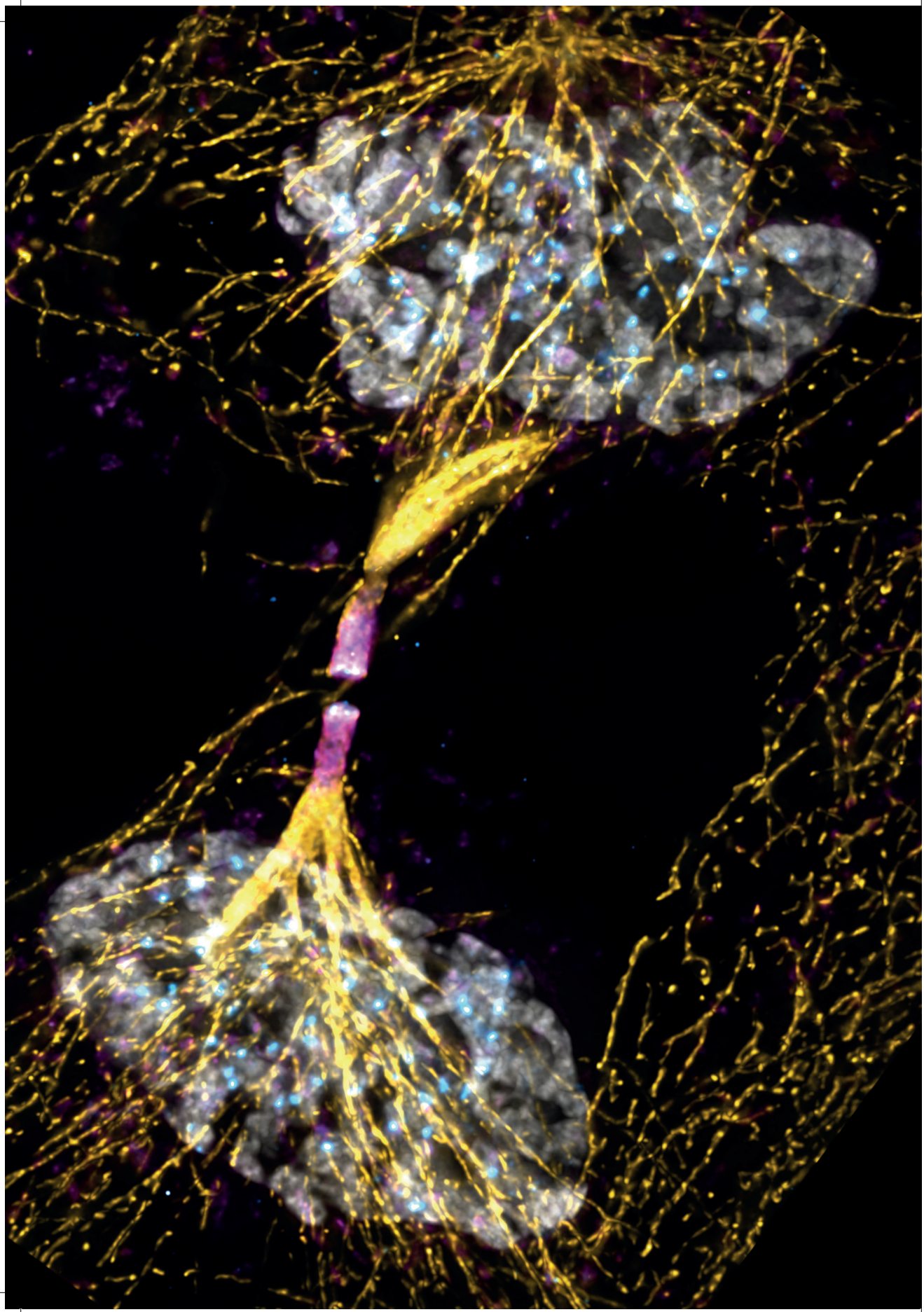

Addendum

References

1. Gordon, D.J., Resio, B. & Pellman, D. Causes and consequences of aneuploidy in cancer. *Nature Reviews Genetics* **13**, 189-203 (2012).
2. Chunduri, N.K. & Storchová, Z. The diverse consequences of aneuploidy. *Nat Cell Biol* **21**, 54-62 (2019).
3. Hinchcliffe, E.H. *et al.* Chromosome missegregation during anaphase triggers p53 cell cycle arrest through histone H3.3 Ser31 phosphorylation. *Nat Cell Biol* **18**, 668 (2016).
4. Santaguida, S. *et al.* Chromosome Mis-segregation Generates Cell-Cycle-Arrested Cells with Complex Karyotypes that Are Eliminated by the Immune System. *Developmental Cell* **41**, 638-651.e635 (2017).
5. Ambartsumyan, G. & Clark, A.T. Aneuploidy and early human embryo development. *Human Molecular Genetics* **17**, R10-R15 (2008).
6. Cromie, Gareth A. & Dudley, Aimée M. Aneuploidy: Tolerating Tolerance. *Current Biology* **25**, R771-R773 (2015).
7. Antonarakis, S.E., Lyle, R., Dermitzakis, E.T., Reymond, A. & Deutsch, S. Chromosome 21 and Down syndrome: from genomics to pathophysiology. *Nature Reviews Genetics* **5**, 725-738 (2004).
8. Helm, S. & Mitelman, F. Nonrandom Chromosome Abnormalities in Cancer—An Overview. *Cancer Cytogenetics*, 25-43 (2010).
9. Hanahan, D. & Weinberg, Robert A. Hallmarks of Cancer: The Next Generation. *Cell* **144**, 646-674 (2011).
10. Duijf, P.H.G., Schultz, N. & Benezra, R. Cancer cells preferentially lose small chromosomes. *International Journal of Cancer* **132**, 2316-2326 (2013).
11. Zack, T.I. *et al.* Pan-cancer patterns of somatic copy number alteration. *Nat Genet* **45**, 1134-1140 (2013).
12. Janssen, A., van der Burg, M., Szuhai, K., Kops, G.J.P.L. & Medema, R.H. Chromosome segregation errors as a cause of DNA damage and structural chromosome aberrations. *Science* **333**, 1895-1898 (2011).
13. Weaver, B.A.A. & Cleveland, D.W. Does aneuploidy cause cancer? *Current Opinion in Cell Biology* **18**, 658-667 (2006).
14. Weaver, B.A.A. & Cleveland, D.W. The role of aneuploidy in promoting and suppressing tumors. *The Journal of Cell Biology* **185**, 935-937 (2009).
15. Santaguida, S. & Amon, A. Short- and long-term effects of chromosome mis-segregation and aneuploidy. *Nat Rev Mol Cell Biol* **16**, 473 (2015).
16. Thompson, S.L., Bakhoum, S.F. & Compton, D.A. Mechanisms of chromosomal instability. *Curr Biol* **20**, R285-295 (2010).
17. Thompson, S.L. & Compton, D.A. Examining the link between chromosomal instability and aneuploidy in human cells. *J Cell Biol* **180**, 665-672 (2008).
18. Lengauer, C., Kinzler, K.W. & Vogelstein, B. Genetic instabilities in human cancers. *Nature* **396**, 643-649 (1998).
19. Vogelstein, B. *et al.* Cancer Genome Landscapes. *Science* **339**, 1546 (2013).
20. Cahill, D.P. *et al.* Mutations of mitotic checkpoint genes in human cancers. *Nature* **392**, 300-303 (1998).
21. Sotillo, R., Schvartzman, J.-M., Socci, N.D. & Benezra, R. Mad2-induced chromosome instability leads to lung tumour relapse after oncogene withdrawal. *Nature* **464**, 436-440 (2010).
22. Schvartzman, J.-M., Duijf, Pascal H.G., Sotillo, R., Coker, C. & Benezra, R. Mad2 Is a Critical Mediator of the Chromosome Instability Observed upon Rb and p53 Pathway Inhibition. *Cancer Cell* **19**, 701-714 (2011).
23. Malumbres, M. & Barbacid, M. To cycle or not to cycle: a critical decision in cancer. *Nature Reviews Cancer* **1**, 222-231 (2001).
24. Coudreuse, D. & Nurse, P. Driving the cell cycle with a minimal CDK control network. *Nature* **468**, 1074 (2010).
25. Lukas, C. *et al.* Accumulation of cyclin B1 requires E2F and cyclin-A-dependent

rearrangement of the anaphase-promoting complex. *Nature* **401**, 815-818 (1999).
26. Krasinska, L. *et al.* Protein Phosphatase 2A Controls the Order and Dynamics of Cell-Cycle Transitions. *Molecular Cell* **44**, 437-450 (2011).
27. Mueller, P.R., Coleman, T.R. & Dunphy, W.G. Cell cycle regulation of a Xenopus Wee1-like kinase. *Mol Biol Cell* **6**, 119-134 (1995).
28. Jackman, M., Lindon, C., Nigg, E.A. & Pines, J. Active cyclin B1–Cdk1 first appears on centrosomes in prophase. *Nat Cell Biol* **5**, 143-148 (2003).
29. Larochelle, S. *et al.* Requirements for Cdk7 in the Assembly of Cdk1/Cyclin B and Activation of Cdk2 Revealed by Chemical Genetics in Human Cells. *Molecular Cell* **25**, 839-850 (2007).
30. Tuck, C., Zhang, T.L., Potapova, T., Malumbres, M. & Novak, B. Robust mitotic entry is ensured by a latching switch. *Biology Open* **2**, 924-931 (2013).
31. Lindqvist, A., Källström, H., Lundgren, A., Barsoum, E. & Rosenthal, C.K. Cdc25B cooperates with Cdc25A to induce mitosis but has a unique role in activating cyclin B1–Cdk1 at the centrosome. *The Journal of Cell Biology* **171**, 35 (2005).
32. Hoffmann, I., Clarke, P.R., Marcote, M.J., Karsenti, E. & Draetta, G. Phosphorylation and activation of human cdc25-C by cdc2--cyclin B and its involvement in the self-amplification of MPF at mitosis. *The EMBO Journal* **12**, 53-63 (1993).
33. Fisher, D., Krasinska, L., Coudreuse, D. & Novák, B. Phosphorylation network dynamics in the control of cell cycle transitions. *Journal of Cell Science* **125**, 4703 (2012).
34. Baumann, K. Activities of a mitotic master. *Nat Rev Mol Cell Biol* **11**, 389 (2010).
35. Clute, P. & Pines, J. Temporal and spatial control of cyclin B1 destruction in metaphase. *Nat Cell Biol* **1**, 82-87 (1999).
36. Pines, J. & Rieder, C.L. Re-staging mitosis: a contemporary view of mitotic progression. *Nat Cell Biol* **3**, E3-E6 (2001).
37. Peters, J.-M. & Nishiyama, T. Sister Chromatid Cohesion. *Cold Spring Harbor Perspectives in Biology* **4** (2012).
38. Zlotorynski, E. Mitotic chromatin condensin. *Nat Rev Mol Cell Biol* **17**, 610 (2016).
39. Lancaster, Oscar M. *et al.* Mitotic Rounding Alters Cell Geometry to Ensure Efficient Bipolar Spindle Formation. *Developmental Cell* **25**, 270-283 (2013).
40. Coue, M., Lombillo, V.A. & McIntosh, J.R. Microtubule depolymerization promotes particle and chromosome movement in vitro. *The Journal of Cell Biology* **112**, 1165 (1991).
41. McEwen, B.F., Heagle, A.B., Cassels, G.O., Buttle, K.F. & Rieder, C.L. Kinetochore Fiber Maturation in PtK₁ Cells and Its Implications for the Mechanisms of Chromosome Congression and Anaphase Onset. *The Journal of Cell Biology* **137**, 1567 (1997).
42. Koshland, D.E., Mitchison, T.J. & Kirschner, M.W. Polewards chromosome movement driven by microtubule depolymerization in vitro. *Nature* **331**, 499-504 (1988).
43. Putkey, F.R. *et al.* Unstable kinetochore-microtubule capture and chromosomal instability following deletion of CENP-E. *Developmental Cell* **3**, 351-365 (2002).
44. Zhu, C. *et al.* Functional analysis of human microtubule-based motor proteins, the kinesins and dyneins, in mitosis/cytokinesis using RNA interference. *Mol Biol Cell* **16**, 3187-3199 (2005).
45. Giménez-Abián, J.F., Díaz-Martínez, L.A., Wirth, K.G., De la Torre, C. & Clarke, D.J. Proteasome activity is required for centromere separation independently of securin degradation in human cells. *Cell Cycle* **4**, 1558-1560 (2005).
46. Santaguida, S. & Musacchio, A. The life and miracles of kinetochores. *The EMBO Journal* **28**, 2511-2531 (2009).
47. McEwen, B.F. *et al.* CENP-E Is Essential for Reliable Bioriented Spindle Attachment, but Chromosome Alignment Can Be Achieved via Redundant Mechanisms in Mammalian Cells. *Mol Biol Cell* **12**, 2776-2789 (2001).

48. Earnshaw, W.C. & Rothfield, N. Identification of a family of human centromere proteins using autoimmune sera from patients with scleroderma. *Chromosoma* **91**, 313-321 (1985).
49. Masumoto, H., Masukata, H., Muro, Y., Nozaki, N. & Okazaki, T. A human centromere antigen (CENP-B) interacts with a short specific sequence in alphoid DNA, a human centromeric satellite. *The Journal of Cell Biology* **109**, 1963 (1989).
50. Yan, K. *et al.* Structure of the inner kinetochore CCAN complex assembled onto a centromeric nucleosome. *Nature* **574**, 278-282 (2019).
51. Kato, H. *et al.* A Conserved Mechanism for Centromeric Nucleosome Recognition by Centromere Protein CENP-C. *Science* **340**, 1110-1113 (2013).
52. Cheeseman, I.M., Chappie, J.S., Wilson-Kubalek, E.M. & Desai, A. The Conserved KMN Network Constitutes the Core Microtubule-Binding Site of the Kinetochore. *Cell* **127**, 983-997 (2006).
53. Espeut, J., Cheerambathur, D.K., Krenning, L., Oegema, K. & Desai, A. Microtubule binding by KNL-1 contributes to spindle checkpoint silencing at the kinetochore. *The Journal of Cell Biology* (2012).
54. Welburn, J.P.I. *et al.* Aurora B phosphorylates spatially distinct targets to differentially regulate the kinetochore-microtubule interface. *Molecular Cell* **38**, 383-392 (2010).
55. McCleland, M.L. *et al.* The Vertebrate Ndc80 Complex Contains Spc24 and Spc25 Homologs, which Are Required to Establish and Maintain Kinetochore-Microtubule Attachment. *Current Biology* **14**, 131-137 (2004).
56. Wigge, P.A. & Kilmartin, J.V. The Ndc80p Complex from Saccharomyces cerevisiae Contains Conserved Centromere Components and Has a Function in Chromosome Segregation. *The Journal of Cell Biology* **152**, 349 (2001).
57. DeLuca, J.G., Moree, B., Hickey, J.M., Kilmartin, J.V. & Salmon, E.D. hNuf2 inhibition blocks stable kinetochore–microtubule attachment and induces mitotic cell death in HeLa cells. *The Journal of Cell Biology* **159**, 549 (2002).
58. McCleland, M.L. *et al.* The highly conserved Ndc80 complex is required for kinetochore assembly, chromosome congression, and spindle checkpoint activity. *Genes & Development* **17**, 101-114 (2003).
59. Ciferri, C. *et al.* Architecture of the Human Ndc80-Hec1 Complex, a Critical Constituent of the Outer Kinetochore. *Journal of Biological Chemistry* **280**, 29088-29095 (2005).
60. Wei, R.R., Sorger, P.K. & Harrison, S.C. Molecular organization of the Ndc80 complex, an essential kinetochore component. *Proc Natl Acad Sci USA* **102**, 5363 (2005).
61. Emanuele, M.J., McCleland, M.L., Satinover, D.L. & Stukenberg, P.T. Measuring the Stoichiometry and Physical Interactions between Components Elucidates the Architecture of the Vertebrate Kinetochore. *Mol Biol Cell* **16**, 4882-4892 (2005).
62. Suzuki, A., Badger, B.L. & Salmon, E.D. A quantitative description of Ndc80 complex linkage to human kinetochores. *Nature Communications* **6**, 8161 (2015).
63. Dong, Y., Vanden Beldt, K.J., Meng, X., Khodjakov, A. & McEwen, B.F. The outer plate in vertebrate kinetochores is a flexible network with multiple microtubule interactions. *Nat Cell Biol* **9**, 516 (2007).
64. Alushin, G.M. *et al.* The Ndc80 kinetochore complex forms oligomeric arrays along microtubules. *Nature* **467**, 805 (2010).
65. Umbreit, N.T. *et al.* The Ndc80 kinetochore complex directly modulates microtubule dynamics. *Proceedings of the National Academy of Sciences* **109**, 16113 (2012).
66. Volkov, V.A., Huis in 't Veld, P.J., Dogterom, M. & Musacchio, A. Multivalency of NDC80 in the outer kinetochore is essential to track shortening microtubules and generate forces. *eLife* **7**, e36764 (2018).
67. Cheerambathur, D.K. *et al.* Dephosphorylation of the Ndc80 Tail Stabilizes Kinetochore-Microtubule Attachments via the Ska Complex. *Developmental Cell*

41, 424-437.e424 (2017).
68. Nishino, T. *et al.* CENP-T provides a structural platform for outer kinetochore assembly. *The EMBO Journal* (2013).
69. Martin-Lluesma, S., Stucke, V.M. & Nigg, E.A. Role of Hec1 in Spindle Checkpoint Signaling and Kinetochore Recruitment of Mad1/Mad2. *Science* **297**, 2267 (2002).
70. Ciferri, C. *et al.* Implications for Kinetochore-Microtubule Attachment from the Structure of an Engineered Ndc80 Complex. *Cell* **133**, 427-439 (2008).
71. Wei, R.R., Al-Bassam, J. & Harrison, S.C. The Ndc80/HEC1 complex is a contact point for kinetochore-microtubule attachment. *Nature Structural & Molecular Biology* **14**, 54-59 (2007).
72. DeLuca, J.G. *et al.* Kinetochore Microtubule Dynamics and Attachment Stability Are Regulated by Hec1. *Cell* **127**, 969-982 (2006).
73. Guimaraes, G.J., Dong, Y., McEwen, B.F. & DeLuca, J.G. Kinetochore-Microtubule Attachment Relies on the Disordered N-Terminal Tail Domain of Hec1. *Current Biology* **18**, 1778-1784 (2008).
74. Itoh, G. *et al.* Lateral attachment of kinetochores to microtubules is enriched in prometaphase rosette and facilitates chromosome alignment and bi-orientation establishment. *Sci. Rep.* **8**, 3888 (2018).
75. Magidson, V. *et al.* Adaptive changes in the kinetochore architecture facilitate proper spindle assembly. *Nature* (2015).
76. Sacristan, C. *et al.* Dynamic kinetochore size regulation promotes microtubule capture and chromosome biorientation in mitosis. *Nat Cell Biol* **20**, 800-810 (2018).
77. Maiato, H., Gomes, M.A., Sousa, F. & Barisic, M. Mechanisms of Chromosome Congression during Mitosis. *Biology* **6** (2017).
78. Pereira, C. *et al.* Self-Assembly of the RZZ Complex into Filaments Drives Kinetochore Expansion in the Absence of Microtubule Attachment. *Current Biology* (2018).
79. Rodriguez-Rodriguez, J.-A. *et al.* Distinct Roles of RZZ and Bub1-KNL1 in Mitotic Checkpoint Signaling and Kinetochore Expansion. *Current Biology* (2018).
80. Mosalaganti, S. *et al.* Structure of the RZZ complex and molecular basis of its interaction with Spindly. *The Journal of Cell Biology* **216**, 961 (2017).
81. Gama, J.B. *et al.* Molecular mechanism of dynein recruitment to kinetochores by the Rod–Zw10–Zwilch complex and Spindly. *The Journal of Cell Biology* **216**, 943 (2017).
82. Chan, Y.W. Mitotic control of kinetochore-associated dynein and spindle orientation by human Spindly. *The Journal of Cell Biology* **185**, 859-874 (2009).
83. Bomont, P., Maddox, P., Shah, J.V., Desai, A.B. & Cleveland, D.W. Unstable microtubule capture at kinetochores depleted of the centromere-associated protein CENP-F. *The EMBO Journal* **24**, 3927-3939 (2005).
84. Vergnolle, M.A.S. & Taylor, S.S. Cenp-F Links Kinetochores to Ndel1/Nde1/Lis1/ Dynein Microtubule Motor Complexes. *Current Biology* **17**, 1173-1179 (2007).
85. Stehman, S.A., Chen, Y., McKenney, R.J. & Vallee, R.B. NudE and NudEL are required for mitotic progression and are involved in dynein recruitment to kinetochores. *The Journal of Cell Biology* **178**, 583 (2007).
86. Faulkner, N.E. *et al.* A role for the lissencephaly gene LIS1 in mitosis and cytoplasmic dynein function. *Nat Cell Biol* **2**, 784-791 (2000).
87. Tai, C.Y., Dujardin, D.L., Faulkner, N.E. & Vallee, R.B. Role of dynein, dynactin, and CLIP-170 interactions in LIS1 kinetochore function. *The Journal of Cell Biology* **156**, 959-968 (2002).
88. Tanenbaum, M.E., Galjart, N., Van Vugt, M.A.T.M. & Medema, R.H. CLIP-170 facilitates the formation of kinetochore–microtubule attachments. *The EMBO Journal* **25**, 45-57 (2006).
89. Gassmann, R. *et al.* Removal of Spindly from microtubule-attached kinetochores controls spindle checkpoint silencing in human cells. *Genes & Development* **24**, 957-971 (2010).

90. Barisic, M. *et al.* Spindly/CCDC99 is required for efficient chromosome congression and mitotic checkpoint regulation. *Mol Biol Cell* **21**, 1968-1981 (2010).
91. Robinett, C.C. *et al.* In vivo localization of DNA sequences and visualization of large-scale chromatin organization using lac operator/repressor recognition. *Journal of Cell Biology* **135**, 1685-1700 (1996).
92. Yao, X., Anderson, K.L. & Cleveland, D.W. The Microtubule-dependent Motor Centromere–associated Protein E (CENP-E) Is an Integral Component of Kinetochore Corona Fibers That Link Centromeres to Spindle Microtubules. *The Journal of Cell Biology* **139**, 435 (1997).
93. Manning, A.L. *et al.* CLASP1, astrin and Kif2b form a molecular switch that regulates kinetochore-microtubule dynamics to promote mitotic progression and fidelity. *The EMBO Journal* **29**, 3531-3543 (2010).
94. Maiato, H. *et al.* Human CLASP1 is an outer kinetochore component that regulates spindle microtubule dynamics. *Cell* **113**, 891-904 (2003).
95. Banerjee, B., Kestner, C.A. & Stukenberg, P.T. EB1 enables spindle microtubules to regulate centromeric recruitment of Aurora B. *J Cell Biol* **204**, 947-963 (2014).
96. Dunsch, A.K., Linnane, E., Barr, F.A. & Gruneberg, U. The astrin-kinastrin/SKAP complex localizes to microtubule plus ends and facilitates chromosome alignment. *The Journal of Cell Biology* **192**, 959-968 (2011).
97. Welburn, J.P.I. *et al.* The Human Kinetochore Ska1 Complex Facilitates Microtubule Depolymerization-Coupled Motility. *Developmental Cell* **16**, 374-385 (2009).
98. Raaijmakers, J.A., Tanenbaum, M.E., Maia, A.F. & Medema, R.H. RAMA1 is a novel kinetochore protein involved in kinetochore-microtubule attachment. *Journal of Cell Science* **122**, 2436 (2009).
99. Hanisch, A., Silljé, H.H.W. & Nigg, E.A. Timely anaphase onset requires a novel spindle and kinetochore complex comprising Ska1 and Ska2. *The EMBO Journal* **25**, 5504-5515 (2006).
100. Gaitanos, T.N. *et al.* Stable kinetochore–microtubule interactions depend on the Ska complex and its new component Ska3/C13Orf3. *The EMBO Journal* **28**, 1442-1452 (2009).
101. Jeyaprakash, A.A. *et al.* Structural and Functional Organization of the Ska Complex, a Key Component of the Kinetochore-Microtubule Interface. *Molecular Cell*, 1-13 (2012).
102. Auckland, P., Clarke, N.I., Royle, S.J. & McAinsh, A.D. Congressing kinetochores progressively load Ska complexes to prevent force-dependent detachment. *The Journal of Cell Biology* (2017).
103. Zhang, G. *et al.* The Ndc80 internal loop is required for recruitment of the Ska complex to establish end-on microtubule attachment to kinetochores. *Journal of Cell Science* (2012).
104. Zhang, Q. *et al.* Ska3 Phosphorylated by Cdk1 Binds Ndc80 and Recruits Ska to Kinetochores to Promote Mitotic Progression. *Current Biology* (2017).
105. Helgeson, L.A. *et al.* Human Ska complex and Ndc80 complex interact to form a load-bearing assembly that strengthens kinetochore–microtubule attachments. *Proceedings of the National Academy of Sciences* **115**, 2740 (2018).
106. Kitajima, T.S., Ohsugi, M. & Ellenberg, J. Complete Kinetochore Tracking Reveals Error-Prone Homologous Chromosome Biorientation in Mammalian Oocytes. *Cell* **146**, 568-581 (2011).
107. Magidson, V. *et al.* The Spatial Arrangement of Chromosomes during Prometaphase Facilitates Spindle Assembly. *Cell* **146**, 555-567 (2011).
108. Harasymiw, L.A., Tank, D., McClellan, M., Panigrahy, N. & Gardner, M.K. Centromere mechanical maturation during mammalian cell mitosis. *Nature Communications* **10**, 1761 (2019).
109. Monda, J.K. & Cheeseman, I.M. The kinetochore–microtubule interface at a glance. *Journal of Cell Science* **131**, jcs214577 (2018).

110. Maresca, T.J. & Salmon, E.D. Intrakinetochore stretch is associated with changes in kinetochore phosphorylation and spindle assembly checkpoint activity. *The Journal of Cell Biology* **184**, 373-381 (2009).
111. Nicklas, R.B. Measurements of the force produced by the mitotic spindle in anaphase. *The Journal of Cell Biology* **97**, 542 (1983).
112. Wan, X. *et al.* Protein Architecture of the Human Kinetochore Microtubule Attachment Site. *Cell* **137**, 672-684 (2009).
113. Waters, J.C., Skibbens, R.V. & Salmon, E.D. Oscillating mitotic newt lung cell kinetochores are, on average, under tension and rarely push. *Journal of Cell Science* **109**, 2823-2831 (1996).
114. Renda, F. *et al.* kSHREC 'Delta' reflects the shape of kinetochore rather than intrakinetochore tension. *bioRxiv*, 811075 (2019).
115. Salmon, E.D. & Bloom, K. Tension sensors reveal how the kinetochore shares its load. *Bioessays* **39**, 1600216 (2017).
116. Akiyoshi, B. *et al.* Tension directly stabilizes reconstituted kinetochore-microtubule attachments. *Nature* **468**, 576-579 (2010).
117. Uchida, K.S.K. *et al.* Kinetochore stretching inactivates the spindle assembly checkpoint. *The Journal of Cell Biology* **184**, 383-390 (2009).
118. Magidson, V. *et al.* Unattached kinetochores rather than intrakinetochore tension arrest mitosis in taxol-treated cells. *The Journal of Cell Biology* **212**, 307 (2016).
119. Lampson, A.M. & Grishchuk, L.E. Mechanisms to Avoid and Correct Erroneous Kinetochore-Microtubule Attachments. *Biology* **6** (2017).
120. Dudka, D. *et al.* Complete microtubule–kinetochore occupancy favours the segregation of merotelic attachments. *Nature Communications* **9**, 2042 (2018).
121. Smith, C.A., McAinsh, A.D. & Burroughs, N.J. Human kinetochores are swivel joints that mediate microtubule attachments. *eLife* **5**, e16159 (2016).
122. Mukherjee, S. *et al.* A Gradient in Metaphase Tension Leads to a Scaled Cellular Response in Mitosis. *Developmental Cell* **49**, 63-76.e10 (2019).
123. Cimini, D. Merotelic kinetochore orientation, aneuploidy, and cancer. *Biochim Biophys Acta* **1786**, 32-40 (2008).
124. Gregan, J., Polakova, S., Zhang, L., Tolić-Nørrelykke, I.M. & Cimini, D. Merotelic kinetochore attachment: causes and effects. *Trends Cell Biol* **21**, 374-381 (2011).
125. Cimini, D., Moree, B., Canman, J.C. & Salmon, E.D. Merotelic kinetochore orientation occurs frequently during early mitosis in mammalian tissue cells and error correction is achieved by two different mechanisms. *Journal of Cell Science* **116**, 4213 (2003).
126. Cimini, D., Cameron, L.A. & Salmon, E.D. Anaphase Spindle Mechanics Prevent Mis-Segregation of Merotelically Oriented Chromosomes. *Current Biology* **14**, 2149-2155 (2004).
127. Tanaka, T.U. *et al.* Evidence that the Ipl1-Sli15 (Aurora Kinase-INCENP) Complex Promotes Chromosome Bi-orientation by Altering Kinetochore-Spindle Pole Connections. *Cell* **108**, 317-329 (2002).
128. Biggins, S. *et al.* The conserved protein kinase Ipl1 regulates microtubule binding to kinetochores in budding yeast. *Genes & Development* **13**, 532-544 (1999).
129. Sessa, F. *et al.* Mechanism of Aurora B activation by INCENP and inhibition by hesperadin. *Molecular Cell* **18**, 379-391 (2005).
130. Carvalho, A., Carmena, M., Sambade, C., Earnshaw, W.C. & Wheatley, S.P. Survivin is required for stable checkpoint activation in taxol-treated HeLa cells. *Journal of Cell Science* **116**, 2987 (2003).
131. Gassmann, R. *et al.* Borealin: a novel chromosomal passenger required for stability of the bipolar mitotic spindle.
. *The Journal of Cell Biology* **166**, 179 (2004).
132. Goto, H., Yasui, Y., Nigg, E.A. & Inagaki, M. Aurora-B phosphorylates Histone H3 at serine28 with regard to the mitotic chromosome condensation. *Genes to Cells* **7**, 11-17 (2002).
133. Hindriksen, S., Lens, S.M.A. & Hadders, M.A. The Ins and Outs of Aurora B

Inner Centromere Localization. *Frontiers in Cell and Developmental Biology* **5**, 112 (2017).
134. Trivedi, P. *et al.* The inner centromere is a biomolecular condensate scaffolded by the chromosomal passenger complex. *Nat Cell Biol* **21**, 1127-1137 (2019).
135. Kitagawa, M. & Lee, S.H. The chromosomal passenger complex (CPC) as a key orchestrator of orderly mitotic exit and cytokinesis. *Frontiers in Cell and Developmental Biology* **3**, 14 (2015).
136. Kelly, A.E. *et al.* Chromosomal Enrichment and Activation of the Aurora B Pathway Are Coupled to Spatially Regulate Spindle Assembly. *Developmental Cell* **12**, 31-43 (2007).
137. Bishop, J.D. & Schumacher, J.M. Phosphorylation of the Carboxyl Terminus of Inner Centromere Protein (INCENP) by the Aurora B Kinase Stimulates Aurora B Kinase Activity. *Journal of Biological Chemistry* **277**, 27577-27580 (2002).
138. Wang, E., Ballister, E.R. & Lampson, M.A. Aurora B dynamics at centromeres create a diffusion-based phosphorylation gradient. *jcb.rupress.org* (2011).
139. Liu, D., Vader, G., Vromans, M.J., Lampson, M.A. & Lens, S.M. Sensing chromosome bi-orientation by spatial separation of aurora B kinase from kinetochore substrates. *Science* **323**, 1350-1353 (2009).
140. Zaytsev, A.V., Sundin, L.J.R., DeLuca, K.F., Grishchuk, E.L. & DeLuca, J.G. Accurate phosphoregulation of kinetochore–microtubule affinity requires unconstrained molecular interactions. *The Journal of Cell Biology* **206**, 45 (2014).
141. Zaytsev, A.V. *et al.* Multisite phosphorylation of the NDC80 complex gradually tunes its microtubule-binding affinity. *Mol Biol Cell* **26**, 1829-1844 (2015).
142. DeLuca, K.F., Lens, S.M.A. & DeLuca, J.G. Temporal changes in Hec1 phosphorylation control kinetochore–microtubule attachment stability during mitosis. *Journal of Cell Science* **124**, 622 (2011).
143. Foley, E.A., Maldonado, M. & Kapoor, T.M. Formation of stable attachments between kinetochores and microtubules depends on the B56-PP2A phosphatase. *Nat Cell Biol* **13**, 1265-1271 (2011).
144. Meppelink, A., Kabeche, L., Vromans, M.J., Compton, D.A. & Lens, S.M. Shugoshin-1 balances Aurora B kinase activity via PP2A to promote chromosome bi-orientation. *Cell Rep* **11**, 508-515 (2015).
145. Xu, P., Raetz, E.A., Kitagawa, M., Virshup, D.M. & Lee, S.H. BUBR1 recruits PP2A via the B56 family of targeting subunits to promote chromosome congression. *Biology Open* **2**, 479 (2013).
146. Kruse, T. *et al.* Direct binding between BubR1 and B56–PP2A phosphatase complexes regulate mitotic progression. *Journal of Cell Science* **126**, 1086 (2013).
147. Liu, D. *et al.* Regulated targeting of protein phosphatase 1 to the outer kinetochore by KNL1 opposes Aurora B kinase. *The Journal of Cell Biology* **188**, 809-820 (2010).
148. Saurin, A.T. Kinase and Phosphatase Cross-Talk at the Kinetochore. *Frontiers in Cell and Developmental Biology* **6** (2018).
149. Suijkerbuijk, S.J.E., Vleugel, M., Teixeira, A. & Kops, G.J.P.L. Integration of Kinase and Phosphatase Activities by BUBR1 Ensures Formation of Stable Kinetochore-Microtubule Attachments. *Developmental Cell* **23**, 745-755 (2012).
150. Nijenhuis, W., Vallardi, G., Teixeira, A., Kops, G.J. & Saurin, A.T. Negative feedback at kinetochores underlies a responsive spindle checkpoint signal. *Nat Cell Biol* **16**, 1257-1264 (2014).
151. Sivakumar, S. & Gorbsky, G.J. Phosphatase-regulated recruitment of the spindle- and kinetochore-associated (Ska) complex to kinetochores. *Biology Open* **6**, 1672 (2017).
152. García-Rodríguez, L.J., Kasciukovic, T., Denninger, V. & Tanaka, T.U. Aurora B-INCENP Localization at Centromeres/Inner Kinetochores Is Required for Chromosome Bi-orientation in Budding Yeast. *Current Biology* **29**, 1536-1544. e1534 (2019).
153. Fischböck-Halwachs, J. *et al.* The COMA complex interacts with Cse4 and

positions Sli15/Ipl1 at the budding yeast inner kinetochore. *eLife* **8**, e42879 (2019).
154. Fuller, B.G. *et al.* Midzone activation of aurora B in anaphase produces an intracellular phosphorylation gradient. *Nature* **453**, 1132-1136 (2008).
155. Caldas, G.V., DeLuca, K.F. & DeLuca, J.G. KNL1 facilitates phosphorylation of outer kinetochore proteins by promoting Aurora B kinase activity. *J Cell Biol* **203**, 957-969 (2013).
156. Posch, M. *et al.* Sds22 regulates aurora B activity and microtubule-kinetochore interactions at mitosis. *The Journal of Cell Biology* **191**, 61-74 (2010).
157. Bekier, M.E., Mazur, T., Rashid, M.S. & Taylor, W.R. Borealin dimerization mediates optimal CPC checkpoint function by enhancing localization to centromeres and kinetochores. *Nature Communications* **6**, 6775 (2015).
158. Shrestha, R.L. *et al.* Aurora-B kinase pathway controls the lateral to end-on conversion of kinetochore-microtubule attachments in human cells. *Nature Communications* **8**, 150 (2017).
159. Campbell, C.S. & Desai, A. Tension sensing by Aurora B kinase is independent of survivin-based centromere localization. *Nature*, 1-5 (2013).
160. Hengeveld, R.C.C., Vromans, M.J.M., Vleugel, M., Hadders, M.A. & Lens, S.M.A. Inner centromere localization of the CPC maintains centromere cohesion and allows mitotic checkpoint silencing. *Nature Communications* **8**, 15542 (2017).
161. McHugh, T. *et al.* The depolymerase activity of MCAK shows a graded response to Aurora B kinase phosphorylation through allosteric regulation. *Journal of Cell Science* **132**, jcs228353 (2019).
162. Kim, Y., Holland, A.J., Lan, W. & Cleveland, D.W. Aurora Kinases and Protein Phosphatase 1 Mediate Chromosome Congression through Regulation of CENP-E. *Cell* **142**, 444-455 (2010).
163. Masuda, N. *et al.* Microtubule stabilization triggers the plus-end accumulation of Kif18A/kinesin-8. *Cell Struct Funct* **36**, 261-267 (2011).
164. Häfner, J., Mayr, M.I., Möckel, M.M. & Mayer, T.U. Pre-anaphase chromosome oscillations are regulated by the antagonistic activities of Cdk1 and PP1 on Kif18A. *Nature Communications* **5** (2014).
165. De Wever, V. *et al.* The human mitotic kinesin KIF18A binds protein phosphatase 1 (PP1) through a highly conserved docking motif. *Biochem. Biophys. Res. Commun.* **453**, 432-437 (2014).
166. Chan, Y.W., Jeyaprakash, A.A., Nigg, E.A. & Santamaria, A. Aurora B controls kinetochore-microtubule attachments by inhibiting Ska complex-KMN network interaction. *The Journal of Cell Biology* (2012).
167. Shrestha, R.L. & Draviam, V.M. Lateral to End-on Conversion of Chromosome-Microtubule Attachment Requires Kinesins CENP-E and MCAK. *Curr Biol* (2013).
168. Tanno, Y. *et al.* Phosphorylation of mammalian Sgo2 by Aurora B recruits PP2A and MCAK to centromeres. *Genes & Development* **24**, 2169-2179 (2010).
169. Knowlton, A.L., Lan, W. & Stukenberg, P.T. Aurora B Is Enriched at Merotelic Attachment Sites, Where It Regulates MCAK. *Current Biology* **16**, 1705-1710 (2006).
170. Kline-Smith, S.L., Khodjakov, A., Hergert, P. & Walczak, C.E. Depletion of Centromeric MCAK Leads to Chromosome Congression and Segregation Defects Due to Improper Kinetochore Attachments. *Mol Biol Cell* **15**, 1146-1159 (2003).
171. Tappan, E. & Chamberlin, A.R. Activation of Protein Phosphatase 1 by a Small Molecule Designed to Bind to the Enzyme's Regulatory Site. *Chemistry & Biology* **15**, 167-174 (2008).
172. Hendrickx, A. *et al.* Docking Motif-Guided Mapping of the Interactome of Protein Phosphatase-1. *Chemistry & Biology* **16**, 365-371 (2009).
173. Rosenberg, J.S., Cross, F.R. & Funabiki, H. KNL1/Spc105 Recruits PP1 to Silence the Spindle Assembly Checkpoint. *Current Biology* **21**, 942-947 (2011).
174. Bajaj, R., Bollen, M., Peti, W. & Page, R. KNL1 Binding to PP1 and Microtubules Is Mutually Exclusive. *Structure* (2018).

175. Meadows, J.C. *et al.* Spindle Checkpoint Silencing Requires Association of PP1 to Both Spc7 and Kinesin-8 Motors. *Developmental Cell* **20**, 739-750 (2011).
176. Conti, D. Role of phosphatases in the end-on conversion process. (2017).
177. Sivakumar, S. *et al.* The human SKA complex drives the metaphase-anaphase cell cycle transition by recruiting protein phosphatase 1 to kinetochores. *eLife* **5**, e12902 (2016).
178. Nasa, I., Rusin, S.F., Kettenbach, A.N. & Moorhead, G.B. Aurora B opposes PP1 function in mitosis by phosphorylating the conserved PP1-binding RVxF motif in PP1 regulatory proteins. *Science Signaling* **11** (2018).
179. Peters, J.-M. The Anaphase-Promoting Complex: Proteolysis in Mitosis and Beyond. *Molecular Cell* **9**, 931-943 (2002).
180. Fang, G., Yu, H. & Kirschner, M.W. Direct binding of CDC20 protein family members activates the anaphase-promoting complex in mitosis and G1. *Molecular Cell* **2**, 163-171 (1998).
181. Visintin, R., Prinz, S. & Amon, A. CDC20 and CDH1: A Family of Substrate-Specific Activators of APC-Dependent Proteolysis. *Science* **278**, 460 (1997).
182. Kramer, E.R., Scheuringer, N., Podtelejnikov, A.V., Mann, M. & Peters, J.-M. Mitotic Regulation of the APC Activator Proteins CDC20 and CDH1. *Mol Biol Cell* **11**, 1555-1569 (2000).
183. Thornton, B.R. & Toczyski, D.P. Securin and B-cyclin/CDK are the only essential targets of the APC. *Nat Cell Biol* **5**, 1090-1094 (2003).
184. Primorac, I. & Musacchio, A. Panta rhei: The APC/C at steady state. *The Journal of Cell Biology* **201**, 177-189 (2013).
185. Sivakumar, S. & Gorbsky, G.J. Spatiotemporal regulation of the anaphase-promoting complex in mitosis. *Nat Rev Mol Cell Biol* **16**, 82 (2015).
186. Dick, A.E. & Gerlich, D.W. Kinetic framework of spindle assembly checkpoint signalling. *Nature Cell Biol* (2013).
187. Rieder, C.L., Cole, R.W., Khodjakov, A. & Sluder, G. The checkpoint delaying anaphase in response to chromosome monoorientation is mediated by an inhibitory signal produced by unattached kinetochores. *The Journal of Cell Biology* **130**, 941 (1995).
188. Collin, P., Nashchekina, O., Walker, R. & Pines, J. The spindle assembly checkpoint works like a rheostat rather than a toggle switch. *Nature Cell Biol* (2013).
189. Burke, D.J. & Stukenberg, P.T. Linking kinetochore-microtubule binding to the spindle checkpoint. *Developmental Cell* **14**, 474-479 (2008).
190. Yamaguchi, M. *et al.* Cryo-EM of Mitotic Checkpoint Complex-Bound APC/C Reveals Reciprocal and Conformational Regulation of Ubiquitin Ligation. *Molecular Cell* (2016).
191. Herzog, F. *et al.* Structure of the Anaphase-Promoting Complex/Cyclosome Interacting with a Mitotic Checkpoint Complex. *Science* **323**, 1477-1481 (2009).
192. Chao, W.C.H., Kulkarni, K., Zhang, Z., Kong, E.H. & Barford, D. Structure of the mitotic checkpoint complex. *Nature* **484**, 208-213 (2012).
193. Izawa, D. & Pines, J. The mitotic checkpoint complex binds a second CDC20 to inhibit active APC/C. *Nature* **517**, 631 (2014).
194. Alfieri, C. *et al.* Molecular basis of APC/C regulation by the spindle assembly checkpoint. *Nature* **advance online publication** (2016).
195. Li, R. & Murray, A.W. Feedback control of mitosis in budding yeast. *Cell* **66**, 519-531 (1991).
196. Hoyt, M.A., Totis, L. & Roberts, B.T. S. cerevisiae genes required for cell cycle arrest in response to loss of microtubule function. *Cell* **66**, 507-517 (1991).
197. Li, Y., Gorbea, C., Mahaffey, D., Rechsteiner, M. & Benezra, R. MAD2 associates with the cyclosome/anaphase-promoting complex and inhibits its activity. *Proceedings of the National Academy of Sciences* **94**, 12431 (1997).
198. Uzunova, K. *et al.* APC15 mediates CDC20 autoubiquitylation by APC/CMCC and disassembly of the mitotic checkpoint complex. *Nat Struct Mol Biol* **19**, 1116-

1123 (2012).
199. Mansfeld, J., Collin, P., Collins, M.O., Choudhary, J.S. & Pines, J. APC15 drives the turnover of MCC-CDC20 to make the spindle assembly checkpoint responsive to kinetochore attachment. *Nat Cell Biol* **13**, 1234-1243 (2011).
200. Foster, S.A. & Morgan, D.O. The APC/C Subunit Mnd2/Apc15 Promotes Cdc20 Autoubiquitination and Spindle Assembly Checkpoint Inactivation. *Cell* (2012).
201. Nilsson, J., Yekezare, M., Minshull, J. & Pines, J. The APC/C maintains the spindle assembly checkpoint by targeting Cdc20 for destruction. *Nat Cell Biol* **10**, 1411-1420 (2008).
202. Foe, I.T. *et al.* Ubiquitination of Cdc20 by the APC Occurs through an Intramolecular Mechanism. *Current Biology* **21**, 1870-1877 (2011).
203. King, E.M.J., van der Sar, S.J.A. & Hardwick, K.G. Mad3 KEN Boxes Mediate both Cdc20 and Mad3 Turnover, and Are Critical for the Spindle Checkpoint. *PLoS ONE* **2**, e342 (2007).
204. Sironi, L. *et al.* Mad2 binding to Mad1 and Cdc20, rather than oligomerization, is required for the spindle checkpoint. *The EMBO Journal* **20**, 6371-6382 (2001).
205. Taylor, S.S., Hussein, D., Wang, Y., Elderkin, S. & Morrow, C.J. Kinetochore localisation and phosphorylation of the mitotic checkpoint components Bub1 and BubR1 are differentially regulated by spindle events in human cells. *Journal of Cell Science* **114**, 4385-4395 (2001).
206. Jablonski, S.A., Chan, G.K.T., Cooke, C.A., Earnshaw, W.C. & Yen, T.J. The hBUB1 and hBUBR1 kinases sequentially assemble onto kinetochores during prophase with hBUBR1 concentrating at the kinetochore plates in mitosis. *Chromosoma* **107**, 386-396 (1998).
207. Johnson, V.L. Bub1 is required for kinetochore localization of BubR1, Cenp-E, Cenp-F and Mad2, and chromosome congression. *Journal of Cell Science* **117**, 1577-1589 (2004).
208. Vleugel, M. *et al.* Arrayed BUB recruitment modules in the kinetochore scaffold KNL1 promote accurate chromosome segregation. *J Cell Biol* **203**, 943-955 (2013).
209. Lischetti, T., Zhang, G., Sedgwick, G.G., Bolanos-Garcia, V.M. & Nilsson, J. The internal Cdc20 binding site in BubR1 facilitates both spindle assembly checkpoint signalling and silencing. *Nature Communications* **5**, 5563 (2014).
210. Li, D., Morley, G., Whitaker, M. & Huang, J.Y. Recruitment of Cdc20 to the Kinetochore Requires BubR1 but Not Mad2 in Drosophila melanogaster. *Molecular and Cellular Biology* **30**, 3384-3395 (2010).
211. Luo, X. *et al.* Structure of the Mad2 spindle assembly checkpoint protein and its interaction with Cdc20. *Nat Struct Biol* **7**, 224-229 (2000).
212. Mapelli, M., Massimiliano, L., Santaguida, S. & Musacchio, A. The Mad2 conformational dimer: structure and implications for the spindle assembly checkpoint. *Cell* **131**, 730-743 (2007).
213. Sironi, L. *et al.* Crystal structure of the tetrameric Mad1–Mad2 core complex: implications of a'safety belt'binding mechanism for the spindle checkpoint. *The EMBO Journal* **21**, 2496-2506 (2002).
214. Yang, M. *et al.* Insights into Mad2 Regulation in the Spindle Checkpoint Revealed by the Crystal Structure of the Symmetric Mad2 Dimer. *PLoS Biol* **6**, e50 (2008).
215. De Antoni, A. *et al.* The Mad1/Mad2 Complex as a Template for Mad2 Activation in the Spindle Assembly Checkpoint. *Current Biology* **15**, 214-225 (2005).
216. Luo, X., Tang, Z., Rizo, J. & Yu, H. The Mad2 Spindle Checkpoint Protein Undergoes Similar Major Conformational Changes Upon Binding to Either Mad1 or Cdc20. *Molecular Cell* **9**, 59-71 (2002).
217. Skinner, J.J., Wood, S., Shorter, J., Englander, S.W. & Black, B.E. The Mad2 partial unfolding model: regulating mitosis through Mad2 conformational switching. *The Journal of Cell Biology* **183**, 761-768 (2008).
218. Han, J.S. *et al.* Catalytic Assembly of the Mitotic Checkpoint Inhibitor BubR1-Cdc20 by a Mad2-Induced Functional Switch in Cdc20. *Cell* (2013).
219. Sudakin, V., Chan, G.K.T. & Yen, T.J. Checkpoint inhibition of the APC/C in HeLa

cells is mediated by a complex of BUBR1, BUB3, CDC20, and MAD2. *The Journal of Cell Biology* **154**, 925 (2001).
220. Faesen, A.C. *et al.* Basis of catalytic assembly of the mitotic checkpoint complex. *Nature* **542**, 498 (2017).
221. Rodriguez-Bravo, V. *et al.* Nuclear pores protect genome integrity by assembling a premitotic and Mad1-dependent anaphase inhibitor. *Cell* **156**, 1017-1031 (2014).
222. Kim, D.H. *et al.* TRIP13 and APC15 drive mitotic exit by turnover of interphase- and unattached kinetochore-produced MCC. *Nat Commun* **9**, 4354 (2018).
223. Westhorpe, F.G., Tighe, A., Lara-Gonzalez, P. & Taylor, S.S. p31comet-mediated extraction of Mad2 from the MCC promotes efficient mitotic exit. *Journal of Cell Science* **124**, 3905-3916 (2011).
224. Hewitt, L. *et al.* Sustained Mps1 activity is required in mitosis to recruit O-Mad2 to the Mad1-C-Mad2 core complex. *The Journal of Cell Biology* **190**, 25-34 (2010).
225. Lee, S.H., Sterling, H., Burlingame, A. & McCormick, F. Tpr directly binds to Mad1 and Mad2 and is important for the Mad1-Mad2-mediated mitotic spindle checkpoint. *Genes & Development* **22**, 2926-2931 (2008).
226. Schweizer, N. *et al.* Spindle assembly checkpoint robustness requires Tpr-mediated regulation of Mad1/Mad2 proteostasis. *J Cell Biol* **203**, 883-893 (2013).
227. Rajanala, K. *et al.* Phosphorylation of nucleoporin Tpr governs its differential localization and is required for its mitotic function. *Journal of Cell Science* **127**, 3505-3520 (2014).
228. Osswald, M. *et al.* Mps1 releases Mad1 from nuclear pores to ensure a robust mitotic checkpoint and accurate chromosome segregation. *bioRxiv*, 659938 (2019).
229. London, N., Ceto, S., Ranish, J.A. & Biggins, S. Phosphoregulation of Spc105 by Mps1 and PP1 Regulates Bub1 Localization to Kinetochores. *Current Biology* (2012).
230. Shepperd, L.A. *et al.* Phosphodependent Recruitment of Bub1 and Bub3 to Spc7/KNL1 by Mph1 Kinase Maintains the Spindle Checkpoint. *Current Biology* (2012).
231. Yamagishi, Y., Yang, C.-H., Tanno, Y. & Watanabe, Y. MPS1/Mph1 phosphorylates the kinetochore protein KNL1/Spc7 to recruit SAC components. *Nat Cell Biol* **14**, 1-9 (2012).
232. Vleugel, M. *et al.* Sequential multisite phospho-regulation of KNL1-BUB3 interfaces at mitotic kinetochores. *Mol Cell* **57**, 824-835 (2015).
233. Primorac, I. *et al.* Bub3 reads phosphorylated MELT repeats to promote spindle assembly checkpoint signaling. *eLife* **2**, e01030-e01030 (2013).
234. Mora-Santos, Maria del M. *et al.* Bub3-Bub1 Binding to Spc7/KNL1 Toggles the Spindle Checkpoint Switch by Licensing the Interaction of Bub1 with Mad1-Mad2. *Current Biology* (2016).
235. Ji, Z., Gao, H., Jia, L., Li, B. & Yu, H. A sequential multi-target Mps1 phosphorylation cascade promotes spindle checkpoint signaling. *eLife* **6**, e22513 (2017).
236. London, N. & Biggins, S. Mad1 kinetochore recruitment by Mps1-mediated phosphorylation of Bub1 signals the spindle checkpoint. *Genes Dev* **28**, 140-152 (2014).
237. Zhang, G. *et al.* Bub1 positions Mad1 close to KNL1 MELT repeats to promote checkpoint signalling. *Nature Communications* **8**, 15822 (2017).
238. Vleugel, M. *et al.* Dissecting the roles of human BUB1 in the spindle assembly checkpoint. *Journal of Cell Science* **128**, 2975-2982 (2015).
239. Maciejowski, J. *et al.* Mps1 Regulates Kinetochore-Microtubule Attachment Stability via the Ska Complex to Ensure Error-Free Chromosome Segregation. *Developmental Cell* **41**, 143-156.e146 (2017).
240. Santaguida, S., Tighe, A., D'Alise, A.M., Taylor, S.S. & Musacchio, A. Dissecting the role of MPS1 in chromosome biorientation and the spindle checkpoint through the small molecule inhibitor reversine. *J Cell Biol* **190**, 73-87 (2010).
241. Kops, G.J.P.L. *et al.* ZW10 links mitotic checkpoint signaling to the structural

kinetochore. *The Journal of Cell Biology* **169**, 49 (2005).
242. Silió, V., McAinsh, Andrew D. & Millar, Jonathan B. KNL1-Bubs and RZZ Provide Two Separable Pathways for Checkpoint Activation at Human Kinetochores. *Developmental Cell* **35**, 600-613 (2015).
243. Zhang, G. *et al.* Efficient mitotic checkpoint signaling depends on integrated activities of Bub1 and the RZZ complex. *The EMBO Journal*, e100977 (2019).
244. Alfonso-Perez, T., Hayward, D., Holder, J., Gruneberg, U. & Barr, F.A. MAD1-dependent recruitment of CDK1-CCNB1 to kinetochores promotes spindle checkpoint signaling. *J Cell Biol* **218**, 1108-1117 (2019).
245. Jackman, M. *et al.* Cyclin B1-Cdk1 binding to MAD1 links nuclear pore disassembly to chromosomal stability. *bioRxiv*, 701474 (2019).
246. Allan, L.A. *et al.* Cyclin B1 scaffolds MAD1 at the corona to activate the spindle assembly checkpoint. *bioRxiv*, 726224 (2019).
247. D'Angiolella, V., Mari, C., Nocera, D., Rametti, L. & Grieco, D. The spindle checkpoint requires cyclin-dependent kinase activity. *Genes Dev* **17**, 2520-2525 (2003).
248. Stucke, V.M., Silljé, H.H.W., Arnaud, L. & Nigg, E.A. Human Mps1 kinase is required for the spindle assembly checkpoint but not for centrosome duplication. *The EMBO Journal* **21**, 1723-1732 (2002).
249. Hardwick, K.G., Weiss, E., Luca, F.C., Winey, M. & Murray, A.W. Activation of the budding yeast spindle assembly checkpoint without mitotic spindle disruption. *Science* **273**, 953-956 (1996).
250. Fisk, H.A., Mattison, C.P. & Winey, M. Human Mps1 protein kinase is required for centrosome duplication and normal mitotic progression. *Proc Natl Acad Sci USA* **100**, 14875-14880 (2003).
251. Jelluma, N. *et al.* Chromosomal Instability by Inefficient Mps1 Auto-Activation Due to a Weakened Mitotic Checkpoint and Lagging Chromosomes. *PLoS ONE* **3**, e2415 (2008).
252. Sliedrecht, T., Zhang, C., Shokat, K.M. & Kops, G.J.P.L. Chemical Genetic Inhibition of Mps1 in Stable Human Cell Lines Reveals Novel Aspects of Mps1 Function in Mitosis. *PLoS ONE* **5**, e10251 (2010).
253. Stucke, V., Baumann, C. & Nigg, E. Kinetochore localization and microtubule interaction of the human spindle checkpoint kinase Mps1. *Chromosoma* **113**, 1-15 (2004).
254. Pachis, S.T., Hiruma, Y., Tromer, E.C., Perrakis, A. & Kops, G.J.P.L. Interactions between N-terminal Modules in MPS1 Enable Spindle Checkpoint Silencing. *Cell Rep* **26**, 2101-2112.e2106 (2019).
255. Nijenhuis, W. *et al.* A TPR domain-containing N-terminal module of MPS1 is required for its kinetochore localization by Aurora B. *J Cell Biol* **201**, 217-231 (2013).
256. Chu, M.L.H., Chavas, L.M.G., Douglas, K.T., Eyers, P.A. & Tabernero, L. Crystal structure of the catalytic domain of the mitotic checkpoint kinase Mps1 in complex with SP600125. *J Biol Chem* **283**, 21495-21500 (2008).
257. Zhang, X. *et al.* Two LXXLL motifs in the N terminus of Mps1 are required for Mps1 nuclear import during G2/M transition and sustained spindle checkpoint responses. *Cell Cycle* **10**, 2742-2750 (2011).
258. Mills, G.B. *et al.* Expression of TTK, a novel human protein kinase, is associated with cell proliferation. *J Biol Chem* **267**, 16000-16006 (1992).
259. Kang, J., Chen, Y., Zhao, Y. & Yu, H. Autophosphorylation-dependent activation of human Mps1 is required for the spindle checkpoint. *Proceedings of the National Academy of Sciences* **104**, 20232-20237 (2007).
260. Mattison, C.P. *et al.* Mps1 activation loop autophosphorylation enhances kinase activity. *J Biol Chem* **282**, 30553-30561 (2007).
261. Lee, S. *et al.* Characterization of spindle checkpoint kinase Mps1 reveals domain with functional and structural similarities to tetratricopeptide repeat motifs of Bub1 and BubR1 checkpoint kinases. *Journal of Biological Chemistry* **287**, 5988-

6001 (2012).
262. Combes, G. *et al.* Mps1 Phosphorylates Its N-Terminal Extension to Relieve Autoinhibition and Activate the Spindle Assembly Checkpoint. *Current Biology* **28**, 872-883.e875 (2018).
263. Kwiatkowski, N. *et al.* Small-molecule kinase inhibitors provide insight into Mps1 cell cycle function. *Nature Chemical Biology* **6**, 359-368 (2010).
264. Meraldi, P., Draviam, V.M. & Sorger, P.K. Timing and checkpoints in the regulation of mitotic progression. *Developmental Cell* **7**, 45-60 (2004).
265. Hiruma, Y. *et al.* Competition between MPS1 and microtubules at kinetochores regulates spindle checkpoint signaling. *Science* **348**, 1264 (2015).
266. Ji, Z., Gao, H. & Yu, H. CELL DIVISION CYCLE. Kinetochore attachment sensed by competitive Mps1 and microtubule binding to Ndc80C. *Science* **348**, 1260-1264 (2015).
267. Morin, V. *et al.* CDK-Dependent Potentiation of MPS1 Kinase Activity Is Essential to the Mitotic Checkpoint. *Current Biology*, 1-7 (2012).
268. Wang, X. *et al.* Dynamic Autophosphorylation of Mps1 Kinase Is Required for Faithful Mitotic Progression. *PLoS ONE* **9**, e104723 (2014).
269. Isokane, M. *et al.* ARHGEF17 is an essential spindle assembly checkpoint factor that targets Mps1 to kinetochores. *The Journal of Cell Biology* **212**, 647-659 (2016).
270. Saurin, A.T., van der Waal, M.S., Medema, R.H., Lens, S.M. & Kops, G.J. Aurora B potentiates Mps1 activation to ensure rapid checkpoint establishment at the onset of mitosis. *Nat Commun* **2**, 316 (2011).
271. Yuan, I. *et al.* Generation of a Spindle Checkpoint Arrest from Synthetic Signaling Assemblies. *Current Biology* (2017).
272. Kasbek, C. *et al.* Preventing the degradation of mps1 at centrosomes is sufficient to cause centrosome reduplication in human cells. *Mol Biol Cell* **18**, 4457-4469 (2007).
273. Winey, M., Goetsch, L., Baum, P. & Byers, B. MPS1 and MPS2: novel yeast genes defining distinct steps of spindle pole body duplication. *The Journal of Cell Biology* **114**, 745-754 (1991).
274. Liu, S.-T. *et al.* Human MPS1 kinase is required for mitotic arrest induced by the loss of CENP-E from kinetochores. *Mol Biol Cell* **14**, 1638-1651 (2003).
275. Pike, A.N. & Fisk, H.A. Centriole assembly and the role of Mps1: defensible or dispensable? *Cell Division* **6**, 9 (2011).
276. Dou, Z. *et al.* Dynamic distribution of TTK in HeLa cells: insights from an ultrastructural study. *Cell Res* **13**, 443-449 (2003).
277. Maciejowski, J. *et al.* Mps1 directs the assembly of Cdc20 inhibitory complexes during interphase and mitosis to control M phase timing and spindle checkpoint signaling. *The Journal of Cell Biology* **190**, 89-100 (2010).
278. Jelluma, N. *et al.* Mps1 phosphorylates Borealin to control Aurora B activity and chromosome alignment. *Cell* **132**, 233-246 (2008).
279. Espeut, J. *et al.* Phosphorylation Relieves Autoinhibition of the Kinetochore Motor Cenp-E. *Molecular Cell* **29**, 637-643 (2008).
280. Jelluma, N., Dansen, T.B., Sliedrecht, T., Kwiatkowski, N.P. & Kops, G.J. Release of Mps1 from kinetochores is crucial for timely anaphase onset. *J Cell Biol* **191**, 281-290 (2010).
281. Lin, Z., Jia, L., Tomchick, Diana R., Luo, X. & Yu, H. Substrate-Specific Activation of the Mitotic Kinase Bub1 through Intramolecular Autophosphorylation and Kinetochore Targeting. *Structure* **22**, 1616-1627 (2014).
282. Perera, D. & Taylor, S.S. Sgo1 establishes the centromeric cohesion protection mechanism in G2 before subsequent Bub1-dependent recruitment in mitosis. *Journal of Cell Science* **123**, 653-659 (2010).
283. Kawashima, S.A., Yamagishi, Y., Honda, T., Ishiguro, K.-i. & Watanabe, Y. Phosphorylation of H2A by Bub1 Prevents Chromosomal Instability Through Localizing Shugoshin. *Science* **327**, 172 (2010).
284. El Yakoubi, W. *et al.* Mps1 kinase-dependent Sgo2 centromere localisation

mediates cohesin protection in mouse oocyte meiosis I. *Nat Commun* **8**, 694 (2017).
285. Smith, R.J. *et al.* PP1 and PP2A Use Opposite Phospho-dependencies to Control Distinct Processes at the Kinetochore. *Cell Rep* **28**, 2206-2219.e2208 (2019).
286. Peplowska, K., Wallek, A.U. & Storchova, Z. Sgo1 Regulates Both Condensin and Ipl1/Aurora B to Promote Chromosome Biorientation. *PLoS Genet* **10**, e1004411 (2014).
287. Vallardi, G., Allan, L.A., Crozier, L. & Saurin, A.T. Division of labour between PP2A-B56 isoforms at the centromere and kinetochore. *eLife* **8**, e42619 (2019).
288. Liu, H., Jia, L. & Yu, H. Phospho-H2A and Cohesin Specify Distinct Tension-Regulated Sgo1 Pools at Kinetochores and Inner Centromeres. *Current Biology* (2013).
289. Wang, J. *et al.* Crystal structure of a PP2A B56-BubR1 complex and its implications for PP2A substrate recruitment and localization. *Protein & Cell* **7**, 516-526 (2016).
290. Espert, A. *et al.* PP2A-B56 opposes Mps1 phosphorylation of Knl1 and thereby promotes spindle assembly checkpoint silencing. *The Journal of Cell Biology* **206**, 833-842 (2014).
291. Qian, J. *et al.* An Attachment-Independent Biochemical Timer of the Spindle Assembly Checkpoint. *Molecular Cell* (2017).
292. Pinsky, B.A., Nelson, C.R. & Biggins, S. Protein Phosphatase 1 Regulates Exit from the Spindle Checkpoint in Budding Yeast. *Current Biology* **19**, 1182-1187 (2009).
293. Vanoosthuyse, V. & Hardwick, K.G. A Novel Protein Phosphatase 1-Dependent Spindle Checkpoint Silencing Mechanism. *Current Biology* **19**, 1176-1181 (2009).
294. Hayward, D. *et al.* Checkpoint signaling and error correction require regulation of the MPS1 T-loop by PP2A-B56. *J Cell Biol* **218**, 3188-3199 (2019).
295. Moura, M. *et al.* Protein phosphatase 1 inactivates Mps1 to ensure efficient spindle assembly checkpoint silencing. *eLife* **6**, e25366 (2017).
296. Biggins, S. & Murray, A.W. The budding yeast protein kinase Ipl1/Aurora allows the absence of tension to activate the spindle checkpoint. *Genes & Development* **15**, 3118-3129 (2001).
297. Aravamudhan, P., Goldfarb, A.A. & Joglekar, A.P. The kinetochore encodes a mechanical switch to disrupt spindle assembly checkpoint signalling. *Nat Cell Biol* **17**, 868-879 (2015).
298. O'Connell, C.B. *et al.* The spindle assembly checkpoint is satisfied in the absence of interkinetochore tension during mitosis with unreplicated genomes. *The Journal of Cell Biology* **183**, 29 (2008).
299. Wojcik, E. *et al.* Kinetochore dynein: its dynamics and role in the transport of the Rough deal checkpoint protein. *Nat Cell Biol* **3**, 1001-1007 (2001).
300. Howell, B.J. *et al.* Cytoplasmic dynein/dynactin drives kinetochore protein transport to the spindle poles and has a role in mitotic spindle checkpoint inactivation. *The Journal of Cell Biology* **155**, 1159 (2001).
301. Howell, B.J., Hoffman, D.B., Fang, G., Murray, A.W. & Salmon, E.D. Visualization of Mad2 Dynamics at Kinetochores, along Spindle Fibers, and at Spindle Poles in Living Cells. *The Journal of Cell Biology* **150**, 1233 (2000).
302. Maldonado, M. & Kapoor, T.M. Constitutive Mad1 targeting to kinetochores uncouples checkpoint signalling from chromosome biorientation. *Nat Cell Biol* **13**, 475-482 (2011).
303. Qian, J. *et al.* Cdk1 orders mitotic events through coordination of a chromosome-associated phosphatase switch. *Nat Commun* **6** (2015).
304. Holder, J., Poser, E. & Barr, F.A. Getting out of mitosis: spatial and temporal control of mitotic exit and cytokinesis by PP1 and PP2A. *FEBS Letters* **0** (2019).
305. Xia, G.G. *et al.* Conformation-specific binding of p31(comet) antagonizes the function of Mad2 in the spindle checkpoint. *The EMBO Journal* **23**, 3133-3143 (2004).
306. Mapelli, M. *et al.* Determinants of conformational dimerization of Mad2 and its

inhibition by p31comet. *The EMBO Journal* **25**, 1273-1284 (2006).
307. Teichner, A. *et al.* p31comet promotes disassembly of the mitotic checkpoint complex in an ATP-dependent process. *Proceedings of the National Academy of Sciences* **108**, 3187-3192 (2011).
308. Hagan, R.S. *et al.* p31comet acts to ensure timely spindle checkpoint silencing subsequent to kinetochore attachment. *Mol Biol Cell* **22**, 4236-4246 (2011).
309. Lu, S., Qian, J., Guo, M., Gu, C. & Yang, Y. Insights into a Crucial Role of TRIP13 in Human Cancer. *Computational and Structural Biotechnology Journal* **17**, 854-861 (2019).
310. Wang, K. *et al.* Thyroid Hormone Receptor Interacting Protein 13 (TRIP13) AAA-ATPase Is a Novel Mitotic Checkpoint-silencing Protein. *Journal of Biological Chemistry* **289**, 23928-23937 (2014).
311. Alfieri, C., Chang, L. & Barford, D. Mechanism for remodelling of the cell cycle checkpoint protein MAD2 by the ATPase TRIP13. *Nature* **559**, 274-278 (2018).
312. Ye, Q. *et al.* TRIP13 is a protein-remodeling AAA+ ATPase that catalyzes MAD2 conformation switching. *eLife* **4** (2015).
313. Ma, H.T. & Poon, R.Y.C. TRIP13 Functions in the Establishment of the Spindle Assembly Checkpoint by Replenishing O-MAD2. *Cell Rep* **22**, 1439-1450 (2018).
314. Sheltzer, J.M. & Amon, A. The aneuploidy paradox: costs and benefits of an incorrect karyotype. *Trends in Genetics* **27**, 446-453 (2011).
315. Vleugel, M., Hoogendoorn, E., Snel, B. & Kops, G.J.P.L. Evolution and Function of the Mitotic Checkpoint. *Developmental Cell* **23**, 239-250 (2012).
316. Musacchio, A. & Salmon, E.D. The spindle-assembly checkpoint in space and time. *Nat Rev Mol Cell Biol* **8**, 379-393 (2007).
317. Kops, G.J.P.L. & Shah, J.V. Connecting up and clearing out: how kinetochore attachment silences the spindle assembly checkpoint. *Chromosoma* (2012).
318. Mapelli, M. & Musacchio, A. MAD contortions: conformational dimerization boosts spindle checkpoint signaling. *Current Opinion in Structural Biology* **17**, 716-725 (2007).
319. Kulukian, A., Han, J.S. & Cleveland, D.W. Unattached Kinetochores Catalyze Production of an Anaphase Inhibitor that Requires a Mad2 Template to Prime Cdc20 for BubR1 Binding. *Developmental Cell* **16**, 105-117 (2009).
320. Simonetta, M. *et al.* The influence of catalysis on mad2 activation dynamics. *PLoS Biol* **7**, e10 (2009).
321. Kops, G.J.P.L., Weaver, B.A.A. & Cleveland, D.W. On the road to cancer: aneuploidy and the mitotic checkpoint. *Nature Reviews Cancer* **5**, 773-785 (2005).
322. Moyle, M.W. *et al.* A Bub1-Mad1 interaction targets the Mad1-Mad2 complex to unattached kinetochores to initiate the spindle checkpoint. *J Cell Biol* **204**, 647-657 (2014).
323. Basto, R., Gomes, R. & Karess, R.E. Rough Deal and Zw10 are required for the metaphase checkpoint in Drosophila. *Nat Cell Biol* **2**, 939-943 (2000).
324. Brady, D.M. & Hardwick, K.G. Complex formation between Mad1p, Bub1p and Bub3p is crucial for spindle checkpoint function. *Current Biology* **10**, 675-678 (2000).
325. Chan, G.K.T., Jablonski, S.A., Starr, D.A., Goldberg, M.L. & Yen, T.J. Human Zw10 and ROD are mitotic checkpoint proteins that bind to kinetochores. *Nat Cell Biol* **2**, 944-947 (2000).
326. Liu, S.-T., Rattner, J.B., Jablonski, S.A. & Yen, T.J. Mapping the assembly pathways that specify formation of the trilaminar kinetochore plates in human cells. *The Journal of Cell Biology* **175**, 41 (2006).
327. Klebig, C., Korinth, D. & Meraldi, P. Bub1 regulates chromosome segregation in a kinetochore-independent manner. *The Journal of Cell Biology* **185**, 841 (2009).
328. Kim, S., Sun, H., Tomchick, D.R., Yu, H. & Luo, X. Structure of human Mad1 C-terminal domain reveals its involvement in kinetochore targeting. *Proceedings of the National Academy of Sciences* (2012).
329. Tang, Z., Bharadwaj, R., Li, B. & Yu, H. Mad2-Independent inhibition of

APCCdc20 by the mitotic checkpoint protein BubR1. *Developmental Cell* **1**, 227-237 (2001).
330. Elowe, S. *et al.* Uncoupling of the spindle-checkpoint and chromosome-congression functions of BubR1. *Journal of Cell Science* **123**, 84-94 (2010).
331. Fang, G. Checkpoint Protein BubR1 Acts Synergistically with Mad2 to Inhibit Anaphase-promoting Complex. *Mol Biol Cell* **13**, 755-766 (2002).
332. Morrow, C.J. *et al.* Bub1 and aurora B cooperate to maintain BubR1-mediated inhibition of APC/C<sup>Cdc20</sup&gt. *Journal of Cell Science* **118**, 3639 (2005).
333. Tipton, A.R. *et al.* BUBR1 and Closed MAD2 (C-MAD2) Interact Directly to Assemble a Functional Mitotic Checkpoint Complex. *Journal of Biological Chemistry* **286**, 21173-21179 (2011).
334. Davenport, J., Harris, L.D. & Goorha, R. Spindle checkpoint function requires Mad2-dependent Cdc20 binding to the Mad3 homology domain of BubR1. *Experimental Cell Research* **312**, 1831-1842 (2006).
335. Lara-Gonzalez, P., Scott, M.I.F., Diez, M., Sen, O. & Taylor, S.S. BubR1 blocks substrate recruitment to the APC/C in a KEN-box-dependent manner. *Journal of Cell Science*, 1-14 (2011).
336. Pines, J. Cubism and the cell cycle: the many faces of the APC/C. *Nat Rev Mol Cell Biol* **12**, 427-438 (2011).
337. Burton, J.L. & Solomon, M.J. Mad3p, a pseudosubstrate inhibitor of APCCdc20 in the spindle assembly checkpoint. *Genes & Development* **21**, 655-667 (2007).
338. Sczaniecka, M. *et al.* The Spindle Checkpoint Functions of Mad3 and Mad2 Depend on a Mad3 KEN Box-mediated Interaction with Cdc20-Anaphase-promoting Complex (APC/C). *Journal of Biological Chemistry* **283**, 23039-23047 (2008).
339. Reddy, S.K., Rape, M., Margansky, W.A. & Kirschner, M.W. Ubiquitination by the anaphase-promoting complex drives spindle checkpoint inactivation. *Nature* **446**, 921-925 (2007).
340. Varetti, G., Guida, C., Santaguida, S., Chiroli, E. & Musacchio, A. Homeostatic Control of Mitotic Arrest. *Molecular Cell* **44**, 710-720 (2011).
341. Waters, J.C., Chen, R.-H., Murray, A.W. & Salmon, E.D. Localization of Mad2 to Kinetochores Depends on Microtubule Attachment, Not Tension. *The Journal of Cell Biology* **141**, 1181 (1998).
342. Rivera, V.M. *et al.* A humanized system for pharmacologic control of gene expression. *Nature Medicine* **2**, 1028-1032 (1996).
343. Ditchfield, C. *et al.* Aurora B couples chromosome alignment with anaphase by targeting BubR1, Mad2, and Cenp-E to kinetochores. *J Cell Biol* **161**, 267-280 (2003).
344. Howell, B.J. *et al.* Spindle checkpoint protein dynamics at kinetochores in living cells. *Current Biology* **14**, 953-964 (2004).
345. Skoufias, D.A., Andreassen, P.R., Lacroix, F.B., Wilson, L. & Margolis, R.L. Mammalian mad2 and bub1/bubR1 recognize distinct spindle-attachment and kinetochore-tension checkpoints. *Proceedings of the National Academy of Sciences* **98**, 4492 (2001).
346. Hauf, S. *et al.* The small molecule Hesperadin reveals a role for Aurora B in correcting kinetochore–microtubule attachment and in maintaining the spindle assembly checkpoint. *The Journal of Cell Biology* **161**, 281 (2003).
347. Famulski, J.K. & Chan, G.K. Aurora B Kinase-Dependent Recruitment of hZW10 and hROD to Tensionless Kinetochores. *Current Biology* **17**, 2143-2149 (2007).
348. Vázquez-Novelle, M.D. *et al.* Cdk1 Inactivation Terminates Mitotic Checkpoint Surveillance and Stabilizes Kinetochore Attachments in Anaphase. *Current Biology* (2014).
349. Yang, M. *et al.* p31comet Blocks Mad2 Activation through Structural Mimicry. *Cell* **131**, 744-755 (2007).
350. Famulski, J.K., Vos, L.J., Rattner, J.B. & Chan, G.K. Dynein/Dynactin-Mediated

Transport of Kinetochore Components off Kinetochores and onto Spindle Poles Induced by Nordihydroguaiaretic Acid. *PLoS ONE* **6**, e16494 (2011).
351. Foley, E.A. & Kapoor, T.M. Microtubule attachment and spindle assembly checkpoint signalling at the kinetochore. *Nat Rev Mol Cell Biol* **14**, 25-37 (2012).
352. Sacristan, C. & Kops, G.J. Joined at the hip: kinetochores, microtubules, and spindle assembly checkpoint signaling. *Trends Cell Biol* **25**, 21-28 (2015).
353. London, N. & Biggins, S. Signalling dynamics in the spindle checkpoint response. *Nat Rev Mol Cell Biol* **15**, 736-748 (2014).
354. Nicklas, R.B., Waters, J.C., Salmon, E.D. & Ward, S.C. Checkpoint signals in grasshopper meiosis are sensitive to microtubule attachment, but tension is still essential. *Journal of Cell Science* **114**, 4173-4183 (2001).
355. Li, X. & Nicklas, R.B. Mitotic forces control a cell-cycle checkpoint. *Nature* **373**, 630-632 (1995).
356. Stern, B.M. & Murray, A.W. Lack of tension at kinetochores activates the spindle checkpoint in budding yeast. *Current Biology* **11**, 1462-1467 (2001).
357. Rieder, C.L., Schultz, A., Cole, R. & Sluder, G. Anaphase onset in vertebrate somatic cells is controlled by a checkpoint that monitors sister kinetochore attachment to the spindle. *The Journal of Cell Biology* **127**, 1301 (1994).
358. Pinsky, B.A., Kung, C., Shokat, K.M. & Biggins, S. The Ipl1-Aurora protein kinase activates the spindle checkpoint by creating unattached kinetochores. *Nat Cell Biol* **8**, 78-83 (2006).
359. Shannon, K.B., Canman, J.C. & Salmon, E.D. Mad2 and BubR1 function in a single checkpoint pathway that responds to a loss of tension. *Mol Biol Cell* **13**, 3706-3719 (2002).
360. Khodjakov, A. & Pines, J. Centromere tension: A divisive issue. *Nat Cell Biol* **12**, 919-923 (2010).
361. Nezi, L. & Musacchio, A. Sister chromatid tension and the spindle assembly checkpoint. *Current Opinion in Cell Biology* **21**, 785-795 (2009).
362. Pinsky, B.A. & Biggins, S. The spindle checkpoint: Tension versus attachment. *Trends Cell Biol* **15**, 486-493 (2005).
363. Tanaka, T.U. Kinetochore-microtubule interactions: Steps towards bi-orientation. *EMBO Journal* **29**, 4070-4082 (2010).
364. Santaguida, S., Vernieri, C., Villa, F., Ciliberto, A. & Musacchio, A. Evidence that Aurora B is implicated in spindle checkpoint signalling independently of error correction. *EMBO J* **30**, 1508-1519 (2011).
365. Vader, G. *et al.* The chromosomal passenger complex controls spindle checkpoint function independent from its role in correcting microtubule-kinetochore interactions. *Mol Biol Cell* **18**, 4553-4564 (2007).
366. Kallio, M.J., McCleland, M.L., Todd Stukenberg, P. & Gorbsky, G.J. Inhibition of Aurora B kinase blocks chromosome segregation, overrides the spindle checkpoint, and perturbs microtubule dynamics in mitosis. *Current Biology* **12**, 900-905 (2002).
367. Petersen, J. & Hagan, I.M. S. pombe aurora kinase/survivin is required for chromosome condensation and the spindle checkpoint attachment response. *Current Biology* **13**, 590-597 (2003).
368. Tooley, J.G., Miller, S.A. & Stukenberg, P.T. The Ndc80 complex uses a tripartite attachment point to couple microtubule depolymerization to chromosome movement. *Mol Biol Cell* **22**, 1217-1226 (2011).
369. Sundin, L.J.R., Guimaraes, G.J. & Deluca, J.G. The NDC80 complex proteins Nuf2 and Hec1 make distinct contributions to kinetochore-microtubule attachment in mitosis. *Mol Biol Cell* **22**, 759-768 (2011).
370. Ogo, N. *et al.* Synthesis and biological evaluation of l-cysteine derivatives as mitotic kinesin Eg5 inhibitors. *Bioorganic and Medicinal Chemistry Letters* **17**, 3921-3924 (2007).
371. Zhu, T. *et al.* Phosphorylation of microtubule-binding protein Hec1 by mitotic kinase Aurora B specifies spindle checkpoint kinase Mps1 signaling at the

kinetochore. *jbc.org* (2013).
372. Cheerambathur, D.K., Gassmann, R., Cook, B., Oegema, K. & Desai, A. Crosstalk Between Microtubule Attachment Complexes Ensures Accurate Chromosome Segregation. *Science* **342**, 1239-1242 (2013).
373. Suzuki, A. *et al.* Spindle microtubules generate tension-dependent changes in the distribution of inner kinetochore proteins. *Journal of Cell Biology* **193**, 125-140 (2011).
374. Vleugel, M., Hoogendoorn, E., Snel, B. & Kops, G. Evolution and Function of the Mitotic Checkpoint. *Developmental Cell* **23**, 239-250 (2012).
375. Holland, A.J., Fachinetti, D., Han, J.S. & Cleveland, D.W. Inducible, reversible system for the rapid and complete degradation of proteins in mammalian cells. *Proceedings of the National Academy of Sciences* **109**, E3350-3357 (2012).
376. Gibson, D.G. *et al.* Enzymatic assembly of DNA molecules up to several hundred kilobases. *Nat Meth* **6**, 343-345 (2009).
377. Duijf, P.H. & Benezra, R. The cancer biology of whole-chromosome instability. *Oncogene* **32**, 4727-4736 (2013).
378. Knouse, K.A., Davoli, T., Elledge, S.J. & Amon, A. Aneuploidy in Cancer: Seq-ing Answers to Old Questions. *Annual Review of Cancer Biology* **1**, 335-354 (2017).
379. van Jaarsveld, R.H. & Kops, G.J.P.L. Difference Makers: Chromosomal Instability versus Aneuploidy in Cancer. *Trends in Cancer* **2**, 561-571 (2016).
380. Tanaka, T.U. Bi-orienting chromosomes: acrobatics on the mitotic spindle. *Chromosoma* **117**, 521-533 (2008).
381. Pachis, S.T. & Kops, G. Leader of the SAC: molecular mechanisms of Mps1/TTK regulation in mitosis. *Open Biol* **8**, 180109 (2018).
382. Kemmler, S. *et al.* Mimicking Ndc80 phosphorylation triggers spindle assembly checkpoint signalling. *EMBO J* **28**, 1099-1110 (2009).
383. Hayward, D. *et al.* CDK1-CCNB1 creates a spindle checkpoint-permissive state by enabling MPS1 kinetochore localization. *J Cell Biol* **218**, 1182-1199 (2019).
384. Musacchio, A. The Molecular Biology of Spindle Assembly Checkpoint Signaling Dynamics. *Current Biology* **25**, R1002-R1018 (2015).
385. van der Waal, M.S. *et al.* Mps1 promotes rapid centromere accumulation of Aurora B. *EMBO Rep*, 1-8 (2012).
386. Kagami, Y. *et al.* Mps1 phosphorylation of condensin II controls chromosome condensation at the onset of mitosis. *J Cell Biol* **205**, 781-790 (2014).
387. Wei, J.-H. *et al.* TTK/hMps1 Participates in the Regulation of DNA Damage Checkpoint Response by Phosphorylating CHK2 on Threonine 68. *Journal of Biological Chemistry* **280**, 7748-7757 (2005).
388. Etemad, B. *et al.* Spindle checkpoint silencing at kinetochores with submaximal microtubule occupancy. *J Cell Sci* **132**, jcs231589 (2019).
389. Zaytsev, A.V. *et al.* Bistability of a coupled Aurora B kinase-phosphatase system in cell division. *eLife* **5**, e10644 (2016).
390. O'Connor, A. *et al.* Requirement for PLK1 kinase activity in the maintenance of a robust spindle assembly checkpoint. *Biol Open* **5**, 11-19 (2015).
391. Macurek, L. *et al.* Polo-like kinase-1 is activated by aurora A to promote checkpoint recovery. *Nature* **455**, 119-123 (2008).
392. Bruinsma, W., Macurek, L., Freire, R., Lindqvist, A. & Medema, R.H. Bora and Aurora-A continue to activate Plk1 in mitosis. *J Cell Sci* **127**, 801-811 (2014).
393. Alexander, J. *et al.* Spatial exclusivity combined with positive and negative selection of phosphorylation motifs is the basis for context-dependent mitotic signaling. *Sci Signal* **4**, ra42 (2011).
394. Dou, Z. *et al.* Quantitative mass spectrometry analysis reveals similar substrate consensus motif for human Mps1 kinase and Plk1. *PLoS ONE* **6**, e18793 (2011).
395. Goedhart, J. *et al.* Structure-guided evolution of cyan fluorescent proteins towards a quantum yield of 93%. *Nature Communications* **3**, 751-759 (2012).
396. Koch, A., Maia, A., Janssen, A. & Medema, R.H. Molecular basis underlying resistance to Mps1/TTK inhibitors. *Oncogene* **35**, 2518-2528 (2016).

397. Hennrich, M.L. *et al.* Universal quantitative kinase assay based on diagonal SCX chromatography and stable isotope dimethyl labeling provides high-definition kinase consensus motifs for PKA and human Mps1. *J Proteome Res* **12**, 2214-2224 (2013).
398. Lenart, P. *et al.* The small-molecule inhibitor BI 2536 reveals novel insights into mitotic roles of polo-like kinase 1. *Curr Biol* **17**, 304-315 (2007).
399. Etemad, B., Kuijt, T.E.F. & Kops, G.J.P.L. Kinetochore–microtubule attachment is sufficient to satisfy the human spindle assembly checkpoint. *Nat Commun* **6**, 8987 (2015).
400. Tauchman, E.C., Boehm, F.J. & DeLuca, J.G. Stable kinetochore-microtubule attachment is sufficient to silence the spindle assembly checkpoint in human cells. *Nat Commun* **6**, 10036 (2015).
401. Dou, Z. *et al.* Dynamic localization of Mps1 kinase to kinetochores is essential for accurate spindle microtubule attachment. *Proc Natl Acad Sci U S A* **112**, E4546-4555 (2015).
402. Gavet, O. & Pines, J. Activation of cyclin B1-Cdk1 synchronizes events in the nucleus and the cytoplasm at mitosis. *J Cell Biol* **189**, 247-259 (2010).
403. Cheeseman, I.M. & Desai, A. Molecular architecture of the kinetochore-microtubule interface. *Nat Rev Mol Cell Biol* **9**, 33-46 (2008).
404. Holland, A.J. & Cleveland, D.W. Losing balance: the origin and impact of aneuploidy in cancer. *EMBO Rep* **13**, 501-514 (2012).
405. Berg, K.C.G. *et al.* Multi-omics of 34 colorectal cancer cell lines - a resource for biomedical studies. *Mol Cancer* **16**, 116 (2017).
406. Lengauer, C., Kinzler, K.W. & Vogelstein, B. Genetic instability in colorectal cancers. *Nature* **386**, 623-627 (1997).
407. van de Wetering, M. *et al.* Prospective derivation of a living organoid biobank of colorectal cancer patients. *Cell* **161**, 933-945 (2015).
408. Bolhaqueiro, A.C.F. *et al.* Ongoing chromosomal instability and karyotype evolution in human colorectal cancer organoids. *Nat Genet* **51**, 824-834 (2019).
409. von Schubert, C. *et al.* Plk1 and Mps1 Cooperatively Regulate the Spindle Assembly Checkpoint in Human Cells. *Cell Rep* **12**, 66-78 (2015).
410. Ballister, E.R., Riegman, M. & Lampson, M.A. Recruitment of Mad1 to metaphase kinetochores is sufficient to reactivate the mitotic checkpoint. *J Cell Biol* **204**, 901-908 (2014).
411. Kuijt, T.E.F., Omerzu, M., Saurin, A.T. & Kops, G.J.P.L. Conditional targeting of MAD1 to kinetochores is sufficient to reactivate the spindle assembly checkpoint in metaphase. *Chromosoma* **123**, 471-480 (2014).
412. Williams, S.J., Abrieu, A. & Losada, A. Bub1 targeting to centromeres is sufficient for Sgo1 recruitment in the absence of kinetochores. *Chromosoma* **126**, 279-286 (2017).
413. Adriaans, I.E., Basant, A., Ponsioen, B., Glotzer, M. & Lens, S.M.A. PLK1 plays dual roles in centralspindlin regulation during cytokinesis. *J Cell Biol* **218**, 1250-1264 (2019).
414. Drost, J. *et al.* Sequential cancer mutations in cultured human intestinal stem cells. *Nature* **521**, 43-47 (2015).
415. Suijkerbuijk, S.J. *et al.* Molecular causes for BUBR1 dysfunction in the human cancer predisposition syndrome mosaic variegated aneuploidy. *Cancer Res* **70**, 4891-4900 (2010).
416. Schindelin, J. *et al.* Fiji: an open-source platform for biological-image analysis. *Nat Methods* **9**, 676-682 (2012).
417. Krenn, V., Overlack, K., Primorac, I., van Gerwen, S. & Musacchio, A. KI Motifs of Human Knl1 Enhance Assembly of Comprehensive Spindle Checkpoint Complexes around MELT Repeats. *Current Biology* (2013).
418. Wu, J.Q. *et al.* PP1-mediated dephosphorylation of phosphoproteins at mitotic exit is controlled by inhibitor-1 and PP1 phosphorylation. *Nat Cell Biol* **11**, 644-651 (2009).

419. Lara-Gonzalez, P. *et al.* The G2-to-M Transition Is Ensured by a Dual Mechanism that Protects Cyclin B from Degradation by Cdc20-Activated APC/C. *Developmental Cell* (2019).
420. Chen, Q., Zhang, X., Jiang, Q., Clarke, P.R. & Zhang, C. Cyclin B1 is localized to unattached kinetochores and contributes to efficient microtubule attachment and proper chromosome alignment during mitosis. *Cell Res* **18**, 268-280 (2008).
421. Zeitlin, S.G., Barber, C.M., Allis, C.D. & Sullivan, K. Differential regulation of CENP-A and histone H3 phosphorylation in G2/M. *Journal of Cell Science* **114**, 653 (2001).
422. Dumitru, A.M.G., Rusin, S.F., Clark, A.E.M., Kettenbach, A.N. & Compton, D.A. Cyclin A/Cdk1 modulates Plk1 activity in prometaphase to regulate kinetochore-microtubule attachment stability. *eLife* **6**, e29303 (2017).
423. Schmidt, J.C. *et al.* Aurora B kinase controls the targeting of the Astrin–SKAP complex to bioriented kinetochores. *The Journal of Cell Biology* **191**, 269 (2010).
424. Schmidt, Jens C. *et al.* The Kinetochore-Bound Ska1 Complex Tracks Depolymerizing Microtubules and Binds to Curved Protofilaments. *Developmental Cell* **23**, 968-980 (2012).
425. Abad, M.A. *et al.* Structural basis for microtubule recognition by the human kinetochore Ska complex. *Nature Communications* **5**, 2964 (2014).
426. Janssen, L.M.E. *et al.* Loss of Kif18A Results in Spindle Assembly Checkpoint Activation at Microtubule-Attached Kinetochores. *Current Biology* **28**, 2685-2696. e2684 (2018).
427. Li, J., Dang, N., Wood, D.J. & Huang, J.-Y. The kinetochore-dependent and -independent formation of the CDC20-MAD2 complex and its functions in HeLa cells. *Sci. Rep.* **7**, 41072 (2017).
428. Choi, E., Zhang, X., Xing, C. & Yu, H. Mitotic Checkpoint Regulators Control Insulin Signaling and Metabolic Homeostasis. *Cell* (2016).
429. Choi, E. & Yu, H. Spindle Checkpoint Regulators in Insulin Signaling. *Frontiers in Cell and Developmental Biology* **6**, 161 (2018).
430. Wang, W., Wu, T. & Kirschner, M.W. The master cell cycle regulator APC-Cdc20 regulates ciliary length and disassembly of the primary cilium. *eLife* **3**, e03083 (2014).
431. Huang, J. & Bonni, A. A decade of the anaphase-promoting complex in the nervous system. *Genes & Development* **30**, 622-638 (2016).
432. Kim, A.H. *et al.* A Centrosomal Cdc20-APC Pathway Controls Dendrite Morphogenesis in Postmitotic Neurons. *Cell* **136**, 322-336 (2009).
433. Hadjihannas, M.V., Bernkopf, D.B., Brückner, M. & Behrens, J. Cell cycle control of Wnt/β-catenin signalling by conductin/axin2 through CDC20. *EMBO Rep* **13**, 347-354 (2012).
434. Hori, T., Haraguchi, T., Hiraoka, Y., Kimura, H. & Fukagawa, T. Dynamic behavior of Nuf2-Hec1 complex that localizes to the centrosome and centromere and is essential for mitotic progression in vertebrate cells. *Journal of Cell Science* **116**, 3347 (2003).
435. Gascoigne, K.E. & Cheeseman, I.M. CDK-dependent phosphorylation and nuclear exclusion coordinately control kinetochore assembly state. *The Journal of Cell Biology* **201**, 23-32 (2013).
436. Buffin, E., Lefebvre, C., Huang, J., Gagou, M.E. & Karess, R.E. Recruitment of Mad2 to the Kinetochore Requires the Rod/Zw10 Complex. *Current Biology* **15**, 856-861 (2005).
437. Flegg, C.P. *et al.* Nuclear Export and Centrosome Targeting of the Protein Phosphatase 2A Subunit B56α: ROLE OF B56α IN NUCLEAR EXPORT OF THE CATALYTIC SUBUNIT. *Journal of Biological Chemistry* **285**, 18144-18154 (2010).
438. Varadkar, P., Abbasi, F., Takeda, K., Dyson, J.J. & McCright, B. PP2A-B56γ is required for an efficient spindle assembly checkpoint. *Cell Cycle* **16**, 1210-1219 (2017).
439. Sontag, E., Nunbhakdi-Craig, V., Bloom, G.S. & Mumby, M.C. A novel pool of

protein phosphatase 2A is associated with microtubules and is regulated during the cell cycle. *The Journal of Cell Biology* **128**, 1131 (1995).
440. Kishi, K., van Vugt, M.A.T.M., Okamoto, K.-i., Hayashi, Y. & Yaffe, M.B. Functional Dynamics of Polo-Like Kinase 1 at the Centrosome. *Molecular and Cellular Biology* **29**, 3134-3150 (2009).
441. Izumi, H. *et al.* BubR1 localizes to centrosomes and suppresses centrosome amplification via regulating Plk1 activity in interphase cells. *Oncogene* **28**, 2806 (2009).
442. Ferrell, J.E. Self-perpetuating states in signal transduction: positive feedback, double-negative feedback and bistability. *Current Opinion in Cell Biology* **14**, 140-148 (2002).
443. Huang, H. *et al.* Phosphorylation sites in BubR1 that regulate kinetochore attachment, tension, and mitotic exit. *The Journal of Cell Biology* **183**, 667-680 (2008).
444. Trinkle-Mulcahy, L. *et al.* Time-lapse imaging reveals dynamic relocalization of PP1gamma throughout the mammalian cell cycle. *Mol Biol Cell* **14**, 107 (2003).
445. Grallert, A. *et al.* A PP1–PP2A phosphatase relay controls mitotic progression. *Nature* (2014).
446. Gut, G., Herrmann, M.D. & Pelkmans, L. Multiplexed protein maps link subcellular organization to cellular states. *Science* **361**, eaar7042 (2018).
447. Murakoshi, H., Shibata, A.C.E., Nakahata, Y. & Nabekura, J. A dark green fluorescent protein as an acceptor for measurement of Förster resonance energy transfer. *Sci. Rep.* **5**, 15334 (2015).
448. Murakoshi, H. & Shibata, A.C.E. ShadowY: a dark yellow fluorescent protein for FLIM-based FRET measurement. *Sci. Rep.* **7**, 6791 (2017).
449. Bertolin, G. *et al.* Optimized FRET Pairs and Quantification Approaches To Detect the Activation of Aurora Kinase A at Mitosis. *ACS Sensors* **4**, 2018-2027 (2019).

Nederlandse samenvatting

Celdeling en chromosoomsegregatie

De ontwikkeling, groei en het in standhouden van een gezond lichaam berust op het structureel aanvullen en vernieuwen van cellen, de eenheden waaruit ons lichaam is opgebouwd. Door middel van celdeling of mitose, splits één moedercel zich in twee identieke dochtercellen. In één dag vinden er naar schatting twéé biljoen celdelingen plaats in een volwassen menselijk lichaam. Bij iedere deling worden alle eigenschappen van de moedercel nauwkeurig overgedragen op de dochtercellen. Een zeer belangrijk onderdeel hierin is het erfelijk materiaal waarop instructies liggen opgeslagen die de cel nodig heeft om correct te functioneren en communiceren binnen ons lichaam.

Ons erfelijk materiaal bestaat uit strengen DNA en deze zijn opgevouwen tot 46 chromosomen in de kern van een menselijke cel. Zowel de vader als de moeder leveren een sets van 23 unieke chromosomen aan die in hun nakomelingen een set van 2 x 23 chromosomen vormen (46 chromosomen in totaal). Het DNA codeert de instructies om moleculaire machines, eiwitten genaamd, te maken en eiwitten zijn de voornaamste functionele componenten in cellen.

Voordat een cel kan delen wordt de inhoud van de cel gerepliceerd waaronder een exact kopie van ieder chromosomen. Gerepliceerde chromosomen (2x 46 chromosomen) worden bij elkaar gehouden, als zusterchromatiden, zodat tijdens de segregatie van de chromosomen in mitose iedere dochtercel een van de twee kopieën toegedeeld krijgt. Het eerlijk doorgeven van de chromosomen (de instructiesets) is essentieel voor het correct functioneren van cellen in het lichaam. Fouten in de verdelen van chromosomen heeft als gevolg dat in dochtercellen delen van de instructieset ontbreken, een staat die aneuploïdie genoemd wordt. Aneuploïdie verstoord de cellulaire balans en kan de fitheid van cellen verminderen wat kan leiden tot het ontstaan van ziektes of problemen in de ontwikkeling van een organisme. In de ziektes die tezamen kanker genoemd wordt, is in veel gevallen aneuploïdie aanwezig in de kankercellen.

Het segregeren van de zusterchromatiden wordt mogelijk gemaakt door de mitotische spoel, een georganiseerd netwerk van trekdraden (microtubuli) die vanuit twee centrale, tegenover elkaar liggende punten (centrosomen) een bipolaire spoel vormt. De mitotische spoel bindt aan de zusterchromatiden om deze vervolgens naar tegenover elkaar liggende centrosomen te slepen (**Figuur 1B, introductie**). Hierdoor krijgt ieder dochtercel één volledige set van 46 chromosomen toegedeeld. Ieder zusterchromosoom kan binden aan microtubuli via een specifiek domein, de kinetochoor. Om zusterchromatiden correct te segregeren naar iedere dochtercel is het essentieel dat de ene zusterkinetochoor aan microtubuli vanuit de ene pool bindt en de andere kinetochoor aan microtubuli van de andere pool. Deze configuratie is amfitelisch

genaamd en alleen deze configuratie kan gelijke segregatie van zusterchromatiden produceren. Alleen wanneer alle 46 chromosoom paren deze configuratie hebben verworven, genaamd metafase (**Figuur 1B, introductie**), kan gelijke segregatie van zusterchromatiden voltrekken.

Het spindle assembly checkpoint en error correction

Tijdens mitose worden kinetochoor-microtubuli configuraties gevormd die gelijke chromosoomsegregaties niet kunnen waarmaken (**Figuur 3, introductie**). Cellen beschikken over mechanismen die de status van de kinetochoor-microtubuli verbinding detecteert en reguleert. Deze mechanismen voorkomen dat incorrecte verbindingen leiden tot fouten in de segregatie van chromosomen en aneuploïde dochtercellen ontstaan. Eén zo'n mechanisme, genaamd het spindle assembly checkpoint (SAC), is actief op kinetochoren die niet verbonden zijn aan microtubuli en zendt een signaal uit om te voorkomen dat de cel overgaat tot het segregeren van de chromosomen. Een tweede mechanisme, het error correction pathway, detecteert incorrecte kinetochoor-microtubuli interacties en destabiliseert deze om de kans te vergroten dat amfitelische verbindingen daaropvolgend vormen.

Het SAC wordt aangestuurd door MPS1, een enzym dat op de kinetochoor actief is wanneer deze niet gebonden is aan microtubuli. MPS1 zorgt ervoor dat andere SAC-eiwitten op de kinetochoor clusteren, een diffuus SAC-signaal produceren en de celdeling vertragen. Binding van microtubuli aan de kinetochoor verstoot MPS1 van de kinetochoor en hiermee neemt de activiteit van dit enzym af waardoor het SAC-signaal gedempt wordt. Daarnaast worden SAC-eiwitten van de kinetochoor verwijderd om het SAC-signaal verder te dempen. Het SAC-mechanisme is zo effectief dat één niet verbonden kinetochoor voldoende SAC-signaal uitzendt om celdeling te vertragen.

De stabiliteit van kinetochoor-microtubuli verbindingen wordt gereguleerd door het enzym Aurora B. Door de kinetochoor chemisch te modificeren, neemt de affiniteit van de kinetochoor voor microtubuli af en laat de kinetochoor de microtubuli los. De chemische modificaties op de kinetochoor wordt continu verwijderd en hiermee ontstaat een dynamisch systeem voor de regulatie van kinetochoor-microtubuli verbindingen. Microtubuli trekken aan de kinetochoor en alleen amfitelische verbindingen kunnen de trekkrachten van microtubuli weerstaan doordat de activiteit van Aurora B afneemt in deze configuratie.

De destabilisatie van kinetochoor-microtubuli verbindingen zorgt ervoor dat de kinetochoor niet verbonden is aan microtubuli en hierdoor een SAC-signaal afgeeft. Deze twee mechanismen zijn onlosmakelijk aan elkaar verbonden. Daarbovenop bevorderen Aurora B en MPS1 elkaars activiteit en zijn er nog veel meer eiwitten bij betrokken die deze processen reguleren tijdens mitose. Tezamen zorgen het error correction pathway en SAC ervoor dat cellen niet delen zolang er incorrecte kinetochoor-

microtubuli verbindingen aanwezig zijn en hiermee beschermen zij tegen het verlies van chromosomen tijdens mitose.

Het onderzoek beschreven in dit proefschrift

De onderzoeksresultaten beschreven in dit proefschrift geven meer inzicht in de fundamentele werking en regulatie van SAC-signalering en de activator van de SAC, MPS1. In **Hoofdstuk 1** wordt een algemene introductie gegeven over het celdelingsproces, de onderliggende regulatiemechanismen en de functie van betrokken eiwitten in deze mechanismen.

In **Hoofdstuk 2** behandelen we de vraag welke stap essentieel is voor het dempen van het SAC-signaal op de kinetochoor. Het uitzetten van het SAC-signaal gebeurt via verschillende mechanismes die nauw samenwerken. Door een proefopstelling op te zetten waarin wij een specifiek SAC-eiwit terugzetten op de kinetochoor, achterhalen we de cruciale stap voor SAC-demping op de kinetochoor. Onze studie laat zien dat het door MPS1-gerecruiteerde eiwit MAD1 van de kinetochoor te verwijderen het SAC-signaal uitgezet wordt. Verder onthullen wij dat de activiteit van MPS1 niet volledig gedempt is op het moment dat het SAC-signaal uit staat in metafase.

In **Hoofdstuk 3** adresseren we de vraag welke moleculaire verandering op de kinetochoor ten grondslag ligt voor het uitzetten van het SAC-signaal. De kinetochoor en onderliggend DNA van het chromosoom worden door de trekkrachten van microtubuli vervormt waarbij de afstand tussen DNA en de kinetochoor groter wordt. In de afwezigheid van deze kinetochoor-rek, zorgt Aurora B activiteit ervoor dat microtubuli de kinetochoor loslaten en hiermee geeft de kinetochoor een SAC-signaal af. Het is onduidelijk of het vormen van kinetochoor-microtubuli verbindingen of de kinetochoor-rek het SAC-signaal uitzet. Wij tonen aan dat het vormen van kinetochoor-microtubuli verbinden voldoende is om het SAC-signaal uit te zetten in de afwezigheid van enige meetbare kinetochoor-rek. Dit toont de onderliggende werking van het SAC-signaal aan en roept vragen op waarom en wat kinetochoor-rek voor een functie heeft.

In **Hoofdstuk 4** onderzoeken we de regulatie van MPS1 activatie en modulatie van MPS1 activiteit in detail. Door een moleculaire sensor specifiek voor MPS1 (MPS1sen) te ontwikkelen kunnen we met lichtmicroscopie de activiteit van MPS1 op specifieke plekken in de cel ten alle tijden meten. Met MPS1sen onthullen wij dat initiatie van MPS1 activiteit 9-12 minuten voor de start van mitose plaats vindt met een kinetiek gelijkend op het omzetten van een schakelaar. De kinetochoor is belangrijk voor de activatie van MPS1 en vorming van kinetochoor-microtubuli verbindingen verminderen activiteit gemeten met MPS1sen in cellen. Wij onthullen dat MPS1 activatie gereguleerd wordt door de fosfatase PP2A-B56, het SAC-eiwit BUBR1 en de kinase Aurora B. Tot slot passen wij MPS1sen toe in dikke darmtumor cellijnen en dikke darmtumor 3D-miniorganen en beschrijven dat MPS1 activiteit verminderd is in tumorcellen.

Curriculum Vitae

Timoteo Enrique Felipe Kuijt was born in Bogota, Colombia on July 12th, 1987. In 2004 he obtained his HAVO high school diploma from the Jacob Roelandlyceum in Boxtel, The Netherlands. In this same year he enrolled in the bachelor programme for Applied Sciences at the Fontys University of Applied Sciences in Eindhoven. As part of his bachelor studies he undertook a research internship in the lab of Prof. dr. Gerco Angenent at Plant Research International, Wageningen University, under supervision of dr. Stefan de Folter. His second rotation was completed in the cell biology department headed by Prof. dr. Ger Strous, in the lab of dr. Peter van der Sluijs, the University Medical Centre Utrecht. In the year 2008 he completed his B.Sc. studies and enrolled in the Master Molecular and Cellular Life Sciences programme at Utrecht University. He then started a one-year rotation in the lab of Prof. dr. Johannes Boonstra under supervision of dr. Elsa Regan-Klapisz at University Utrecht. Subsequently, he started a rotation in the lab of Prof. dr. Geert Kops at University Medical Centre Utrecht under the supervision of dr. Adrian Saurin. After completing his Master degree, he started his doctoral studies in this same lab in 2011, postponing these studies in 2014. In the year 2016 he reinitiated his doctoral studies, the results of which are described in this work.

&

List of publications

Kuijt, T.E.F., S. Weterings, B. Ponsioen, A.C.F. Bolhaqueiro, D. Staijen, and G.J.P.L. Kops. 2020. A biosensor for the mitotic kinase MPS1 reveals spatiotemporal activity dynamics and regulation. *In revision at Current Biology*.

Etemad, B., A. Vertesy, **T.E.F. Kuijt**, C. Sacristan, A. van Oudenaarden, and G.J.P.L. Kops. 2019. Spindle checkpoint silencing at kinetochores with submaximal microtubule occupancy. *Journal of Cell Science*. 132:jcs231589.

Hiruma, Y., C. Sacristan, S.T. Pachis, A. Adamopoulos, **T.E.F. Kuijt**, M. Ubbink, E. von Castelmur, A. Perrakis, and G.J.P.L. Kops. 2015. Competition between MPS1 and microtubules at kinetochores regulates spindle checkpoint signaling. *Science*. 348:1264.

Etemad, B., **T.E.F. Kuijt**, and G.J.P.L. Kops. 2015. Kinetochore–microtubule attachment is sufficient to satisfy the human spindle assembly checkpoint. *Nature Communications*. 6:8987.

Kuijt, T.E.F., M. Omerzu, A.T. Saurin, and G.J.P.L. Kops. 2014. Conditional targeting of MAD1 to kinetochores is sufficient to reactivate the spindle assembly checkpoint in metaphase. *Chromosoma*. 123:471-480.

Dankwoord

Zo, dit *opus* is klaar! Na een lange zit (reken zelf maar uit hoe lang), is het dan toch tot een boekje gekomen. Een boekje waar ik zelf tros op ben maar nooit tot stand was gekomen zonder de steun en hulp van een flink aantal mensen. Een duit in eigen zakje, ik heb niet altijd blijk gegeven dat ik er veel plezier in heb gehad, edoch zijn er voornamelijk positieve herinneringen die mij bijstaan. Voornamelijk de mensen om mij heen vormen deze goede herinneringen, en daarom verdienen zij genoemd en geprezen te worden.

Te beginnen met de dirigent, **Geert**. De runner-up 'best PhD supervisor of the year 2016', maar wat mij betreft had je de eerste prijs verdient! Ik ben je zeer dankbaar dat ik met jou samen heb mogen werken en van dichtbij zo veel van je hebt mogen leren. Je wetenschappelijke talent is groot en hiermee breng je op een ogenschijnlijk eenvoudige manier verschillende vakgebieden samen in je onderzoeksgroep, dit vind ik heel bijzonder. Je bezorgdheid voor iedereen binnen de groep creëert een geweldige omgeving waarin iedereen zich optimaal kan ontwikkelen met veel creatieve vrijheid. De groep wetenschappers die je weet samen te brengen vormen een bron voor deze zelfontwikkeling, zowel wetenschappelijk als op persoonlijk vlak. Ik hoop dat het appendix hoofdstuk (juist, het werk dat dit boekje niet heeft gehaald), de aandacht krijgt om te ontpoppen tot een heerlijk complex signaaltransductie werk waar ik zo naar verlangde om te ontrafelen. Nogmaals, Geert enorm bedankt voor al je toewijding, vertrouwen en mentorschap.

Leden van de PhD-commissie (**Jacco van Rheenen** en **Paul Coffer**), bedankt voor het altijd klaar staan met nuttige adviezen tijdens de jaarlijkse evaluaties. Tevens ook heel veel dank dat jullie zitting hebben genomen in de leescommissie om dit proefschrift te beoordelen. The other members of the assessment committee (**Catherine Rabouille**, **Judith Klumperman** and **Adrian Saurin**), thank you for taking time and interest in assessing this doctoral dissertation. Adrian, I am very excited you are part of the assessment committee and look forward to spending time with you discussing science. Your drive for performing science at the highest standard is astonishing and I admire your ambition and dedication. You have really inspired me to tackle complex signalling pathways and I still draw up models on white boards like old times. Furthermore, I would like to thank **Lukas Kapitein, Anastassis Perrakis** and **Michael Hadders** for taking seat at the opposition table during my defense, I look forward to the exchange of thoughts.

Ik heb veel geluk gehad met de master studenten die onder mij hoede terecht zijn gekomen. Allereerst **Debbie**, bedankt dat je het grondwerk voor hoofdstuk 4 hebt verricht, dit was geen eenvoudige klus. Zonder dit deel was er nooit een boekje geweest, daarom ben ik je zeer dankbaar voor je bijdrage! Ik heb onze samenwerking altijd als heel plezierig en zeer leerzaam ervaren, relaxed was ik minder in die tijd. Veel succes met het uitstippelen van je toekomst, het ga je goed. Daarna kwam **Sonja** (Son)

uit het niets tevoorschijn! Ook jij hebt een belangrijke bijdrage aan hoofdstuk 4 en de daaruit voortvloeiende publicatie gedaan (we zijn er bijna!). Dat verdient sowieso een paar stickers, of beter een roze Japans cute-cuddly-toy! Ik heb veel genoten van onze samenwerking, en je assertiviteit en zelfstandigheid waren geruststellend om te zien in een master-student. Ik mis je geweldige verhalen en soms iets wat platte humor in het lab. Nu ga je zelfstandig aan de slag als kersverse PhD-student en dus zal ook jij masterstudenten gaan begeleiden. Doen! Het is heel leuk, tenminste als je een tweede Son als student krijgt.

Current members of the Kops lab: A big thank you to you all, as this group is made special by each of your personalities and commitment to each other as colleagues and friends. **Nannette**, it is time for me to check out at '*Hotel California*'. I admire your approach to do science, your critical insights and how you always share those in a calm way to help your colleagues improve their work. Sweet and caring is how I would describe you in two words **Banafsheh**. I was very excited when you decided to stay in '*Hotel California*', as a big hole would arise if you were to have left the group. Thank you for all your sweet words and friendship, you would have been my third paranimf, but then I would fix this tradition for all eternity. The B-Rex, **Bas**, you have the ability to always see the coin from another direction and take approaches no one could come up with. This skill will bring you far in life, just don't forget to add minimal the controls where needed. I enjoyed 'Men's Night' and 'Movie Night' at *Spíti tis Sofia and Bas*. Good luck with writing up the very interesting story on *CC48D(?)* or *HRT-ATC* or whatever this month's acronym is. **Kim**, my buddy from the start. Your perseverance has brought you far and will carry you further still. I admire you for also thinking about the curriculum beyond just science and your active involvement in developing this further for your colleagues. You are always ready for friends and this draws people to like you and enjoy your company. **Joana**, the next warrior princess to tackle the complexity that the organoid group faces. You avoid no battles and obstacles will not slow you down much. You are very caring and provide a listening ear to those in need for one, thank you for this. **Jingchao**, you are calm yet work hard and quietly on very complex stuff. I am sure you will finish this story soon and think **Tim** will help you a great deal in this. **Emine**, you are a very kind and generous person, willing to help whenever needed. Also, thank you for sharing all these nice snacks you bring for us from distant places or family recipes your mother prepared. **Sjoerd**, you stun people with your humor and special ways to push people's buttons. I know the lab feels empty without that one person so special to you, but luckily you have managed to get passed this already. Good luck finishing up your PhD, should be in 2020 no? no pressure, not at all! **Bastiaan**, de vroege vogel. Wat fijn dat jij naast me zat, de rust die je uitstraalt is merkbaar. Hulde voor de manier waarop je alle touwtjes in handen houdt, geen gemakkelijke taak maar je doet 't echt goed. **Pim**, 'mister sunshine', jij maakt ongeacht de situatie altijd het beste ervan en kan mensen altijd opvrolijken. Je energie is oneindig en je bent altijd bereid te helpen

op welke manier dan ook. Ik hoop dat je nog vele jaren de 'Kopsies' zult opvrolijken en nieuwe dingen kunt leren wat toch eigenlijk het leukste is aan deze job! **Anko**, de stille kracht die het Hubrecht en 'Kopies' voor zeker de helft draaiende houdt. Bedankt voor al je toewijding en het uitvoeren van verbeteringen die we in de afgelopen jaren hebben bedacht. Ik hoop dat je eindelijk eens versterking krijgt omdat dit verdient en met de continue expansie van het instituut ook nodig is. **Dani**, je brengt leve in de brouwerij! Daarnaast ben ik blij dat je je enorme berg aan kennis en ervaring deelt met ons! De man die weet van aanpakken, **Nico**! Bedankt dat je zo efficiënt en vol energie de taak als lab-manager ben komen opvullen. En meer dan dat, je brengt veel kennis en veel humor mee waar we allemaal ook zeer van genieten. Binnenkort maar eens wat cellijnen naar de stikstof brengen? **Marta**, you quietly joined the group, yet I am very happy you found us. Thank you for de gezelligheid and good luck with filming those pesky oocytes, you got this!

Kopsies from the past but nonetheless not forgotten: **Spiros**, you are such a delightful person to have around. I miss you but am glad you pop up at various occasions, so until we meet again. '*Fire in the hacienda*', baby! **Richard**, ik ben heel blij dat je een positie hebt gevonden waarin je op je stek zit en verder kunt groeien. Je nuchtere en kritische blik op het leven en wetenschap mis ik. De eerste dinner-date is geschied, ik vond het gezellig **Camilla** en stond versteld van je cooking-skills . Beetje schuiven in de agenda, dan gaat het vast lukken! **Ana F**, your strong energy always broke the boring routines that can creep up on us unknowingly. I miss our nice chats and your dedication to coming up with nice SKA-avond events. You brought so much life to the lab, and thank you for your time and effort to last minute help out pimping chapter 4! **Richarda**, bedankt voor de gezelligheid! Ook al ben je al een tijdje niet meer gespot in de gangen ik hoop dat je weer een langs komt. Verder heb ik veel bewondering voor je wetenschappelijke inzichten en management skills! **Eelco**, je toewijding om een bijdrage aan de wetenschap te maken is indrukwekkend en je verzet onmenselijke hoeveelheden werk om dit te bereiken. Verder heb ik altijd genoten van je verhalen en plezierige persoonlijkheid. Ik hoop je snel weer eens te spreken. **Wilma**, ik heb genoten van onze praatjes en je bent nooit bang om buiten je comfortzone te treden. Een hele belangrijke eigenschap daarnaast ben je een echt gezelligheidsdier, wat fijn om je als collega te hebben gehad. **Ajit**, ik ben blij dat je de keuze hebt durven maken om een carrière switch uit te voeren. Enerzijds moest het wel, maar er was ook een verlangen naar vrijheid. Deze heb je gevonden en daarnaast heb je een 'little lion' rondlopen die je vol liefde stopt. *The little lion will roar one day like his farther!* **Alexandra,** mijn grote zus van een andere moeder (en vader). Ik heb enorm genoten van onze tijd samen in het lab. Jammer dat ik zo'n slechte student Spaans was, ik vond het heel fijn een beetje Colombia naast me te hebben, ik mis je. **Antoinette**, je inzet en toewijding voor het organiseren van het lab waren van groot belang. Daarnaast heb je veel collega's ondersteund zowel in het lab als op de momenten waarop de emoties hoog waren. **Claudia**, je energie was altijd welkom

in de groep, fijn dat je altijd een praatje wilde maken en helpen wanneer nodig. **Debora**, you were a silent workhorse in the lab. At first glance you were a quiet and sweet person who spoke so calmly. Yet you have much passion inside you for life and it was very nice to get to know you a bit. **Yoshitake-san**, I am sad that you were stationed in Amsterdam as I always enjoyed the moments you were around. I hope we run into each other again soon, *arigato gozaimashita*. **Jolien**, ik vond het altijd leuk om naar je heldere presentaties te luisteren. De discussies die je hiermee voorbracht hebben mij doen leren buiten mijn eigen expertise te denken. X**iaorong**, you are a warm and hard worker. I enjoyed our discussions on scientific stuff and your energetic personality was very pleasant to have around. I hope you are doing well! Then there are those from another era: **Mattie**, **Tale**, **Wilco**, **Saskia**, **Aniek, Vincent**. Jullie waren de pioniers en hebben een stempel gedrukt op de manier waarop het lab zich heeft ontwikkeld. Dit heeft mij ook beïnvloed en de gezelligheid was uniek, bedankt!

Besides the Kops-group, many other people have contributed whom deserve mentioning. Ten eerste, **Bas Ponsioen**. Je toewijding aan de wetenschap is een beetje intimiderend alsmede je kennis van alles omtrent microscopie. Zonder jou waren een hoop projecten, waaronder hoofdstuk 4, niet van de grond gekomen! Mijn go-to voor advies, reagentia en borrels het Lens-Lab. **Susanne Lens** bedankt voor al je input op projecten in de tijd dat we nog gezamenlijke werkbesprekingen voerden. **Martijn**, bedankt dat je altijd bereid bent om snel vragen te beantwoorden en spullen wilde delen. Jij bent de super manager van het lab en bezit enorm veel kennis. Jammer dat ik niet meer van je eigen bier brouwsels heb kunnen proeven. **Ingrid**! Je besloot toch maar even te bellen voor een promotiedatum, waarom niet? Ik bewonder de manier waarop je je eigen weg beloopt in de wetenschap en in het leven zelf. Verder geniet ik nog wel eens na van de toptijd die we in hadden in Philly, *fire in the hacienda*! **Michael**, yup een tweede vermelding zowaar. Ik waardeer en bewonder je kritische blik die je werpt op de wetenschap en relaxed houding. **Livio**, bedankt voor alle fijne praatjes, feestjes en hulp met het aanslingeren van microscopen. Ik heb veel van je geleerd! **Amanda**, **Sanne**, **Sippe**, ik hoop dat jullie alle een mooie nieuwe plek hebben gevonden waar jullie je lieve persoonlijkheden zo veel gewaardeerd worden als op het Lens lab het geval was.

From the van Rooij-lab, thank you, **Brian**, **Anne**, **Marta, Jantine**, **Maya**, **Bas, Hesther**, **Jennie**, **Iliana**, **Andrea**, **Ilaria**, **Arwa, Eirini** for your kindness and fun times. Mijn Imaris buddy, **Dennis**! Leuk dat je vaak naast me zat, een praatje maken maakt acht uur data-analyse doen dragelijk. People from the Tanenbaum-groep, **Tim**, **Sanne**, **Lenno**, **Deepak**, **Bram**, **Stijn** thank you for fun times and all the pie! Stijn, ook enorm bedankt voor het verrichten van wonderen in MatLab. **Matilde**, fijn dat je onze werkbespreking hebt verrijkt met je kritische blik en een heel interessant onderwerp waar je aan werkt. **Gabby**, I adore your sense of humour! Yes, I consider you are lost member of the Kops-group, thank you for sharing many fun moments and I wish you much strength and joy. **Lotte**, jij ben een enorm lief en open persoon en je gevoel voor humor is geweldig.

Helaas dat je onze groep niet zo vaak meer vergezelt. **Corina**, **Sammy**, **Silke** and **Kim** you are the mascots of the Kind-group with your open and friendly personalities. I wish you all the best of luck in finishing the necessary chapters and remember to enjoy the rollercoaster-ride a PhD can be. **Annabel, Euclides** and **Lorenzo** from the Korswagen-group, thank you for the fun times and enjoy D-day (defense-day)! Lorenzo, you threw a stellar party I will remember for long! Annabel, PhD-buddy, ik ben blij dat onze kinders prima op eigen benen kunnen staan en vond het heel leuk om samen met jou dit traject te pionieren. **Maaike** and **Jens**, you are both very smart and your drive to do science will bring you far, remember to enjoy the ride! **Stefan**, bedankt voor het flexibel zijn en vertrouwen in mij zodat ik zelfstandig wat dingetjes mocht uitvoeren. Dit is heel leerzaam geweest en hulde voor de manier waarop je al de balletjes hoog weet te houden! **John**, bedankt voor het maken van een praatje en begrip voor die momenten waarop het er even niet in zat vanwege de werkdruk. Je inzet voor dit instituut kan niet onopgemerkt gaan en ik ben je heel dankbaar hiervoor, neem je rust waar het kan! De Medema's. **Rene**, bedankt voor je kritische blik die je altijd werpt op de wetenschap, vaak gepaard met een dosis humor en dit bewonder ik enorm. Je hebt mij vanaf dag een al op scherp weten te zetten, ik hoop dat we nog eens de kans krijgen wat vurige discussies te voeren. **Jonne**, **Wytse**, **Mihoko**, **Indra**, **Rob**, **Roy**, **Femke**, en **Mar** een hele hechte groep die altijd open stond voor gezellige praatjes, bedankt! Also, the **Wolthuis**, **Saurin** and **Rowland** labs, thank you for the fun and serious science times we have shared over the years. Then I could go on to mention many more people who have touched me in one way or another. I have to stop myself from writing on and on, and not make this too boring a read, but know this; I remember you warmly.

Carlito, or señor **Carlos**, I admire your seemingly endless creativity and intelligence. I have learned much from seeing you nearly effortlessly carry big projects past unexplored horizons and I will miss discussing exciting and unexplainable results with you. You are able to critically assess complex data and always seem to suggest the critical experiment to carry projects to another level. Your kind and calm personality is have brought me down to earth when needed on several occasions. I hope you find the perfect position in which you can pass on your skills and creativity to the next generation of ambitious scientists. I feel honoured to have someone with so much experience stand beside me as paranimf.

Lab-rookie **Maaike**, maar direct onmisbaar in de groep met je vrolijke en energieke persoonlijkheid. Ik ben blij dat we nog even samen aan de bench staan straks en gezellig verder kunnen kletsen. Ik vind het jammer dat niet al eerder de groep verrijkt hebt, nu zal ik van een afstand moeten toekijken hoe '*the Book of Maaike*' tot stand komt, als musical-thema misschien?. Voor als je diep in een ronde corona staart: "Everything you see exists together in a delicate balance". Ik ben heel blij dat je mijn paranimf wilde zijn en je had geen auditie hoeven doen voor deze rol.

Ana and **Cas**, I am very happy to have shared many great moments of life with you. You two are a powerhouse and I feel relaxed hanging out with you. I am thrilled now that you have decided to return to the mother continent '*From The New World*'. Soon, we will enjoy great conversation, food, drink and board games together again. Thank you for being great friends!! **Tessa**, jij hebt mij misschien wel onwetende een duw gegeven om alsnog dit boekje te schrijven. Ik bewonder je zelfvertrouwen en je intelligentie en het is altijd heel leuk om je te zien. Ik hoop dat ook jij vergevorderde plannen hebt om terug te keren naar het moederland. **Steven**, je enthousiasme voor de wetenschap is verbluffend als is je humor soms. Ik geniet van onze discussies over weet-ik-veel wat en laten dit snel weer een keer op de agenda zetten. **Nicola** and **Claire**, thank you for sharing many enjoyable moments with us. You two are amazing in sharing kindness and I look forward to visiting you again soon, where-ever, whenever, as long as we are together. It goes without saying this will be a place that has good food and wine (e.g. Italy). **Marcelo**, you are strong minded and kind-hearted person. I admire your business-oriented approach to science which is the smart way to go for sure! **Marti**, altijd leuk om een biertje te pakken met jou als gezelschap. Succes met de afronding, wij laatbloeiers gaan die PhD ook gewoon afmaken!

Nadica, you have so much strength and joy to share, thank you for sharing this with me. I admire your stance in life and your openness and kindness towards anybody is heartwarming. You bring the best out in people near you. **Branko**, you are a strong yet very kind person and I hope we get to know each other better still. I will start to work on my Slovenian as of now! **Barbara** and **Stuart**, I am always very excited to see you and enjoy your sense of humour. Your calmness is soothing and I feel relaxed and comfortable around you.

Pap, je hebt me altijd vrijgelaten in het maken van keuzes zodat ik mijn eigen interesses kon najagen. Je bent altijd bereid een duwtje in de juiste richting te geven wanneer nodig om mij richten een goed besluit te bewegen. Je staat altijd klaar en dit wetende geeft mij veel kracht om door te gaan. **Martine**, ik ben enorm blij dat je ons leven hebt verrijkt met je warme en lieve persoonlijkheid. Je geeft veel liefde aan de mensen om je heen, ik voel me thuis. **Marten**, ik mis je omdat je vaak in een land ver weg zit. Ik hoop je dan ook snel weer te zien! Ik hou van jullie.

Manja, mala moja! I'd be *a lost boy* without you; my life would have been but an empty shell from what it is today. Your bright and strong life force bring me joy and leads me to undertake adventures beyond my horizons. You have taught me so many things about experiencing life and defining where you want to go next, you inspire me to dream. I love you and look forward to explore more of this wonderful world together with you. Rad te imam!

&